AD NUMBER

AD020684

NEW LIMITATION CHANGE

TO

Approved for public release, distribution unlimited

FROM

Distribution authorized to U.S. Gov't. agencies and their contractors; Administrative/Operational Use; 23 SEP 1953. Other requests shall be referred to Office of Naval Research, One Liberty Center, 875 North Randolph Street, Arlington, VA 22203-1995.

AUTHORITY

ONR ltr dtd 26 Oct 1977

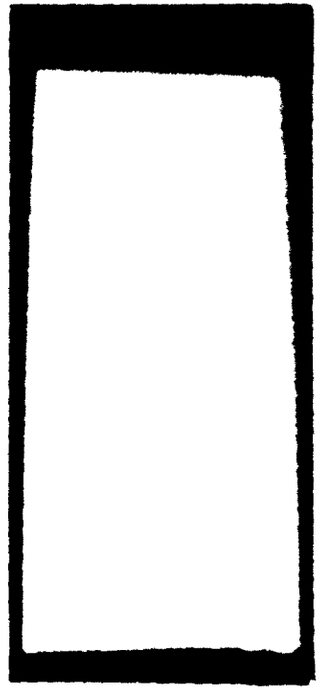

Final Report on

Contract ONR - 24908

to

Office of Naval Research

U. S. Navy

DEFORMATION of BERYLLIUM SINGLE CRYSTALS at 25°C to 500°C

by

H. T. Lee & R. M. Brick

Department of Metallurgical Engineering

Towne Scientific School

University of Pennsylvania

Philadelphia 4, Pa.

Copy No 32

September 23, 1953

CONTENTS

ABSTRACT

Compression tests at room temperature, 300°C, and 500°C have been conducted on single crystals of beryllium for various orientations.

Part I includes experimental observations of the study. Slip and twinning elements were determined from surface markings by microscopic examinations and by x-ray analyses. The operative slip planes at temperatures of 250°, 300°, and 500°C were established as (0001) and $\{10\bar{1}0\}$; the single twinning plane as $\{10\bar{1}2\}$. Cleavage planes were found to be either (0001) or $\{11\bar{2}0\}$. Deformation and kink bands were also observed. A peculiar type of macroscopic band was found present in several specimens with a particular orientation and an explanation accounting for its formation is given. Measurement of the displacement of cracks across slip bands has led to an evaluation of the local strains resulted from basal slip as a comparison to the average shear. A selection rule based on an extension of LeChatelier's principle is advanced for the choosing of active twinning planes from the total ones available.

Part II consists of some crystallographic analyses regarding to twinning and slip. A mathematical relationship is given to describe the atomic movements in twinning of close packed hexagonal metals. Factors of periodicity and crystallographic shear are also considered for their relation with the selection of slip and twinning elements.

Part I - Experimental Observations of Beryllium Single Crystals under Compression

INTRODUCTION

Complications involved in the production of beryllium single crystals (1) of reasonable size and purity have thus far made it impossible to conduct an extensive study of the plastic behavior of this metal. Specimens used in earlier experimental studies of the properties of beryllium were generally the result of chance (2) and often were in the shape of flakes or needles of the order of millimeters in their various dimensions (3) (4). Only recently apparatus and techniques have been developed by Kaufmann and Gordon (5), and Gold (6) to produce beryllium single crystals of reasonably large size.

In 1928, Mathewson and Phillips (7) established the slip and twinning planes of beryllium as (0001) and $(10\bar{1}2)$ respectively. The authors used polycrystalline specimens cut so as to expose two surfaces at right angles. After deformation in a vise the angular relations of the slip lines and twin lamellae in individual larger crystals were studied. Since then no work on the plastic behavior of beryllium single crystals has been reported.

Important applications of beryllium in recent years have required more understanding of this metal. It has been the purpose of the present investigation to make some observations of its single crystals under compression and at various temperatures, so that our knowledge of plasticity of beryllium could be somewhat enlarged.

However, a study of the mechanical properties of beryllium single crystals today is still very much limited by a number of complexities. Our knowledge of beryllium is meager. Many nebulously understood observations concerning beryllium need definite clarification. The various forms of impurities and their effects (1), the much debated possible existence of allotropic forms (1,4,8,9.10,11,12,13,14), and the peculiar imperfection of beryllium crystals (15) all have important bearings to such an investigation. Without a much improved understanding of these complexities, the present study can contribute only semi-quantitative observations.

PREPARATION of SPECIMENS

Two Be ingots 4" in diameter and approximately 6" in length were supplied by Dr. Kaufmann of M.I.T. These ingots were coarse grained, with no more than six grains over the cross section except for clustered small ones about 2mm in size near the pipe. The pipe ran 2" in diameter, and 2" in length.

The material was over 99.8% pure*. X-ray powder patterns from both ingots established the following lattice parameters: a= 2.2871Å, c= 3.5860Å, and c/a= 1.5679. No difference in the two patterns could be detected. However, in both cases, an unidentified extra line was present at the extreme low angle end of the pattern. The given values of lattice constants were much closer to those obtained by Owen, Pickup, Roberts and Richards (4) (13) (14) than to the results of Newburger (12) (16).

* Kaufmann, A.R. ----- private communication.

Slices 3/4" in thickness were first cut across the ingots by means of an abrasive wheel. After the individual orientations had been determined for the grains in a particular slice, compression pieces were cut from it with the aid of a high speed water sprayed glass cut-off wheel. A goniometer stage in front of the blade permitted the slice to be fed into the wheel at different angles. In this way, the desired orientations could be obtained without much difficulty. These pieces, now about 1/2" cubes, were only the rough form of compression specimens. They were carefully hand ground to three sets of parallel surfaces. This was attained by numerous measurements and regrindings on a wet #100 abrasive belt.

Due to the extreme brittleness of Be, even careful hand grinding almost invariably caused cracks to form along the sharp edges of the specimen. Corners were also very easily chipped. This was particularly true for specimens with basal plane inclined about 45° to the compression surfaces, see Fig. 47a, P.62. Cracks at the edges of the specimen were rounded off down to their base and grindings again proceeded on the relevant surfaces. When the grinding proved to be too vigorous for a particular case, the specimen was transferred to a finer grade of polishing paper. This tedious process was continued until a geometrically perfect specimen was obtained.

Specimens were then polished on 240, 400, 600 papers, followed by a deep etching with Tucker's reagent to check if there was any presence of grain boundaries on either of the six surfaces. Quite often an originally overlooked boundary would appear at this stage. Deep etching was found to be the only effective way to bring out high enough contrast among similarly oriented grains. It was, however, avoided as much as possible because its fast action always introduced uneveness and pitting of specimen surfaces, as well as deepening of minute edge cracks.

After a repolishing of the specimens on 600 paper they were then annealed at 1000°C for 1 hr. in vacuum. The annealing treatment eliminated surface twins and insured a comparable initial condition for all the testing specimens.

After annealing, the surfaces of specimens were slightly tarnished. They were polished again on 600 papers lubricated by kerosene, then etched for a last check, and finally polished on silk with Linde fine abrasive. It should be noted that all six faces of a specimen were prepared in such a way. The 4 vertical ones were prepared for subsequent microscopic examination, and the two compression surfaces were given a metallographic polish to insure their smoothness and minimize friction. A dilute HCl wash followed the final polishing, although no measurable change of dimension resulted from this treatment.

This procedure made it difficult if not entirely impossible to attain uniformity of all specimen dimensions. Neverthless, most of the specimens were between 0.1" and 0.2" thick with the exception of a group of nine which were purposely made with greater thickness to attain a higher sensitivity of strain. The cross-sections of the specimens were made to approach closely to a square. Among the 39 specimens, with the exception of nine of them, the perpendicular sides of the cross-section of a particular specimen did not differ more than 0.004" while the lateral dimensions mostly ranged from 0.28" to 0.40". A few larger specimens were made with greater thickness to improve the accuracy in the measurement of stress.

Since the compression strain used in the tests only amounted to a few percent, it is believed the non-uniformity of specimen dimensions would not introduce a serious complication to the experiments. More attention was, therefore, paid to the geometrical perfectness of the specimens rather than to their dimensional uniformity. The thickness of specimens was kept similar to those used by Taylor and Farren (17) so as to minimize the effect of friction at compression surfaces and also to minimize the effect of bulging and barreling. Fig. 7, p.18 shows the initial form of a specimen and another specimen after a 12.7% reduction of thickness. It is clear that the distortion had been quite uniform with the original square section changed to a rhomb.

The dimensions of all specimens are given in Table 1, p.12, for reference. Specimens numbered less than 100 were obtained from one ingot. Those numbered higher than 100 were obtained from a second ingot. Be-12 and Be-109 had a few small grains imbedded in the main crystal. Be-2 was first used for a room temperature test and then again used for 500°C after being repolished and annealed.

COMPRESSION PROCEDURE

The compression unit consisted of a cylindrical hardened steel plunger, an anvil and a container. One end of the plunger was machined to a half sphere to match the depression on a compression plate which was firmly bolted to the cross-head of a Southwark-Emery hydraulic machine. The other end was highly polished to face parallelly the similarly polished surface of the anvil. Compressions were carried out in a series of steps with frequent lubrication.

For the runs at temperatures above atmospheric, the described compression unit was put in a nichrome wound furnace with a controller to maintain the desired temperature.

Tests were carried at three temperatures: 25°C, 300°C, and 500°C. At both room temp. and 300°C, Silicone DC 200 oil was used for lubrication; and at 500°C Houghton's Mar-Temp salt was used. These served the double purpose of lubricating the compression surfaces and protecting the specimens from being exposed to air. The compression unit was first brought up to temperature and specimen was then put in. Owing to the extremely small mass of a specimen as compared to that of the compression unit, temperature equilibrium reached very rapidly.

Strain was measured by a microformer type extensometer attached across the stationary and movable posts of the testing machine. A lever combination connected to the plunger of the microformer enabled several different magnifications of the head movement. Throughout the test a constant rate of head movement of 0.002"/min. was maintained.

Both strain and load were recorded autographically. Prior to each test a blank run was made so that the deformation of the equipment might be evaluated.

Orientation of specimens was determined by the conventional Laue back-reflection method. To correlate the microscopic examination with the X-ray pattern, a special goniometer was constructed with two degrees of freedom of rotation. Angular directions of the slip and twin traces as measured under microscope on each vertical surface were always plotted stereographically to the same reference plane of the original X-ray pattern.

Since frequently there were more than one type of trace on each surface, difficulty arose as to the right combination. For instance, one face might have six twin traces and another face perpendicular to it might also have six twin traces. There were then 21 cases to be analyzed if they were to be determined individually. To facilitate the analysis, the following procedure was adopted throughout the experiments.

Fig. 2 shows a hypothetical case where traces are as indicated. All intersecting faces are 90° apart. The locus of the poles of planes which would make an A° trace on surface II appears as a great circle in Fig. 3 when plotted stereographically with the compression surface I as the plane of projection. This great circle A° to the right of the NS line. In a similar manner the respective locus of the planes containing other traces can also be plotted. For the present case 9 combinations will be obtained simultaneously in the same stereogram. When this is compared with the original orientation of the crystal it could be easily determined which three of the nine possible combinations are the correct ones.

Quite frequently, after considerable distortion, the original square cross-section would turn into a rhomb, as shown by Fig. 4. In such case the procedure would be modified as illustrated by Fig. 5 which is self explanatory.

RESULTS and DISCUSSION

Original orientations of the 39 specimens studied are shown in Fig. 1. The conventional method of orientation notation is adhered to; that is, the pole of the basal plane (0001) has been rotated to the center of the primitive circle, and the position of the compression axis of each specimen is represented by a cross in the basic triangle formed by the poles of three planes (0001), $(10\bar{1}0)$, and $(11\bar{2}0)$. The three triangles show the three groups of specimens compressed at 25°C, 300°C, and 500°C respectively.

A complete tabulated summary of the experimental conditions in these tests is given in Table 1. The angles fixing the position of the compression axis are given as θ and λ, Where θ is the angle between the compression axis and the pole of the basal plane, and λ the angles between the three poles of $\{11\bar{2}0\}$ planes and that of compression surface.

Results of the investigation may be divided into the following groups according to the initial orientation of the specimens:

A. ORIENTATIONS with BASAL PLANE NEARLY PARALLEL to the COMPRESSION SURFACE

This group of specimens included Be-4, Be-5, Be-1, and Be-2, all possessing a θ value smaller than 5°. The first two were compressed at room temperature, and the last two, Be-1 and Be-2, were tested at 300°C and 500°C respectively.

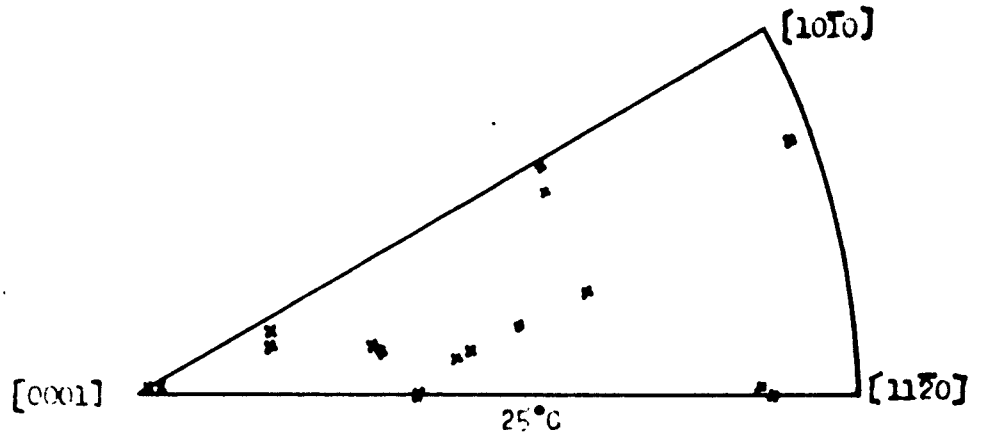

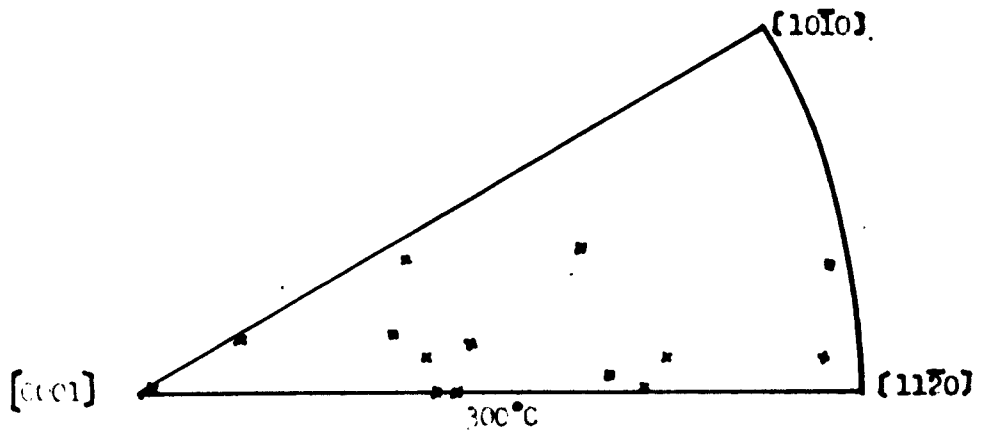

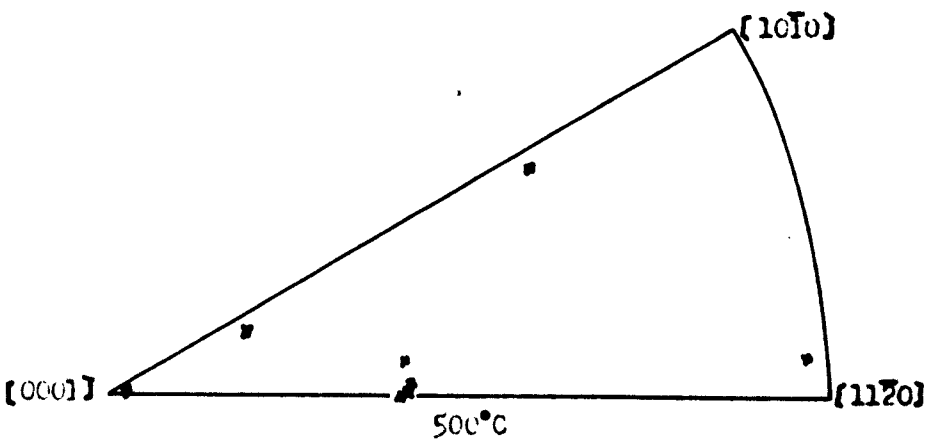

Fig. 1 - Orientation of specimens prior to test.

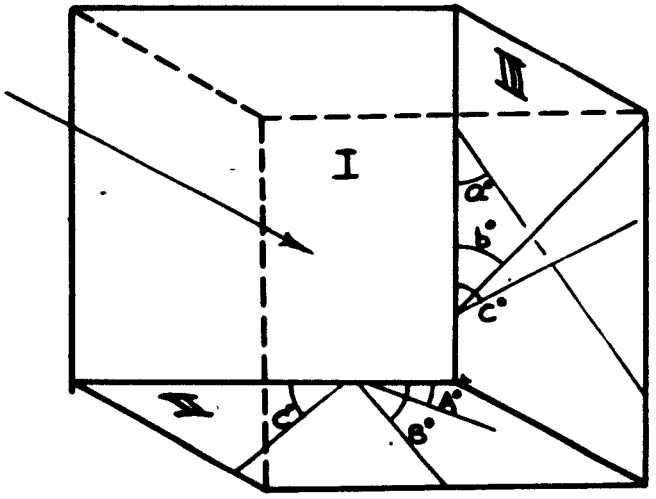

Fig. 2

Deformation traces, Schematic

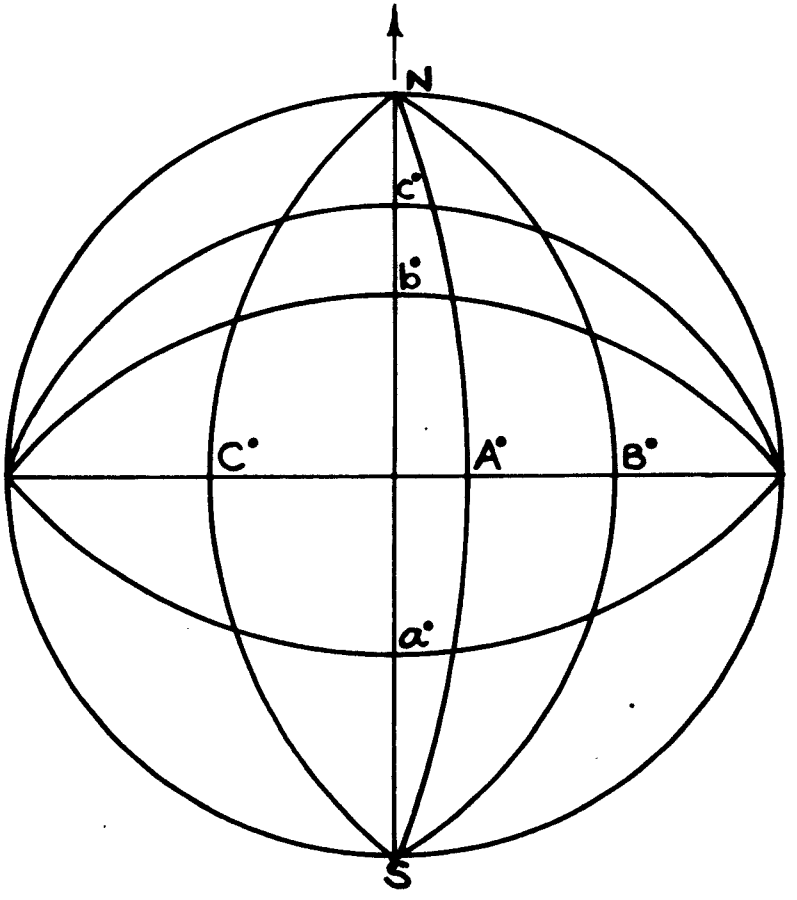

Fig. 3

Projection of locii of poles of the planes containing the various traces.

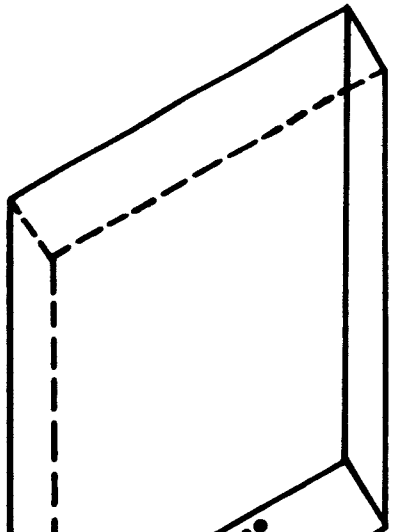

FIG. 4

Deformation trace, Schematic.
Distorted crystal.

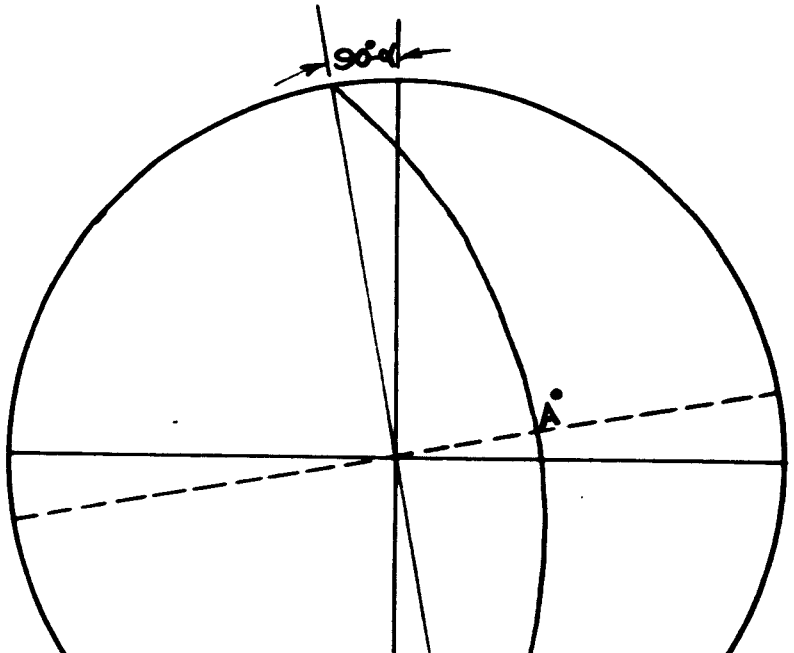

FIG. 5

Projection of locus of plane poles
containing trace A.

Table 1

Testing Conditions of Specimens

Specimen Number	Temperature (°C)	θ	λ	% Red.	Initial Dimensions (in.)	
					Thickness	Area
Be-2	25	4	86,87,89	0	0.1138	0.2895x0.2875
Be-4	25	1	89,89,89	Fract.	0.1751	0.3355x0.3358
Be-5	25	1	89,89,89	Fract.	0.1431	0.3055x0.3048
Be-1	300	?	88,89,90	Fract.	0.1718	0.3239x0.3231
Be-2A	500	4	86,87,89	Fract.	0.1100	0.2865x0.2828
Be-9	25	[illegible]	42,64,73	12.70	0.1650	0.3291x0.3212
Be-11	25	50	40,63,73	3.62	0.1079	0.3104x0.3136
Be-109	25	[illegible]	53,62,66	2.37	0.1604	0.4051x0.4030
Be-113	25	[illegible]	35,57,74	2.35	0.1403	0.4152x0.4286
Be-141	25	[illegible]	47,70,71	3.00	0.2674	0.5020x0.5110
Be-153	25	[illegible]	52,67,77	6.10	0.1067	0.2943x0.2944
Be-12	300	[illegible]	42,62,74	5.50	0.1180	0.3193x0.3180
Be-110	300	[illegible]	52,64,79	3.30	0.1299	0.3219x0.3220
Be-120	300		46,65,74	4.95	0.1931	0.5295x0.5290
Be-142	300		45,69,70	2.75	0.2831	0.4341x0.4342
Be-146	300	[illegible]	43,68,70	5.07	0.2851	0.3538x0.3515
Be-147	300	44	51,55,87	4.80	0.2206	0.4265x0.4247
Be-121	500	45	45,64,74	1.60	0.1908	0.5370x0.5391
Be-143	500	44	46,70,70	4.70	0.2390	0.4037x0.4108
Be-144	500		46,68,71	1.40	0.3053	0.4476x0.4717
Be-145	500		45,68,70	2.11	0.2753	0.4220x0.4312
Be-149	25	[illegible]	69,73,86	20.30	0.1677	0.3960x0.3946
Be-159	25	[illegible]	67,72,88	10.50	0.1570	0.2920x0.3131
Be-14	300	[illegible]	74,75,88	1.20	0.1828	0.3720x0.3705
Be-148	500	[illegible]	68,70,88	1.08	0.1950	0.3966x0.3972
Be-3	25	[illegible]	8,60,62	10.90	0.1503	0.2871x0.2867
Be-6	25	[illegible]	6,60,60	3.86	0.1631	0.3419x0.3424
Be-7	25		20,40,80	1.04	0.1541	0.2498x0.2505
Be-22	300		10,50,70	1.80	0.0890	0.2845x0.2856
Be-151	300	[illegible]	5,57,63	2.66	0.1615	0.3188x0.3190
Be-150	500		4,57,63	2.74	0.2189	0.4241x0.4182
Be-8	25	[illegible]	33,50,77	2.10	0.1342	0.2953x0.2988
Be-155	25	[illegible]	37,38,89	8.30	0.1085	0.3978x0.3966
Be-157	25	[illegible]	35,41,86	8.27	0.1016	0.3821x0.3850
Be-101	300	[illegible]	30,48,79	4.71	0.1485	0.3315x0.3320
Be-117	300	[illegible]	20,59,65	0.31	0.1598	0.3790x0.3770
Be-118	300	[illegible]	20,61,63	0.95	0.1770	0.3871x0.3888
Be-152	300	[illegible]	25,60,65	3.50	0.2392	0.3605x0.3644
Be-156	500	[illegible]	35,40,88	10.60	0.1190	0.2728x0.2685

Typical load and reduction curves for these specimens are shown by Fig. 7. It is clearly seen that the specimen, in this case Be-5, behaved almost completely elastically. Loading was accomplished in three steps: 2790 lbs., 23,600 lbs., and 26,500 lbs. Measurements after first and second compressions did not reveal any change of dimensions from the original. No slip lines or twin traces were observed. The autographic curve was straight without any bend-point or change of slope prior to fracture. Fracture of the room temperature specimens occurred in such a way that the original specimens suddenly were pulverized into numerous fine particles.

Two of the small pieces, however, were large enough to show that the main fracture had been along a plane 45° to the compression surface. X-ray and microscopic examinations established that the basal plane and all three sets of $\{11\bar{2}0\}$ planes also acted as cleavage planes. The orientation of the crystal apparently was in such an unfavorable position for either slip or twinning, that only elastic deformation was allowed. Gradually the elastic energy stored in the specimen built up until it reached the limit that could be sustained by the lattice, followed by fracture. The availability of four cleavage planes made it possible for the specimen to break into many fine pieces.

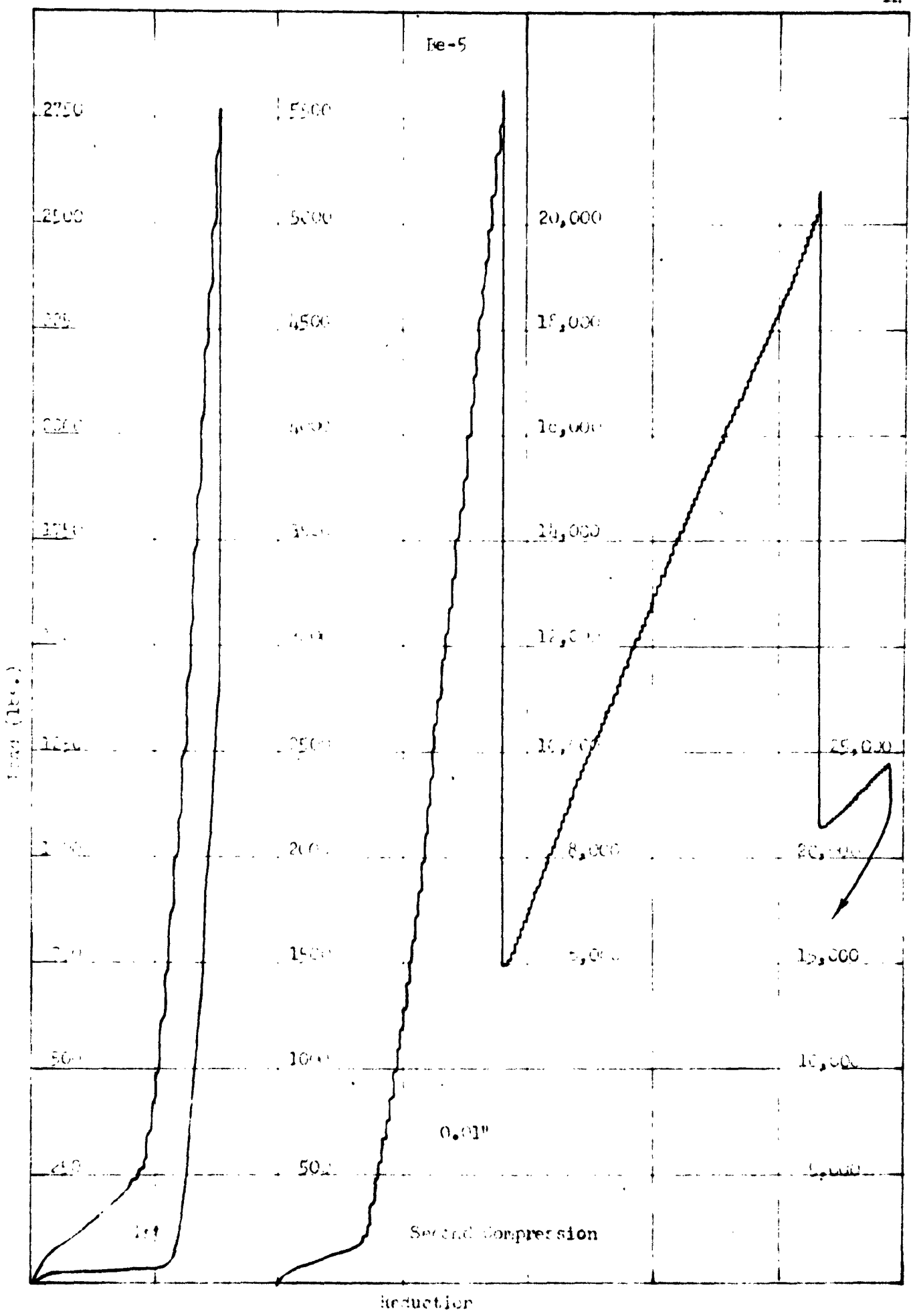

Fig. 7 - Autographic Load-Red. Curves of Fe-5; Stressed at Room Temperature, ⊥(0001).

Both Be-5 and Be-4 behaved exactly in the same manner. In each case, fracture occurred at a stress of 285,000 lbs./in.^{2} based on the initial area.

The autographic load strain curves of these two specimens together with the calibration curve enabled an estimation of the maximum elastic strain energy which could be sustained by the crystals at room temperature. The values obtained are given in Table 2. It is seen that the two values did not differ more than 3%. It seems that these values should be an indication of the cohesive energy of beryllium, and should be corresponding to its heat of sublimation at room temperature. However, a comparison of the present value, 39,900 in-lbs./cu. in. or 0.33 kg. cal/mol. with the sublimation energy of 75 kg. cal/mol as given by Bichowsky and Rossini (19), and Baur and Brunner (20) reveals that there is a more than 200 fold difference. In view of the impurities present in Be as inclusions, the inherent imperfection of the crystal, as well as the crystallographic behavior of fracture in contrast to the isotropic property of heat of sublimation, this discrepancy may not be very surprising. Furthermore, it should also be noted that the heat of sublimation of Be given by most sources were based on the validity of Trauton's Rule, and could only represent a rough approximation.

Table 2

Fracture Data of Beryllium

Specimen Number	θ	Temperature	Fracture Stress (lbs./in.^{2})	Energy Prior to Fracture in-lbs./cu.in.
Be-4	1°	25°C	285,000	39,900
Be-5	1°	25°C	285,000	38,800
Be-1	2°	300°C	215,000	18,000
Be-2A	4°	500°C	227,000	29,900

Figs. 8 and 9 reproduce two fractographs of Be-5. Fig. 9 was taken from on a $(11\bar{2}0)$ cleavage face. A curved, irregular surface was characteristic of all $(11\bar{2}0)$ fractures, whereas the basal cleavage always resulted in a flat surface. Fig. 8 was taken from the approximately 45° surface of fracture. Slip lines are seen associated with the fracture, and so are minute twins. The slip lines ran closely parallel to the compression surface which in this case was only 1° from the basal plane. It was noted that the density of the lines decreased sharply from the compression surface. Farther inside, these lines developed into cracks. $\{11\bar{2}0\}$ cleavages are also seen in these pictures.

X-ray patterns (Figs. 10 and 11) show the difference between the original and the fractured states. One interesting aspect was that asterism only developed along two of the three $\langle 11\bar{2}0 \rangle$ zones. No single rotation or bending axis could account for such an effect. In view of the limited number of slip lines, it seemed quite unlikely that the asterism should be solely derived from the basal slip, although the apparent axis of bending was close to $[10\bar{1}0]$ direction as to be expected. One possible explanation would be that this peculiar bending pattern might be a result from two opposite rotations about $[1\bar{1}00]$ and $[0\bar{1}10]$ axes. Such rotations would possibly have only a very small resultant on the planes of $[1\bar{2}10]$ zone, while the $[11\bar{2}0]$ and $[\bar{2}110]$ zones could still show considerable lattice bending. A distortion like this could very well be introduced by the $\{11\bar{2}0\}$ cleavages. The broken concentric rings in Fig. 11 were identified as the $\{10\bar{1}4\}$ reflections from the small twins. This will be discussed in more detail in a latter section.

Specimens compressed at higher temperatures behaved similarly, except that the final breakages did not result in such small pieces. Also, at 500°C the autographic curve indicated a levelling off just before fracture was reached.

The fracture stress and energy stored prior to fracture for Be-1 and Be-2 are also given in Table 2. Increase in these values at 500°C as compared to those at 300°C may be ascribed to the increased strain and resultant hardening of Be at the former temperature. The slight difference in orientation also may account for part of it.

B. ORIENTATIONS with BASAL PLANE at 45°

This group included 16 specimens. Their θ values ranged from 38° to 57°, although the majority of them had the basal plane inclined to the compression surface only ±2° from 45°. Deformation of these specimens was predominantly by basal slip with one of the $\langle 11\bar{2}0 \rangle$ axes as the direction of the glide.

$(10\bar{1}2)$ twinning occurred in three of these specimens. However, the twins were either very few or very minute.

The (0001) slip lines were straight when no deformation bands were present, and when they were away from inclusions. A typical state is represented by Figure 12. At some locations in a later stage of deformation, the slip lines often formed as clusters which would produce an abrupt off-set at the free surface of the specimen and a basal fracture would thus be initiated. This situation is shown by Figs. 13 and 14.

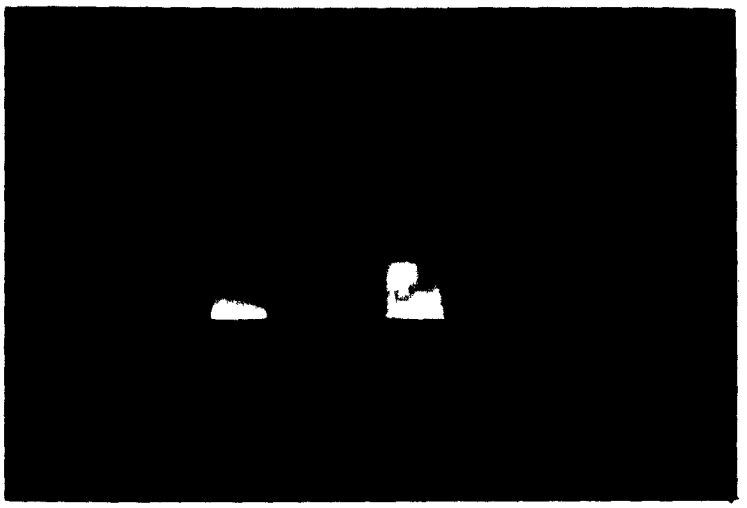

Fig. 7 - Beryllium crystals before and after compression, (IX).

Fig. 8 - Fractograph of Be-5, taken on (0001) cleavage face (150X).

Fig. 9 - Fractograph of Be-5, taken on (11 $\bar{2}$0) cleavage face (100X).

(Be-5, stressed at 25°C perpendicular to basal plane).

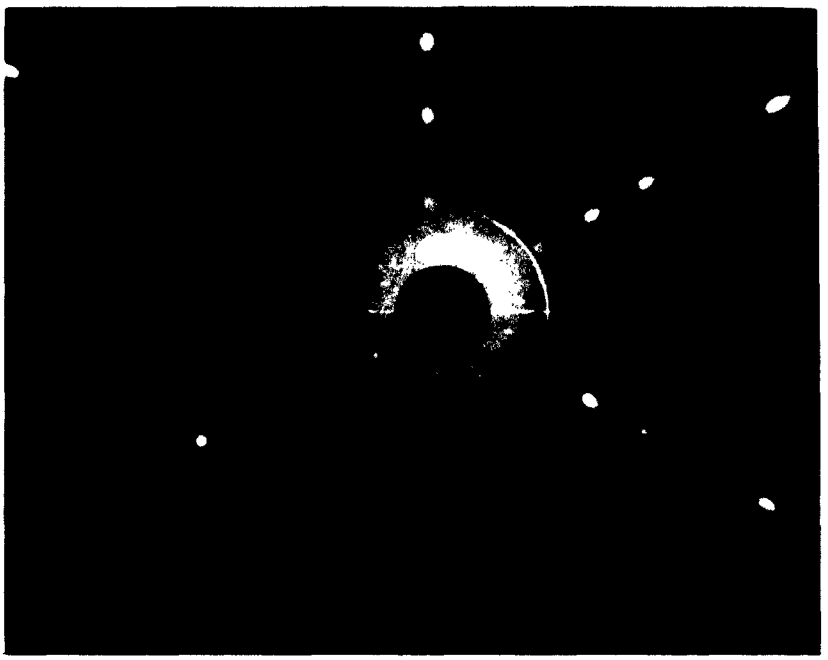

Fig. 10 - Laue pattern of Be-5 before compression.

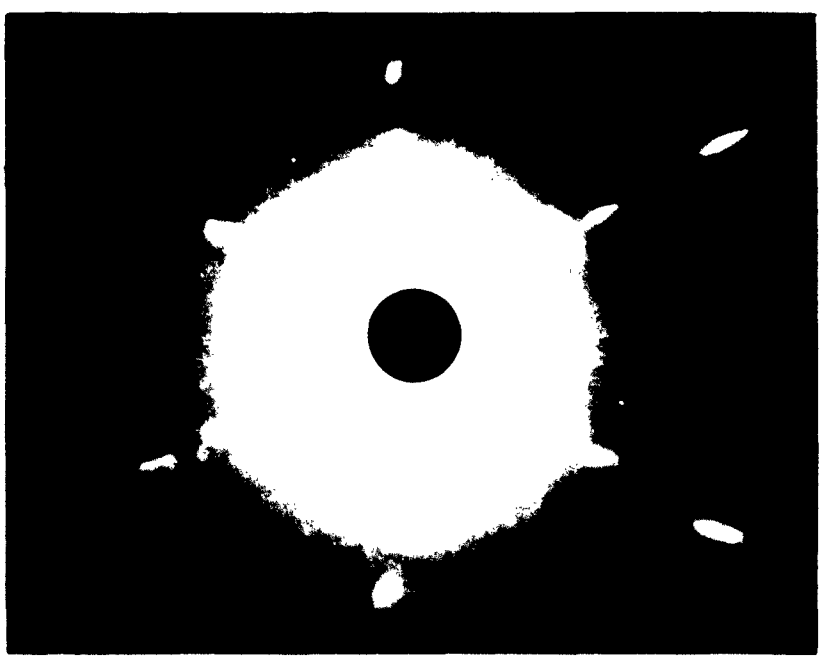

Fig. 11 - Laue pattern of Be-5 after compression, taken perpendicular to an (0001) cleavage face.

Figure 14 also illustrates the effect of a free surface on the gliding. It is seen when the slip lines approached a surface, they were bent in such a way as to be as nearly perpendicular to the surface as possible. This often caused some tear-lines near the compression surface. Furthermore, owing to the extra energy required to break through a solid surface, the slip lines frequently stopped before they could penetrate through. Also the strain hardening near the surface due to lattice bending tended to make the density of slip lines decrease as they were approaching the end. Figure 15 also illustrates these points. Inclusions had similar effects as shown in Figs. 16a and 17.

Deformation bands appeared in many of the specimens. The bands invariably were parallel to the plane of restriction, i.e., the compression surface.

Basal Slip, Room Temperature vs. High Temperature

An important difference seemed apparent between 500°C specimens and those tested at room temperature and 300°C. Crystals compressed at the latter two temperatures did not reveal an appreciable change of slip line spacing, although the 300°C specimens did infrequently show the tendency of branching of slip lines as in Fig. 16. However, 500°C specimens exhibited an obvious increase of slip line spacing as compared to both room temperature and 300°C. A comparison of Fig. 17 and 18 clearly demonstrates this point. Both specimens, in this case, had the same orientation and amount of reduction. They were, therefore, in a comparable state. Moreover, slip lines at 500°C were wavy and often branched to various directions to form an intricate network.

Evidence seemed to indicate that upon deformation at 500°C, the crystal became considerably more imperfect Laue photograms, e.g., Fig 19, showed marked sharp differences of orientation of the mosaics, often amounting to over 2°. This was in contrast with the x-ray pattern obtained from specimens after being compressed at room temperature and 300°C for a comparable amount of reduction, Fig. 20. This increased imperfectness seemed to appreciably strengthen the crystal at 500°C and to account for the waviness and branching of the slip lines The same change was also manifest in the autographic load-reduction curves obtained at different temperatures, Figs. 21 and 22. While curves at both room temperature and 300°C generally possessed a sharp bend-point, the 500°C curves always had only a slight bend and this occurred at a higher resolved shear stress.

Critical Resolved Shear Stress

By utilizing the bend-point of the autographic curves, an attempt was made to determine the critical resolved shear stress of beryllium at the three temperatures studied. Table 3 summarizes the results.

Fig. 12 Basal slip lines on Be-11, strained at 25°C; (0001) 50° from stress axis, (200X).

Fig. 13 Cluster of basal slip lines on Be-9, strained at 25°C; (0001) 50° from stress axis, (300X).

Fig. 14 Crack at terminus of cluster of slip lines of Be-9 at side surface, (200X).

Fig. 15 Basal slip lines on Be-11 at compression surface (top). Crystal strained at 25°C, (200X).

Table 3

Specimen	Temperature, °C	θ	λ	τ_c psi	
Be-9	25	49.5°	41.5°	4420	
Be-8	25	65°	33°	4120	
Be-11	25	50°	41°	4980	Ave. = 4600
Be-141	25	43°	47°	4180	
Be-153	25	38°	52°	5320	
Be-142	300	45°	45°	3910	
Be-147	300	44°	51°	4370	Ave. = 4060
Be-146	300	47°	43°	3910	
Be-143	500	44°	46°	6630	
Be-144	500	44°	46°	6220	Ave. = 6460
Be-145	500	45°	45°	6530	

It is seen that within the limit of accuracy (a 2° difference of both θ and λ would throw the value off 10%) the critical resolved shear stress of Be at 300°C as determined was practically the same as that at room temperature. Values at 500°C were considerably higher. This abnormal affair had been observed by Miller and Milligan [22] in single crystals of silver and aluminum, and was believed to be caused by the increase of thickness of oxide film with increasing temperature [23].

Fig. 16a - Basal slip lines on crystal Be-9 strained at 25°C; effect of inclusion (1000X).

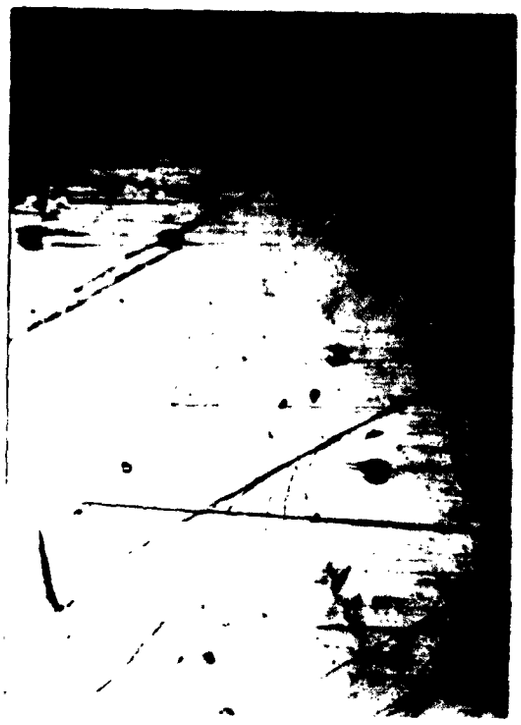

Fig. 16b - Basal slip lines on crystal Be-110 deformed at 300°C. Branching that occasionally was observed (100X).

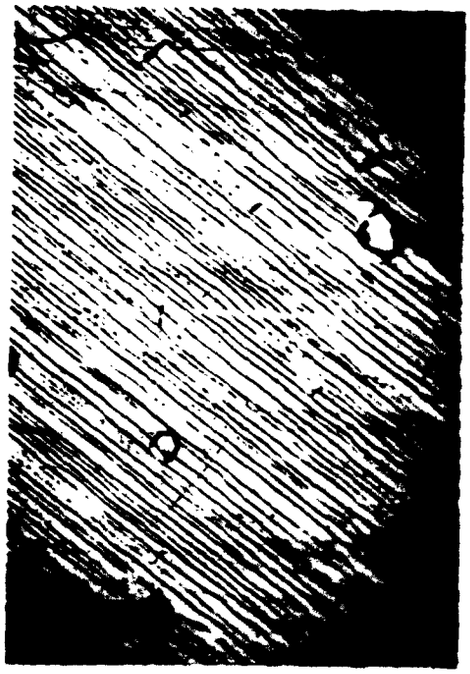

Fig. 17 - Basal slip lines on crystal Be-141 deformed at 25°C (200X).

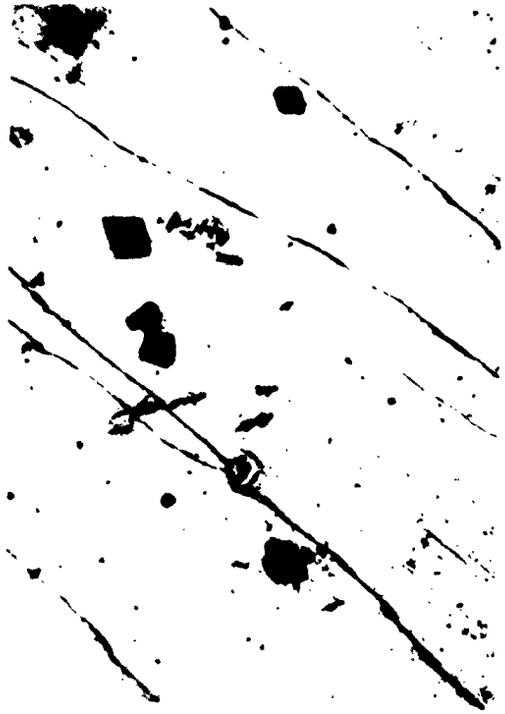

Fig. 18 - Slip lines on crystal Be-145 deformed at 500°C (200X).

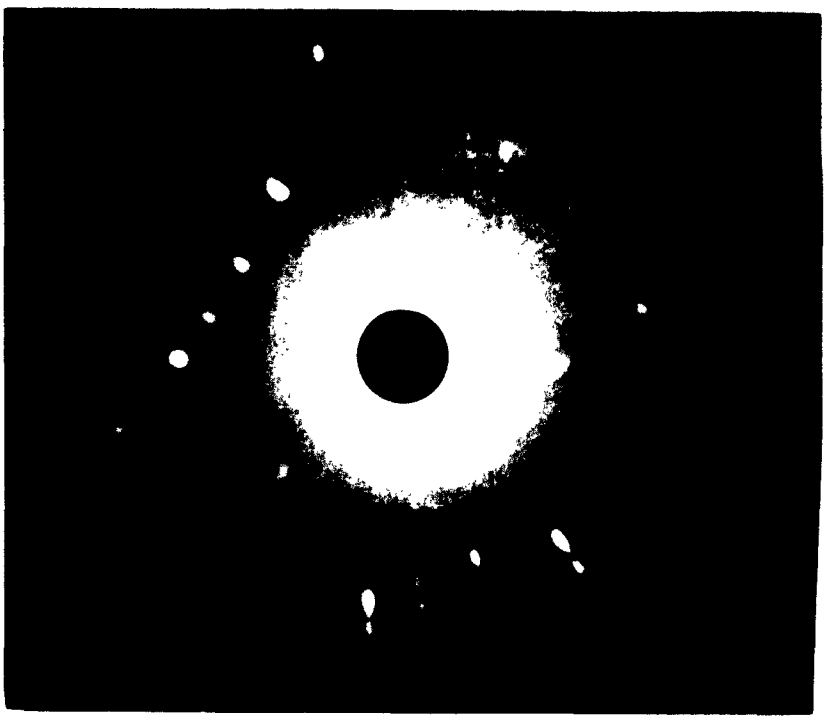

Fig. 19 - Laue photogram of crystal Be-145 after deformation at 500°C; mosaic structure developed upon deformation.

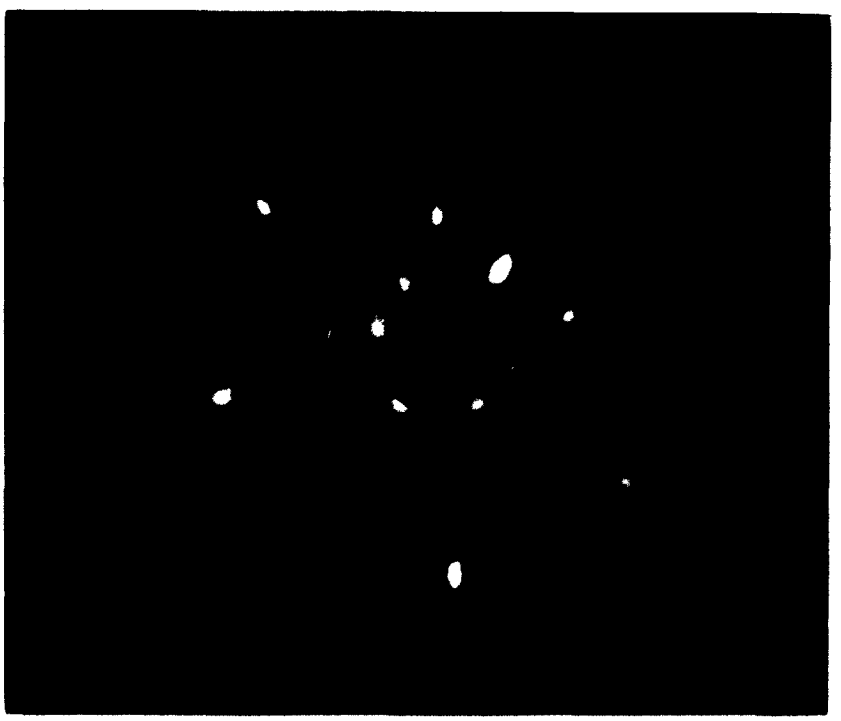

Fig. 20 - Laue photogram of crystal Be-141, of same orientation and equivalent deformation as above but strained at 25°C.

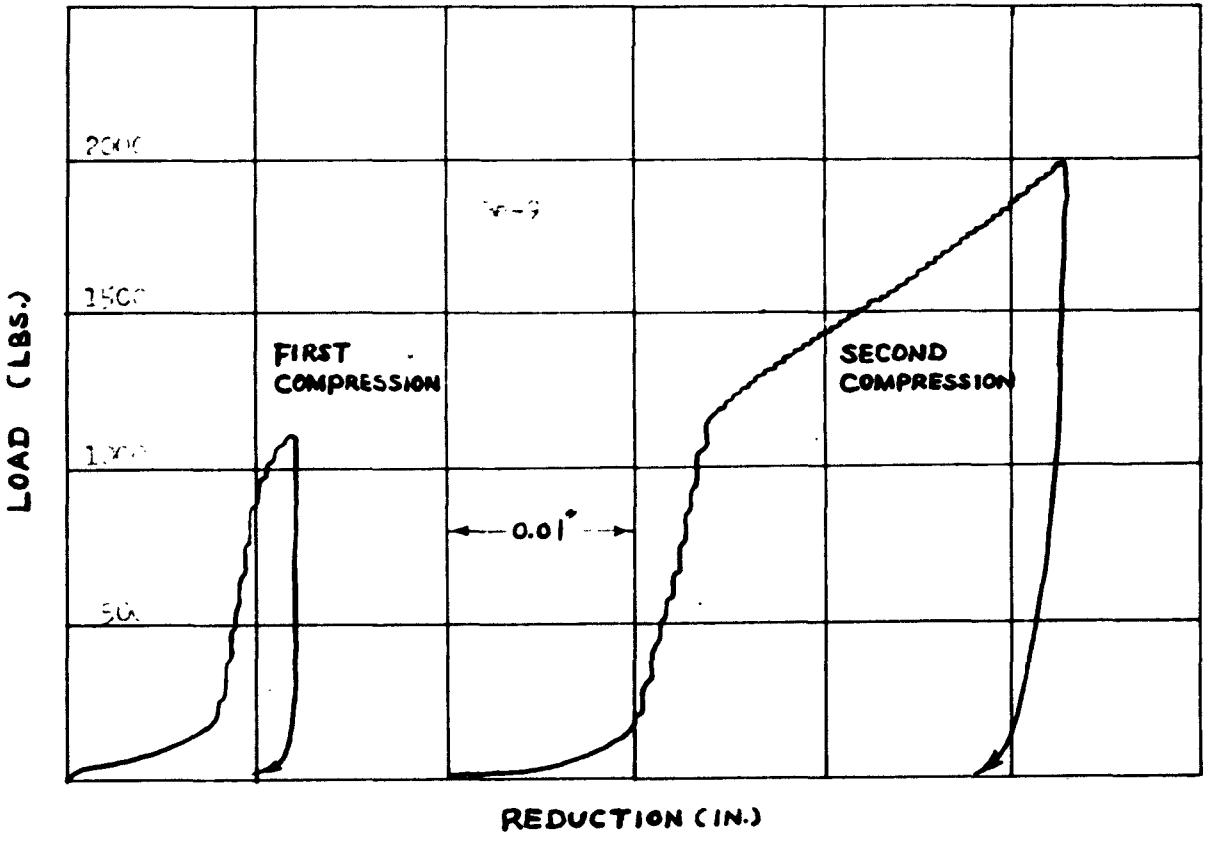

Fig. 12 - Autographic load - reduction curves, Be-9, with (.001) at [illegible] from [illegible] axis; [illegible] at [illegible].

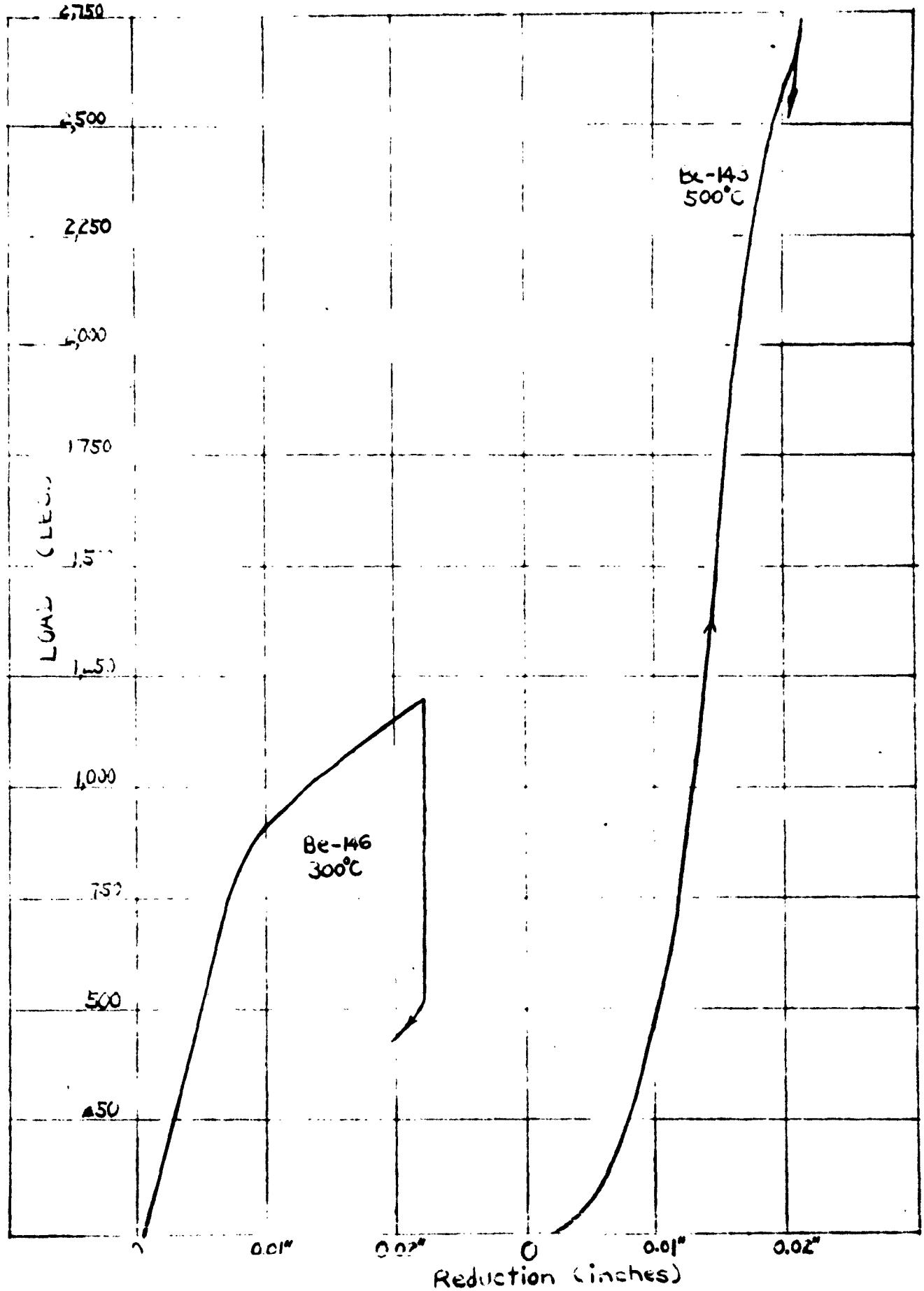

Fig. 22 Load - reduction curves for crystals with stress axis at 47° (Be-146) and 44° (Be-143) from (0001); deformed at 300°C and 500°C respectively.

It is quite probable that in the present case of Be the presence of oxide film might also account partly for the increase of critical resolved shear stress at 500°C. However, it is believed that the rather drastic difference in slip behavior as shown in the last section would constitute a more important factor in contributing to such increase. In view of these two factors, it is doubtful that the values given in Table 3 for 500°C could be regarded as the "true" critical resolved shear stress for Be, although the three specimens tested at this temperature appeared to be in a seemingly comparable state at the moment when the bend-point occurred.

Rotation of Slip Plane

Owing to the restriction of the two compression surfaces, the lattice of the crystal was forced to gradually rotate in such a way that the slip plane would approach parallel to the compression surface as deformation proceeds.

The familiar sine law takes either of the following forms:

$$\frac{l_1}{l_o} = \frac{\sin \lambda_o}{\sin \lambda_1}$$

$$\frac{l_1}{l_o} = \frac{\sin \chi_o}{\sin \chi_1}$$

X-ray patterns of Be-9 before and after a 12.7% reduction gave experimental λ_1 and χ_1 as 50° and 49° respectively. By using the above equations, the corresponding calculated values were 49°21' and 48°2'. The agreement indicates that the geometrical dimensions of the specimens in the present studies were satisfactory.

Analyses of the asterism of the specimens after basal slip also established $\langle 10\bar{1}0 \rangle$ as the rotational axis. This is the direction in the slip plane and perpendicular to the slip direction as had been observed by many workers on other close packed hexagonal metals.

Overall vs. Local Shear Strain

Both the autographic curves and micrometer measurements give only an overall reduction of thickness, which in turn yielded an average value of resolved shear strain along the slip plane.

The relationship between the crystallographic glide strain, a, the initial and the final orientations, and the initial and final thicknesses of the specimen after a certain amount of reduction, is presented by the following equation, adapted from Schmid and Boas[21] to the present case of compression:

$$a = \frac{1}{\sin \chi_o} (\cos \lambda_o - \sqrt{d^2 - \sin^2 \lambda_o}) = \frac{1}{\sin \chi_o} (\cos \lambda_o - d \cos \lambda_1) \quad (1)$$

Where χ_o = angle between slip plane and compression axis before reduction.

λ_o, λ_1 = angle between slip direction and compression axis before and after reduction.

$d = \frac{l_1}{l_o}$, ratio of reduced thickness to the initial.

Applying this expression to Be-9 after a 12.7% reduction ($d = 0.873$, $\chi_o = 40.5°$, $\lambda_o = 41.5°$, $\lambda_1 = 49.5°$), the plastic shear strain was found to be 0.28.

An attempt was made to compare the local shear strains with this theoretical value. The scratches shown in Figs. 13 and 23 (see p.39) were used for this purpose. It is seen that an originally straight and continuous scratch was broken into steps after deformation. By measuring the displacements of the steps and the distance within which the displacements occurred, a value of shear strain can be calculated when other pertinent information was known.

Figure 24 is a schematic drawing to show how the calculations were arrived at. The top plane is the plane of microscopic observation, the front surface is the compression surface with respect to which the x-ray data and angular measurements of any slip lines and scratches are referred to, as in the stereogram of Figure 25. Two slip lines (S.L.) are shown on the surface of observation, together with the scratches (M). The apparent displacement d' is the measured displacement along the slip lines; the apparent spacing, s', is the perpendicular distance between the slip lines in question. d is the true displacement, i.e., the translation resolved along the slip direction (S.D.); and S is the angle between S and S' and β the angle between d and d'. It is easily seen that the crystallographic glide strain, a, may be expressed as:

$$a = \frac{d}{S} = \frac{d'}{S' \cos \alpha \cos \beta} \qquad (2)$$

For specimen Be-9 and the particular plane of observation of Figs. 13 and 23, the α and β values are 28° and 27° respectively, (Fig.25). The crystallographic glide strain, a, calculated within a long range is 0.27, which is practically the same as obtained theoretically from equation (1). However, in more confined localities, the value varies from 0.14 to 0.96. The latter value, being more than three times higher than the average, is obtained within the cluster shown in Fig. 13.

C. ORIENTATIONS with BASAL PLANE at APPROXIMATELY 25°

Four specimens, Be-149 (22°), Be-159 (23°), Be-14 (18°), and Be-148 (24°) were included in this group. The plastic behavior of these specimens may be described as intermediate between the two groups just discussed. No sharp bend point could be detected in the autographic load-reduction curves at any of the temperatures, although slip lines were observed in every case. At room temperature and 300°C the lines were straight, while at 500°C they were forking and wavy, and comparatively much more widely spaced.

Deformation of these specimens seemed to be confined to the regions near to the compression surface. In all cases, there was a macroscopic band present in the diagonally central portion of the specimen faces as shown schematically in Fig. 26.

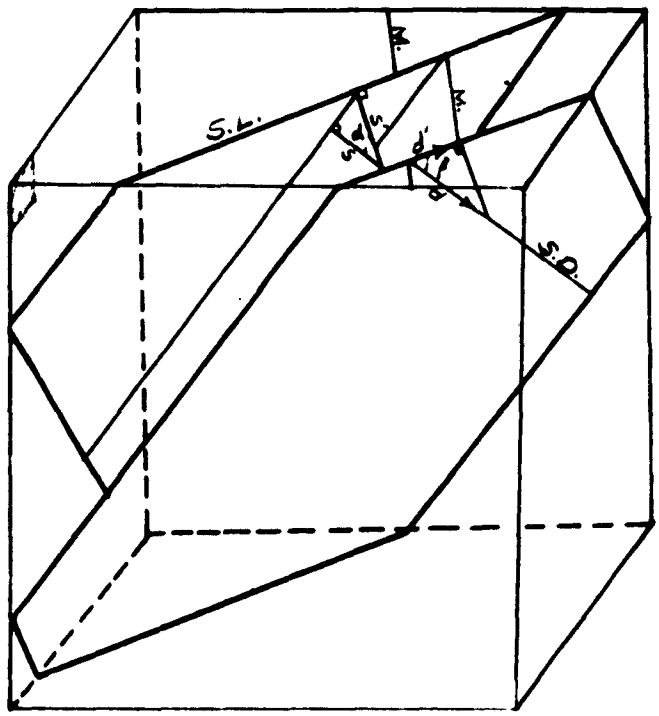

Fig. [illegible]

Schematic representation of relationship among S, S', α, β, d, and d'.

S.L. Slip Lines
S.D. Slip Direction
N Scratches

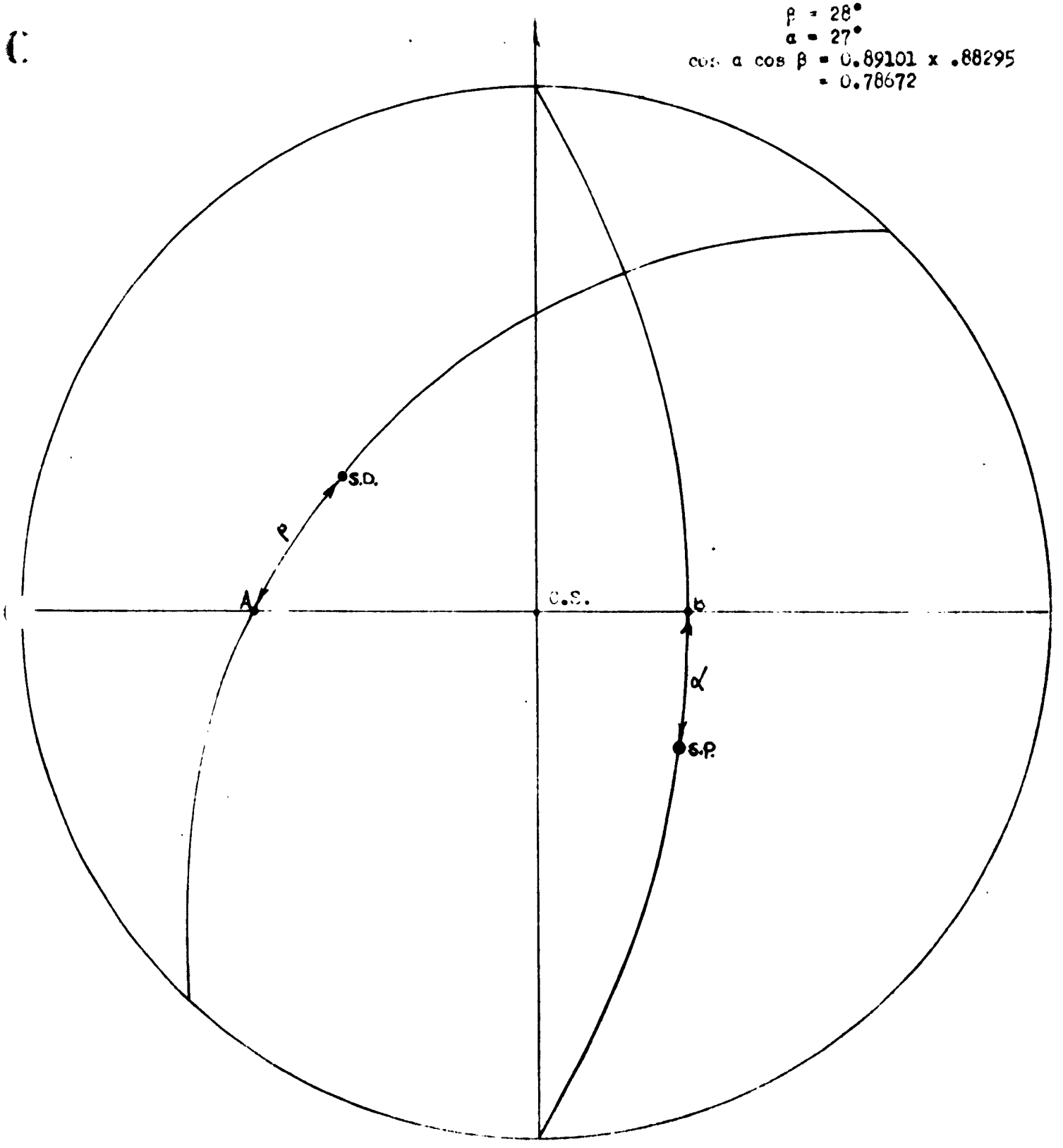

Fig. 25 - α and β of Be-9, deformed at 25°C.

A, direction of slip line
B, direction perpendicular to slip line

Formation of these bands seemed to indicate that the length of the glide direction played an important part during slip. The orientation of this group of specimens was such that a single basal plane ran closely from one specimen edge to another edge diagonally opposite to it, and the projection of the glide direction to the compression plane was approximately parallel to the other set of edges of the compression surface (Fig. 27). As a consequence, there was a gradual difference of length of slip direction from one slip plane to the next. For example, plane A B C D in Fig. 26 obviously possesses a much shorter length of slip direction than the plane A' B' C' D' does. Slip would thus likely prefer those planes near the corners first and then shift gradually inward as the previous planes strain-hardened and ceased to further operate. The cumulative effect of the gradual transfer of slip planes in operation consequently resulted in the split of the two halves of the crystal and a band at the central portion was thus produced. This cumulative effect is believed also to account for the absence of bend-points in the autographic load-reduction curves. In view of the absence of a sharp boundary and also the absence of a sudden drop of load, the bands in the present case were not considered the same as kink bands as first observed by Orowan (24).

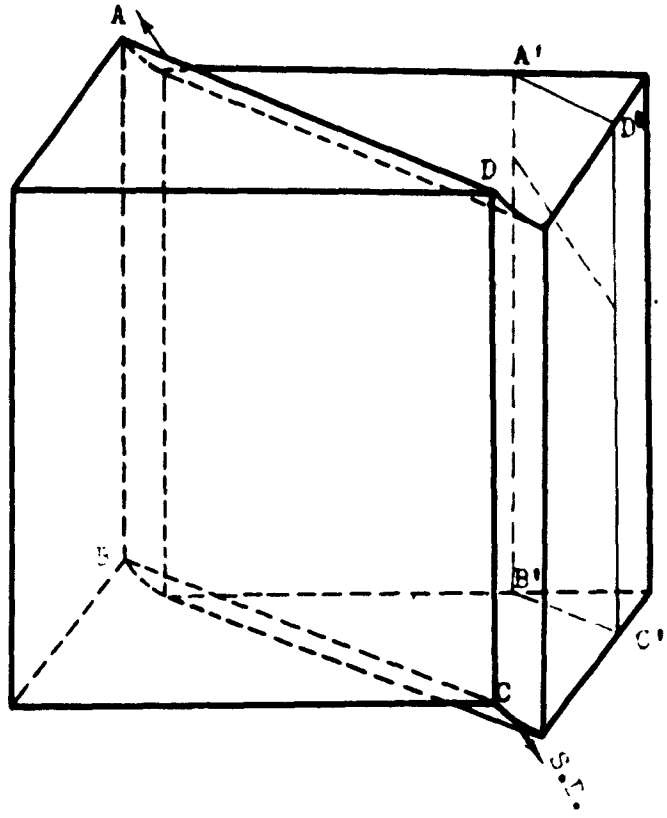

Fig. 20

Formation of the central band, Schematic.

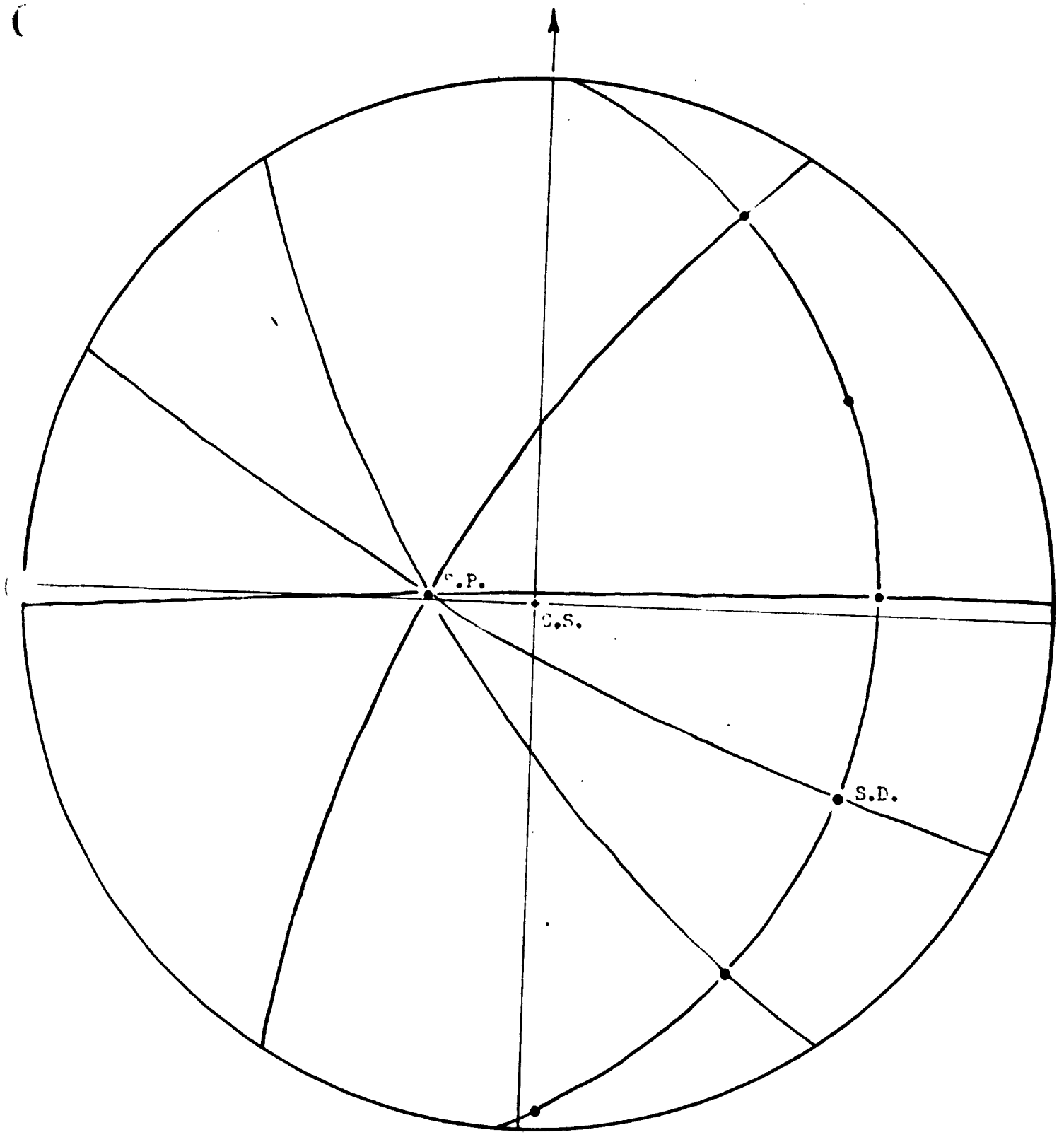

Fig. 27 - Orientation of Be-159, deformed at 25°C.

Wrinkles or folds were also present in this group of specimens, running parallel to the compression surface. This introduced rather high tensile stress on the specimen faces. Minute surface twins were, therefore, frequently observed on top of these folds. Wherever folds were absent, the twins were also not found. It will be observed in later sections that without the presence of folds and the tensile stress thus introduced, specimens of this orientation should not have formed twins under compression.

D. ORIENTATIONS with BASAL PLANE CLOSELY PARALLEL to the COMPRESSION AXIS

The study of this orientation included six specimens whose θ values ranged from 82° to 88°. Deformation of these specimens was predominantly by twinning. Two sets of branching and wavy slip lines were also abundant at all temperatures, particularly at 500°C. They were identified as $\{10\bar{1}0\}$ prismatic slip. Basal slip lines were also present near the compression surface. However, they were generally short and their number was very limited.

The $\{10\bar{1}0\}$ slip lines were in most cases so wavy as to make it difficult to get any consistent angular measurements (Fig. 28, and Figs. 44 and 45 (p.59). Nevertheless, their general direction invariably came close to a $\{10\bar{1}0\}$ plane when plotted stereographically. In some areas of specimens Be-6 and Be-151, the lines were fairly straight (Figs. 29 and 30) and measurements of angles from more than one face established their crystallographic habit with certainty. Quite frequently the $\{10\bar{1}0\}$ slip lines passed through the twins with a slight bend (Fig. 31). This was so because the basal plane of the twins determined by the orientation relationship of twinning, was not more than 8° from the corresponding $\{10\bar{1}0\}$ planes of the matrix.

Twins were very abundant in this group of specimens. They appeared as minute diamond shaped islands, lenses, thin lamellae, or heavy bands running across the entire crystal, (Figs. 31 and 32). Angular measurements have been made in every case, and no twinning plane other than $\{10\bar{1}2\}$ was ever observed.

Load-reduction curves of these specimens bore no sharp bend-point at room temperature and 300°C. No distinct twinning clicks were heard. However, at 500°C the curves showed abrupt drops (Fig. 33) and the twinning clicks were so loud as to be easily mistaken as fracturing. It is believed that the decrease of surface energy at this temperature permitted the twins to penetrate through the specimen surface with comparatively greater easiness. Whereas at room temperature and 300°C, the twins might frequently be restricted within the body of the specimen, and distortion of the lattice was gradually built up at the ends of the twins. This would prevent an effective relaxation of load. While the number of twins at 500°C did not show any increase -- in fact, it appeared to be even less for the same reduction ---- the twins themselves always appeared as continuous heavy bands at this temperature. Owing to the large offset associated with them, these twins could be readily seen without resorting to the use of polarized light.

Fig. 23 - Displacement of scratches by basal slip in crystal Be-9, deformed at 25°C (2000X).

Fig. 28 - Twins formed in crystal Be-6, compressed parallel to (0001) plane at 25°C; also $(10\bar{1}0)$ slip lines (100X).

Fig. 29 - Another view of $(10\bar{1}0)$ slip lines in crystal Be-6, plus mechanical twins (100X).

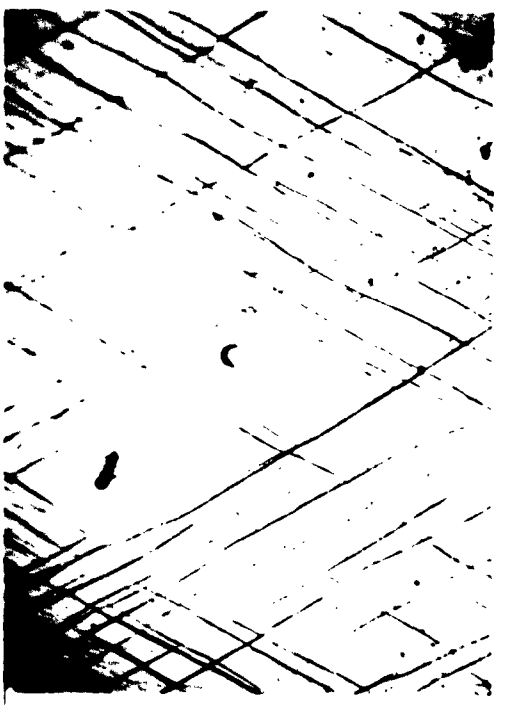

Fig. 30 - $(10\bar{1}0)$ slip lines in crystal Be-151, compressed parallel to (0001) plane at 300°C (200X).

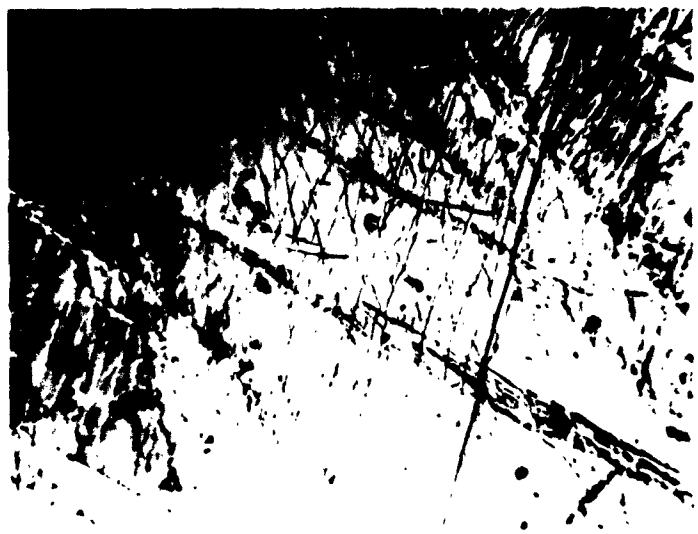

Fig. 31 - $(10\bar{1}0)$ slip lines bending as they pass through $(10\bar{1}2)$ twins; crystal Be-6 deformed at 25°C (100X).

Fig. 32 - Another zone of Be-6 showing only $(10\bar{1}2)$ twins (100X).

Aside from the microscopic measurements of the angular relationship of the twin bands, X-ray method was also used to identify the crystallographic behavior of the twins. Fig. 34 shows the orientation of Be-3. By assuming $\{10\bar{1}2\}$ as the twinning planes and $\langle\bar{1}011\rangle$ the twinning direction, the six new positions of (0001) poles after twinning could be located stereographically as indicated. The X-ray beam was then directed in such a way that it was approximately perpendicular to one of the new (0001) planes, i.e., $(0001)_I$. The Laue pattern thus obtained (Fig. 35) disclosed a distinct 6-fold symmetry, indicating the assumption was valid.

The Laue X-ray pattern taken from Be-3 after a 10.9% reduction showed extreme distortion of the lattice. Asterism has brought the original separated spots into a continuous hyperbola. Spots from the matrix were therefore no longer discernible. Only broken concentric rings were present, resembling a situation of highly preferred orientation. By using characteristic radiation, the pattern of Fig. 36 was obtained where $Cu_K\alpha_1$ and $Cu_K\alpha_2$ lines can be seen separately. The two rings were identified as $(10\bar{1}4)$ and (0004) reflections, the outer one being the latter. New orientations resulted from the four active twinning planes, $(10\bar{1}2)_I$ to $(10\bar{1}2)_{IV}$, were then worked out stereographically, as shown in Figs. 37 to 40, where new $\{10\bar{1}4\}$ and (0001) positions are indicated. By superimposing Fig. 36 onto these orientations, it was found the broken rings originated from the twins (Fig. 41). It should be noted that although the (0001) spot of Fig. 36 coincided perfectly with the $(0001)_{III}$ pole, the $\{10\bar{1}4\}$ spots did not have such good agreement. In view of the extreme distortion of the lattice, this discrepancy of 6° may be considered tolerable.

Slip within the Twins

No particular attempt has been made to investigate the fine structure within the twin bands. In general the exposed surface of the twins were so distorted as to obscure any fine structures present within them. However, in some instances, basal slip lines were observed within the twins.

It was thought that the resolved shear stress factor $\cos\theta' \cos\lambda'$ for the basal plane of a twin orientation as compared to that for the parent material might be a deciding factor to govern whether basal slip should occur within the twins. Examination of three specimens offered no confirmation to such effect. Table 4 shows the results. It is seen for Be-101, even when the ratio $[\cos\theta' \cos\lambda'/\cos\theta \cos\lambda]$ was less than unity, basal slip was still observed within the twins.

Table 4

Comparison of resolved shear stress factor of selected twins vs. matrix

Specimen number	parent orientation $\cos\theta \cos\lambda$	twin orientation $\cos\theta' \cos\lambda'$	$\frac{\cos\theta' \cos\lambda'}{\cos\theta \cos\lambda}$
Be-6 (25°C)	0.120	0.424	3.53
Be-10 (300°C)	0.397	0.317	0.80
Be-117 (300°C)	0.290	0.422	1.46

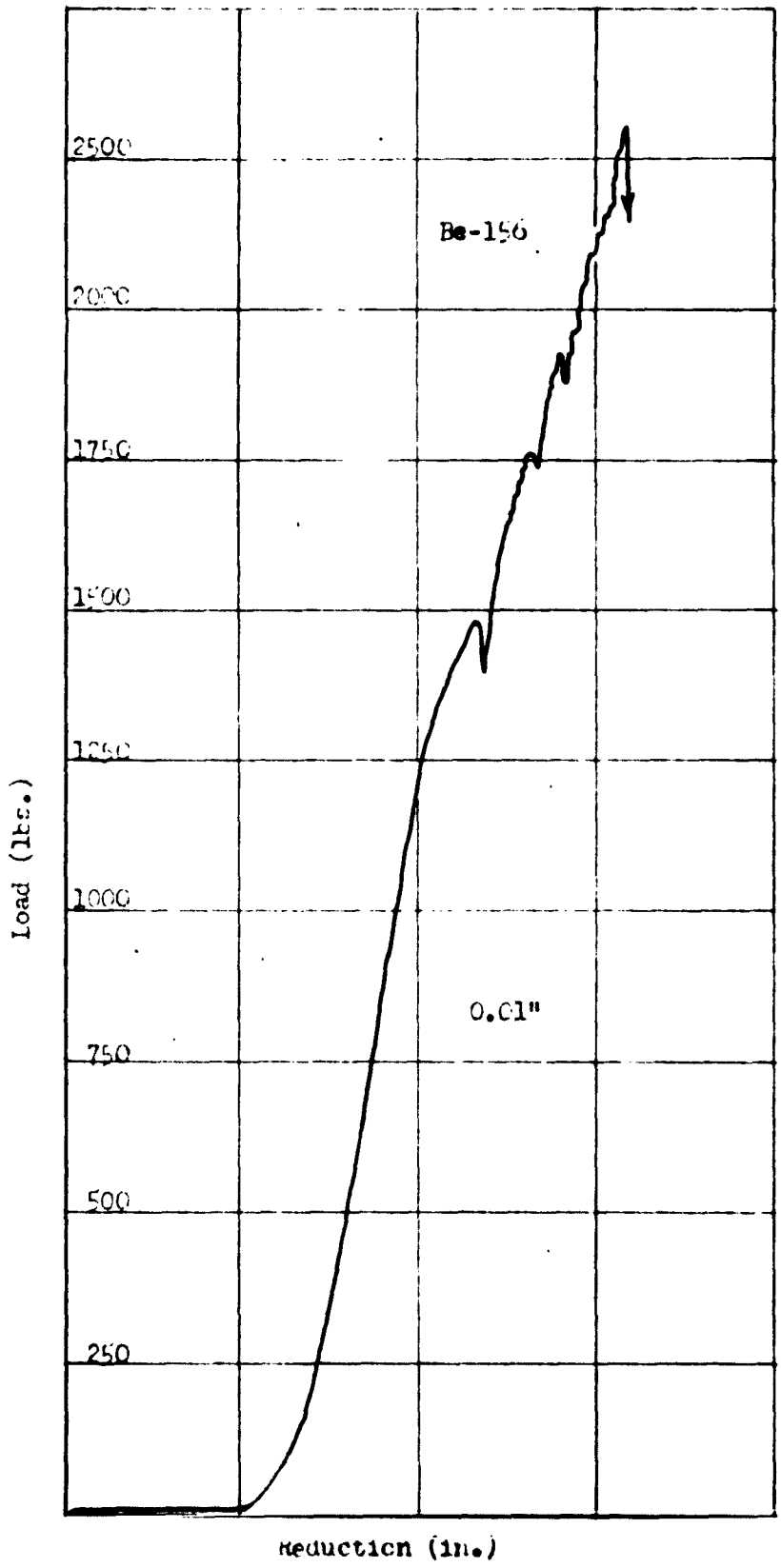

Fig. 33 - Load - deformation graph for crystal Be-156, compressive stress axis 4° from (0001) pole; deformed at 500°C.

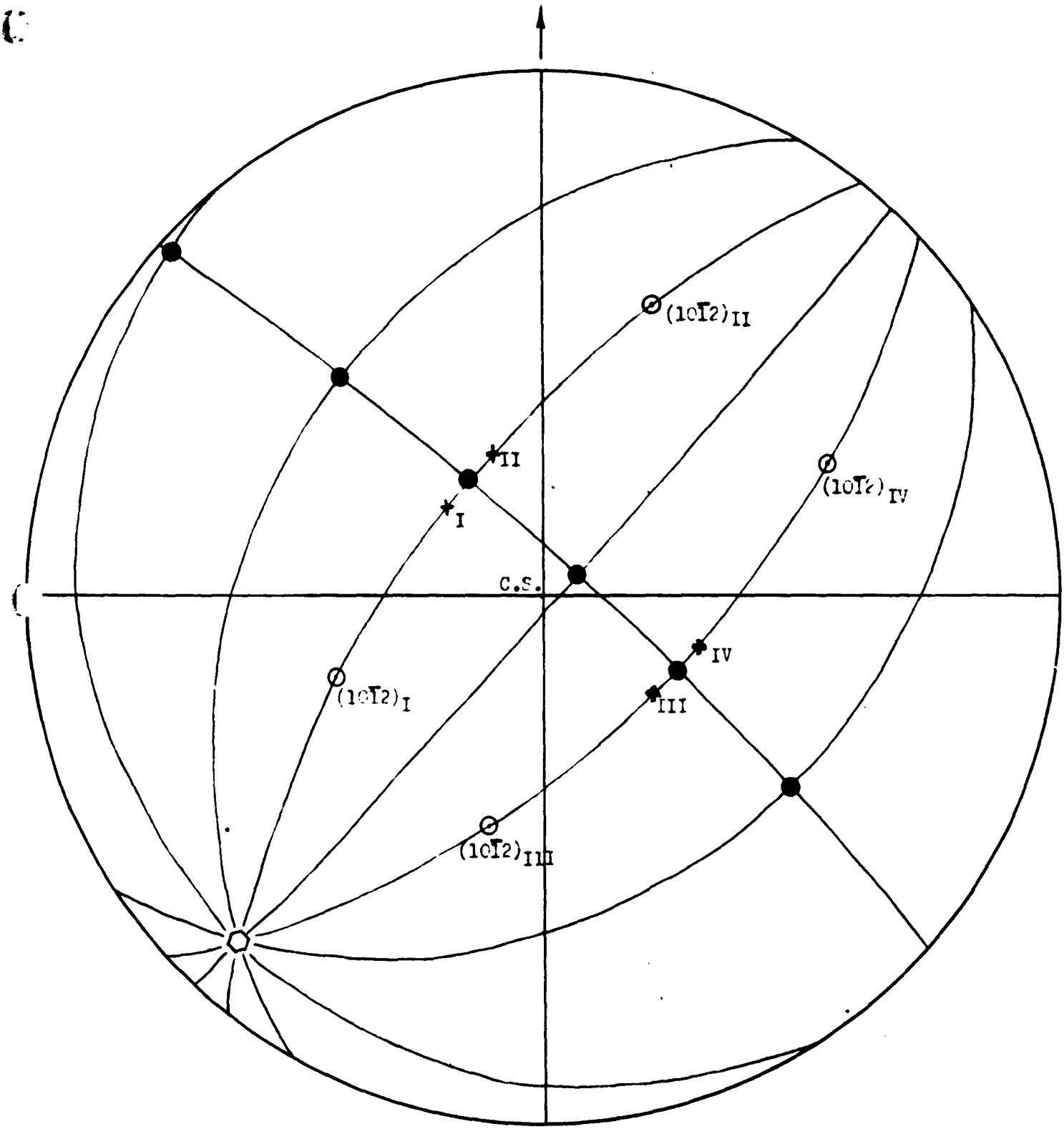

Fig. 34 - Orientations of Be-3, deformed at 25°C.

○ ...(0001) initial; ⊙ $\{10\bar{1}2\}$ initial; ● $\{10\bar{1}0\}$ & $\{11\bar{2}0\}$

+ ...(0001), twinned; C.S., Compression Surface

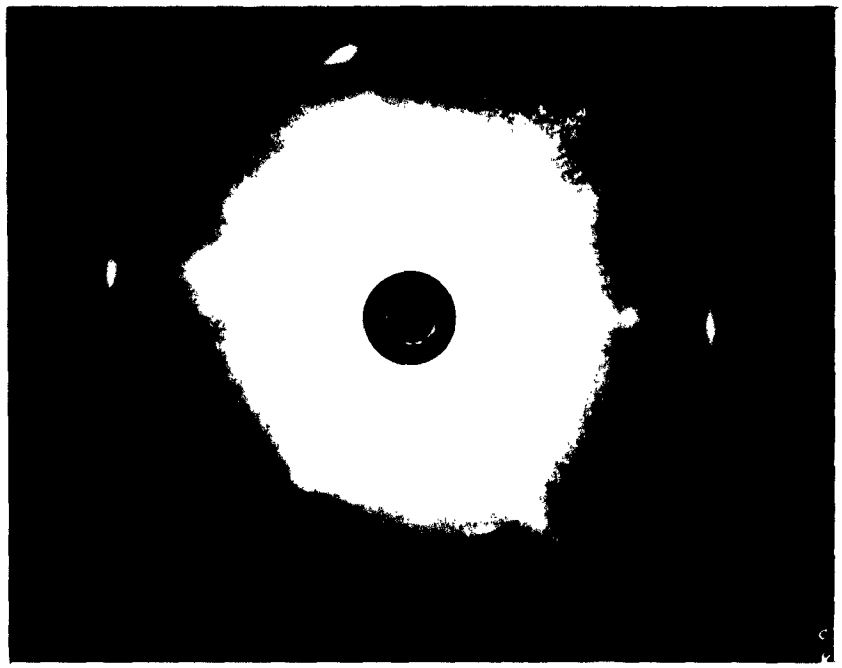

Fig. 35 - Laue photogram of Be-3 after 11% deformation at 25° with abundant twinning. Beam directed perpendicular to the (0001) plane of one set of twins.

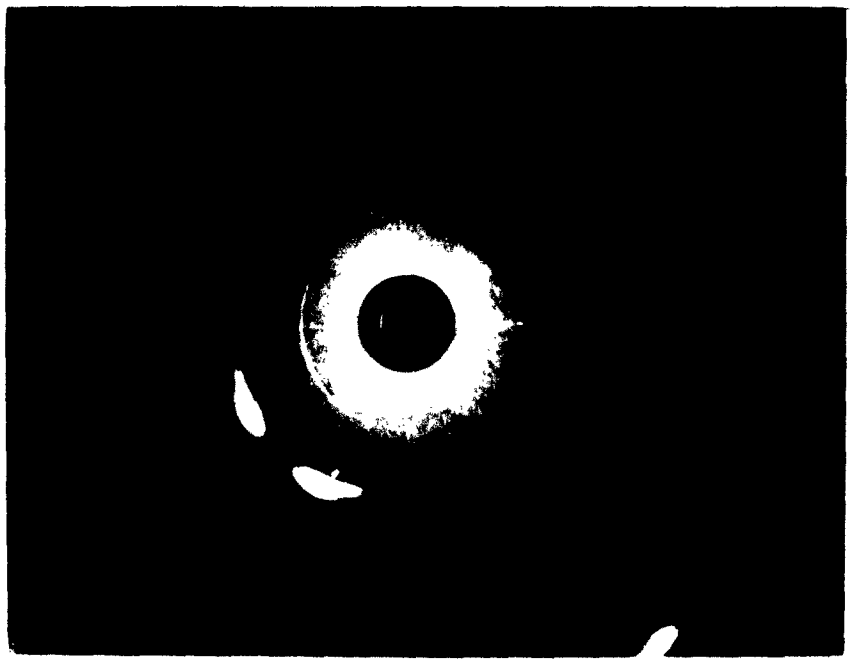

Fig. 36 - Back reflection photogram of Be-3 using Cu K_α radiation. Highly preferred orientation; inner arcs are $(10\bar{1}4)$ and arcs near edge are (0004).

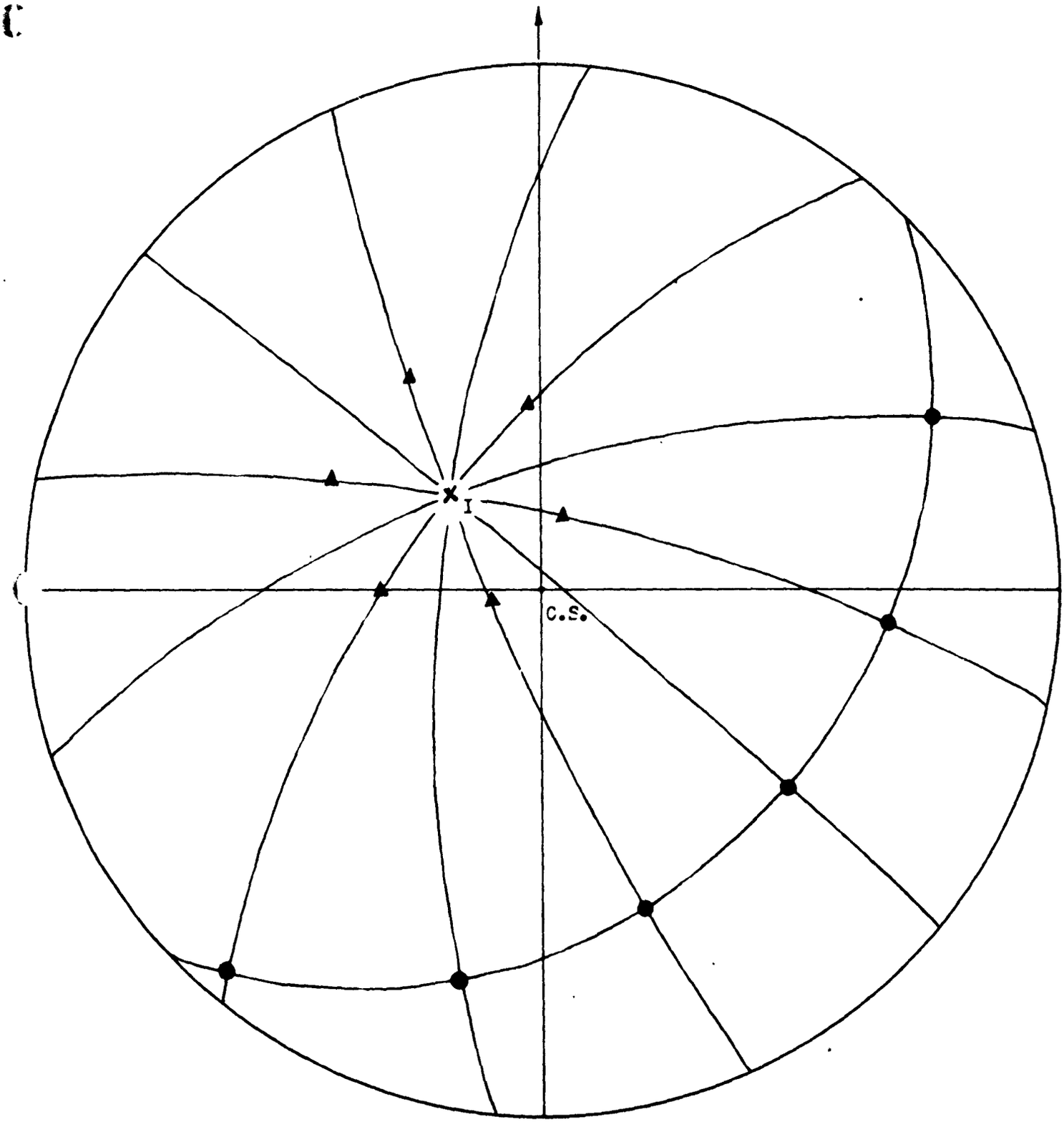

Fig. 37 - New orientation as resulted from $(10\bar{1}2)_I$ twinning.

+ (0001); ▲ $\{10\bar{1}1\}$; ● $\{10\bar{1}0\}$ and $\{11\bar{2}0\}$

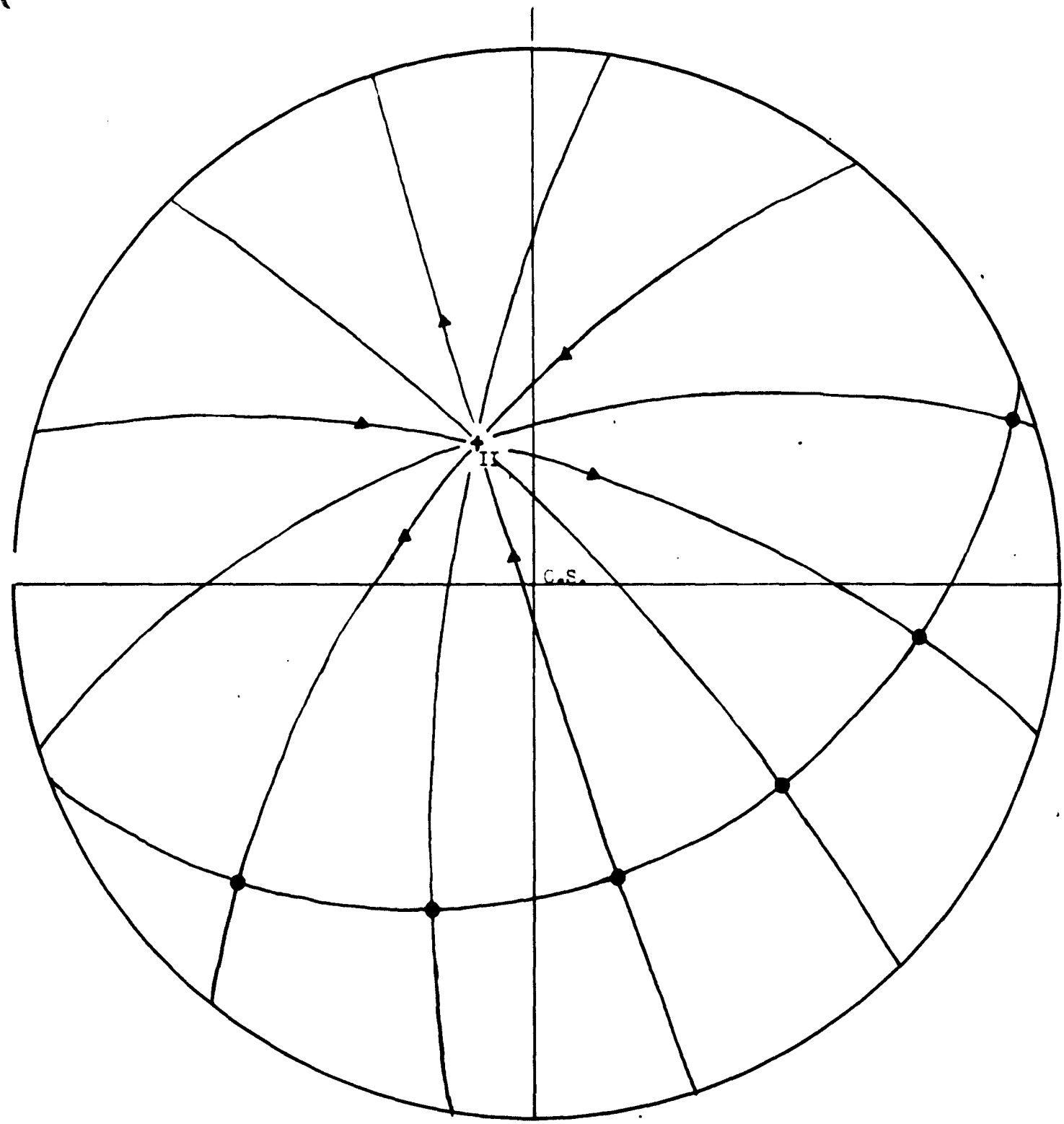

Fig. 38 - New orientation as resulted from $(10\bar{1}2)_{II}$ twinning.

+ (0001); ▲ $\{10\bar{1}4\}$; ● $\{10\bar{1}0\}$ and $\{11\bar{2}0\}$

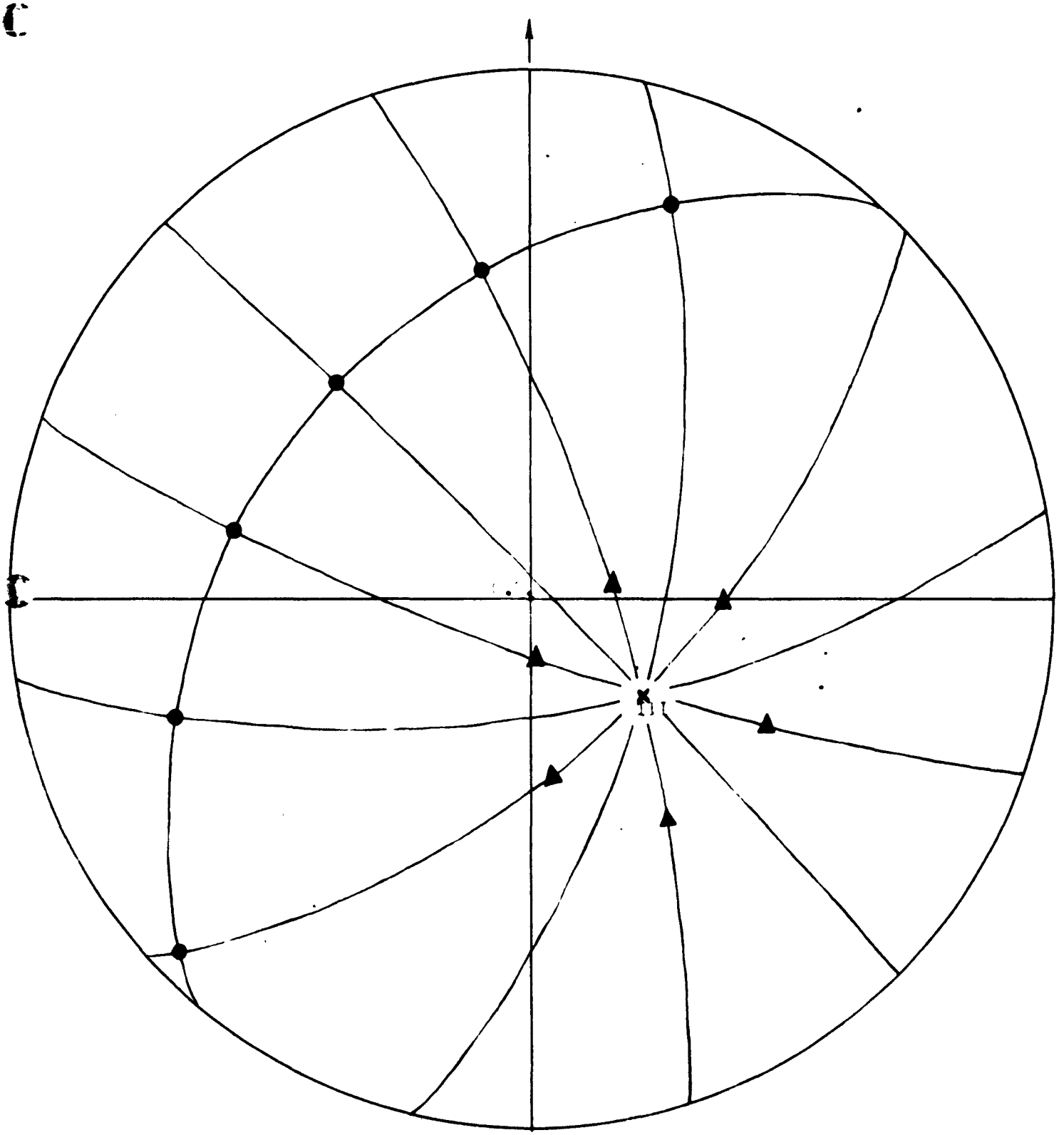

Fig. 3 - New orientation as result of $(10\bar{1}2)$ III twinning.

✚ (0001); ▲$\{10\bar{1}0\}$; ●$\{10\bar{1}0\}$ and $\{11\bar{2}0\}$

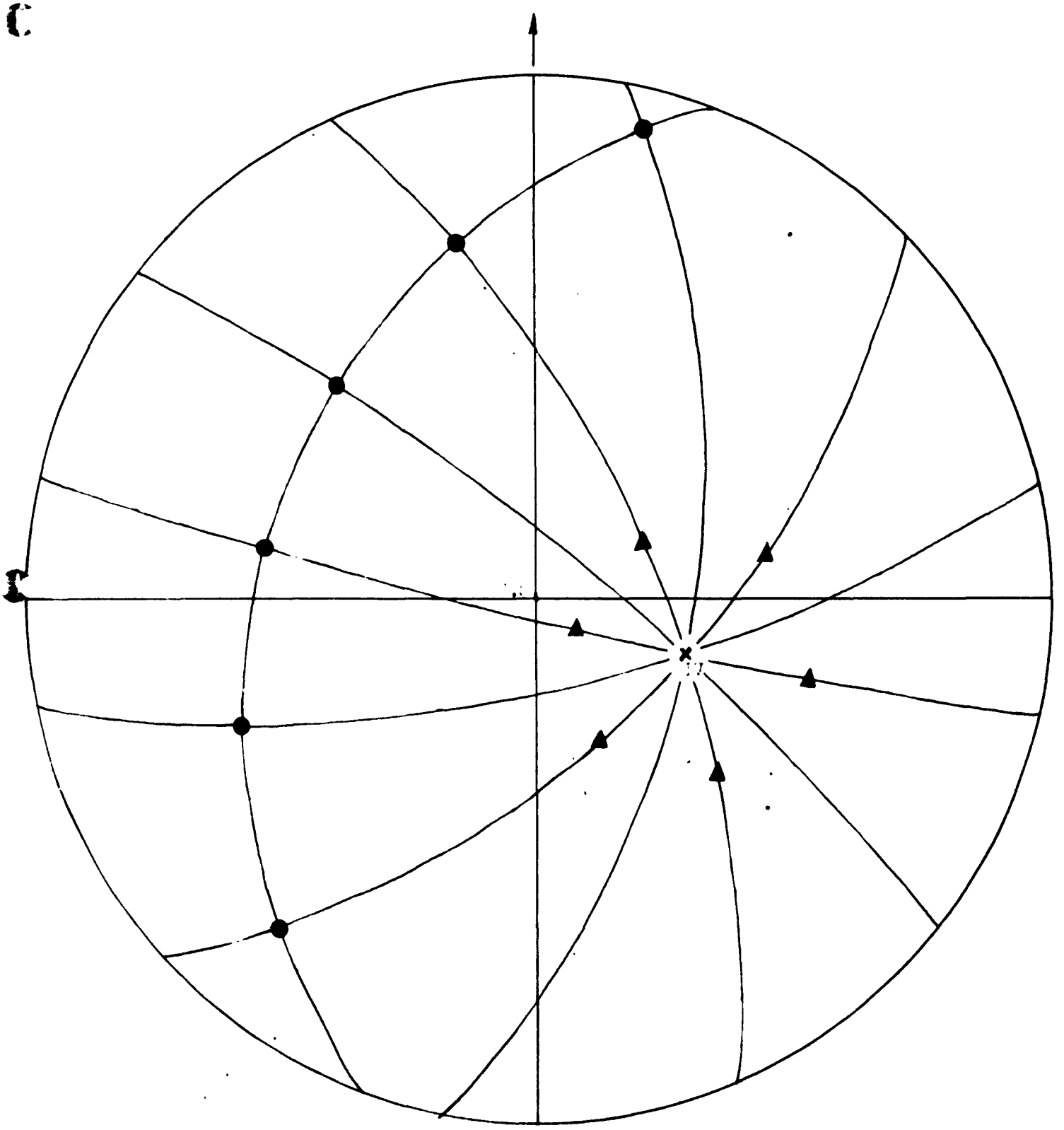

Fig. 10 - Net orientation as resulted from $(10\bar{1}2)_{TV}$ twinning.

+ (0001); ▲ $\{10\bar{1}3\}$; ● $\{10\bar{1}0\}$ and $\{11\bar{2}0\}$

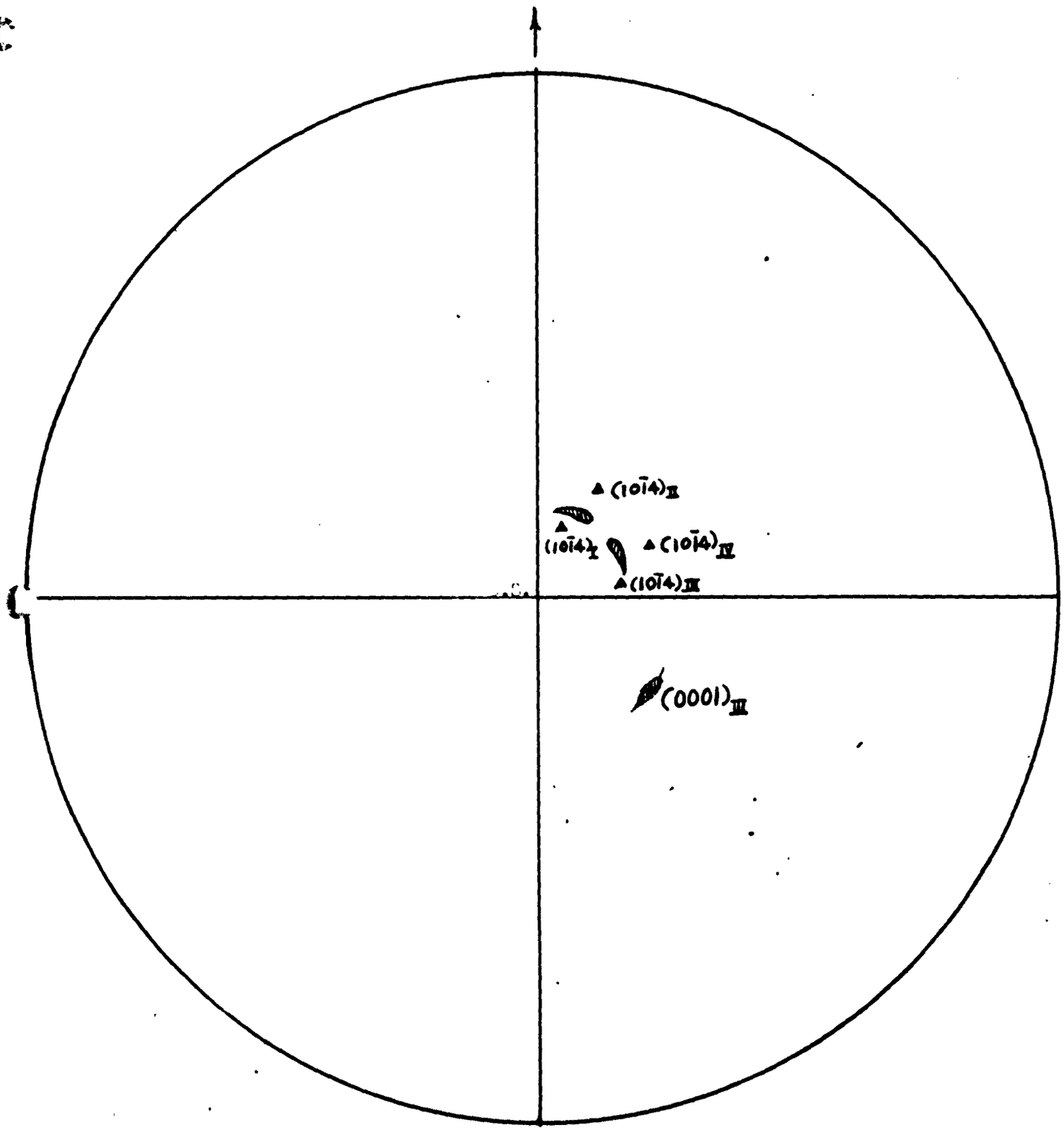

Fig. 41 - Broken concentric rings as a result of twinning.

Here, $\{10\bar{1}0\}$ slip in the parent material might be an important factor complicating the problem. Since the $\{10\bar{1}0\}$ plane of the matrix only differs several degrees from the basal plane of the twin, it is to be expected that the basal slip within the twins might easily be initiated by the active prismatic glide of the parent lattice. In both cases, the same slip direction $\langle 11\bar{2}0\rangle$ is shared.

It must be noted that not all the twins with a ratio of $\cos\theta' \cdot \cos\lambda'/\cos\theta \cos\lambda$ larger than 1 would automatically have basal slip. In general, slip lines could not be observed even in cases where this ratio was 3 or larger.

Selection of Twinning Planes

Compression tests of specimens where twinning had been the significant deformation process also furnished some interesting observations relative to the selection of twinning planes. The basic problem is to determine which of the various twinning planes should be operative and what is the factor governing this selection.

Answers to this question have been provided by a number of workers. Gough (25) in 1933 observed that twinning in zinc crystals took place on the two pairs of planes that did not contain the direction of slip. Andrade and Hutchings (26) in 1935 stated, for the twinning of Hg, "The operative planes are those for which the intersection with the glide plane makes an angle as 90° as is geometrically possible with the glide direction." Bakarian and Mathewson (27) modified this statement to Mg as follows: "The operative pair of planes is the pair for which the intersections with the slip plane makes an angle as nearly as 90° as is geometrically possible with the projection of the compression axis in the same plane."

These statements describe a geometrical factor which governs the selection of twinning planes. And, it is required, by following any of the three rules, that the twinning planes should always operate in pairs. Results of the present investigation found all the rules satisfactory.

However, it seems a more fundamental approach may be followed by simply extending the LeChatelier's principle to this particular problem of twinning. Depending upon the orientation of the crystal in relation to the axis of loading, twinning on some of the $\{10\bar{1}2\}$ planes will lead to an extension of the specimen, while the others will lead to a reduction of specimen length. Diagram in Fig. 42 shows this relationship as adapted from Schmid (21) to the present case of Be. Location of the stress axis in one or another of the triangles A, B, C or D, determines which of the six $\{10\bar{1}2\}$ planes may lead to extension or contraction as noted in the caption. By following LeChatelier's principle, it is natural that in the case of compression, those planes which could lead to the reduction of specimen thickness should be the active ones and those which lead to an extension should not.

Quantitatively, when the orientation of the crystal is known, the amount of reduction of thickness of the specimen as any one of the six $\{10\bar{1}2\}$ planes functions can be calculated by the aid of the following equation (21):

$$\frac{l_o}{l_1} = \sqrt{1 + 2S \sin\chi^* \cos\lambda^* + S^2 \sin\chi^*}$$

Where, l_o, l_1 being the initial and final thicknesses;

χ^*: the angle between compression axis and the twinning plane;

λ^*: the angle between compression axis and the twinning direction.

and s, the twinning shear.

By comparing the calculated values of percent reduction for all six $\{10\bar{1}2\}$ planes, it is possible to find which of them offers the most effective contraction. Consequently the particular planes most likely to be active could be predicted.

This rule has been put to test for all the Be specimens with profuse twinning, and found to be satisfactory in every case. Space does not allow the inclusion of all the data. The result from Be-7 may serve to illustrate the observations.

The orientation of Be-7 (Fig. 43) was such that all six $\{10\bar{1}2\}$ planes would lead to contraction. However, the amount of reduction was different for different planes as shown in Table 5.

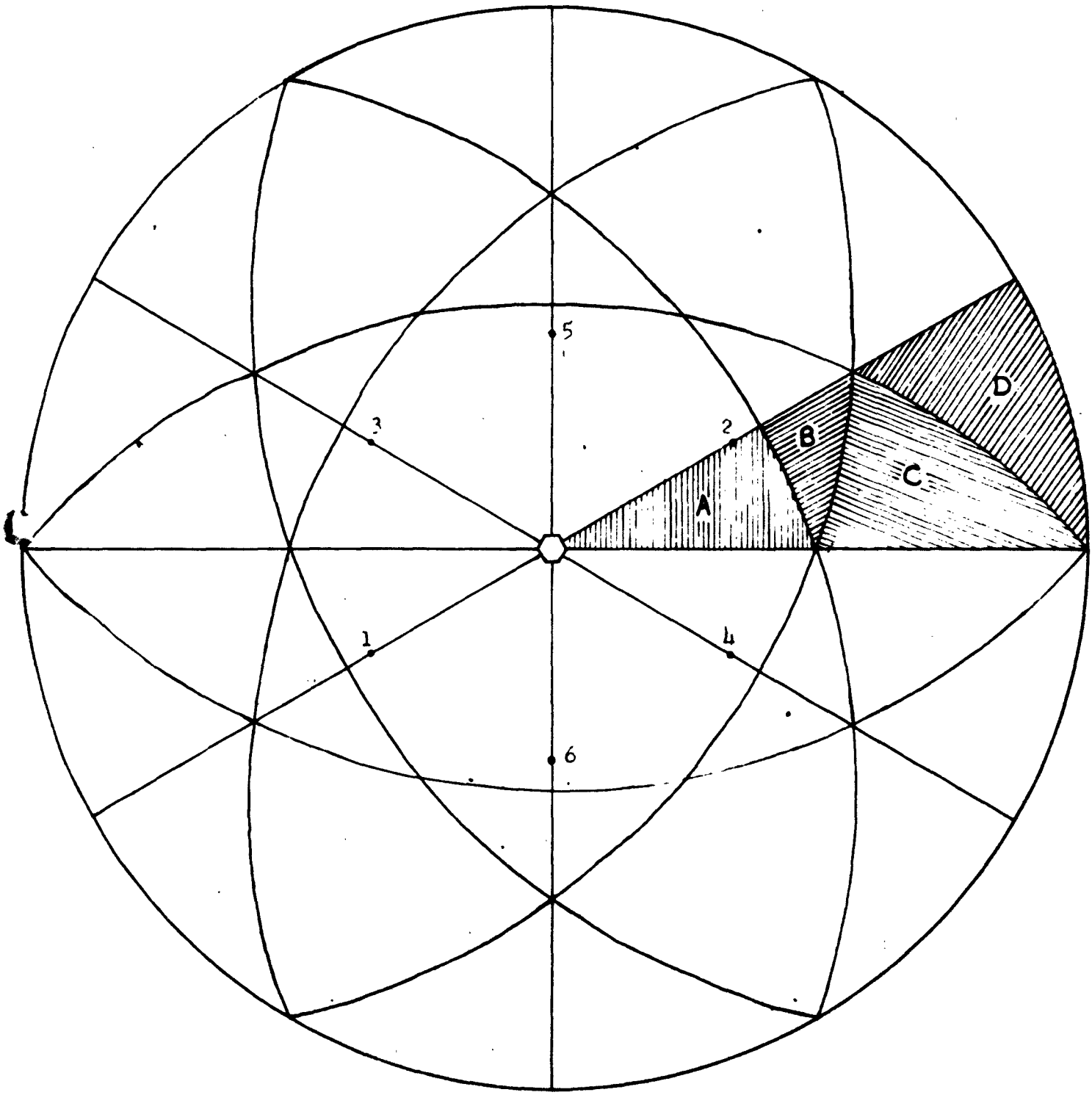

Fig. 42 - Position of compression axis governing extension or contraction of crystal.

A - 1,2,3,4,5,6, Ext. B - 3,4,5,6, Ext.; 1,2, Cont.
C - 5,6, Ext.; 1,2,3,4, Cont. D - 1,2,3,4,5,6, Cont.

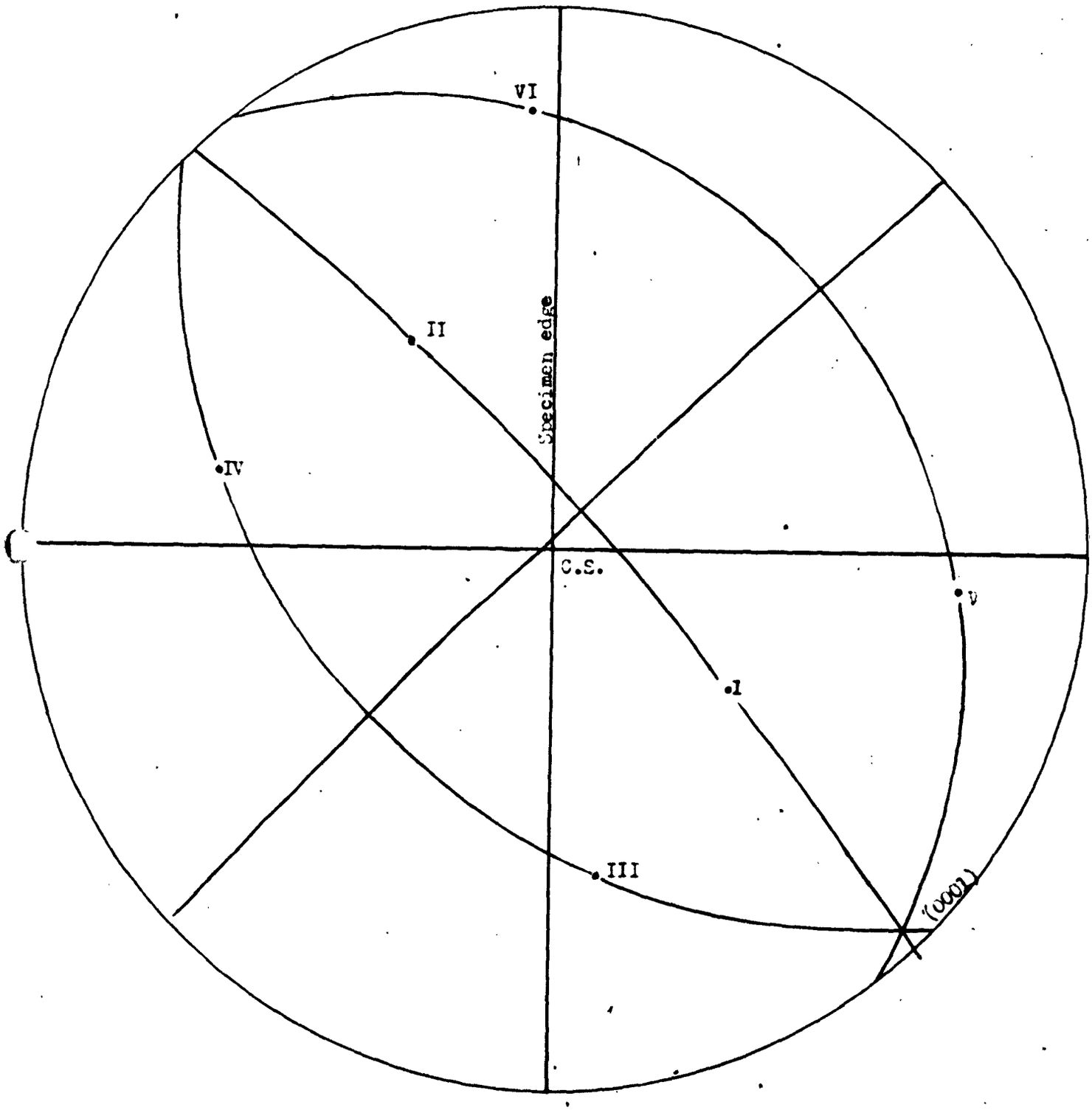

Fig. 43 - Orientation of Be-7, deformed at 25°C.

I, II, III, IV, V, VI $\{10\bar{1}2\}$ poles

Table 5

Reduction of Thickness From Twinning on Each of the $(10\bar{1}2)$ planes, Be-7

$\{10\bar{1}2\}$	χ*	λ*	l_1/l_o	% Reduction	$\cos\theta'\cos\lambda'$	$\frac{\cos\theta'\cos\lambda'}{\cos\theta\cos\lambda}$
I	44°	46°	0.916	8.4	0.173	5.28
II	40°	41°	0.916	8.4	0.187	5.70
III	27°	63°	0.962	3.8	0.493	15.00
IV	24°	61°	0.965	3.5	0.482	14.70
V	15°	76°	0.987	1.3	0.321	9.80
VI	12°	74°	0.987	1.3	0.321	9.80

(S = 0.186 for Be)

Planes I and II offered the greatest reduction, 8.4%; as compared to 3.8%, 3.5% and 1.3% for the others. As a result, twinning should be expected to operate on these two planes in preference to the rest. Subsequent microscopic and stereographic analysis verified this expectation. At a reduction of 1.04%, twins were found only along these two planes. It is interesting to note, as the last two columns of Table 5 indicate, that the ratio $\cos\theta'\cos\lambda'/\cos\theta\cos\lambda$ was by no means a deciding factor in the selection of twinning planes. Planes III and IV, though having a ratio as high as 15 in comparison with 5-6 of I and II, did not operate. In other words, the selection of twinning planes was not governed by the relative effectiveness for subsequent basal slip within the twins.

A quantitative study to determine how the amount of reduction introduced by each twinning plane would affect the thickness and degree of abundance of the twins has been inconclusive. There seemed no such dependence. Also, inconclusive results seemed to indicate there was no shift to new sets of twinning planes upon further deformation.

E. ORIENTATIONS with θ AROUND 65°

This group consisted eight specimens with θ values ranging between 65° and 72°. Their plastic behavior was similar to the group of specimens with basal plane about perpendicular to the compression surface; as just described. The differences were, (1) for this group of specimens, basal slip was more prevalent, (2) $\{10\bar{1}2\}$ twinning less pronounced, as compared to the preceeding group.

The presence of all the features in more or less equal prevalence made the appearance of the deformed surface very complex. Deformation was by no means homogeneous and no sharp bend points occurred with the load-reduction curves. The $\{10\bar{1}0\}$ slip lines in these specimens remained wavy, especially near the specimen or twin surfaces, Fig. 44. They were complicated frequently by the formation of tear lines associated with the emergence of twins, Fig. 45. Basal slip was no longer confined merely to the regions near the compression surface.

Two interesting observations may be here pointed out. Fig. 46a shows a group of twins at the right halve of the pictures. It is seen they appeared as a series of clustered lines outlining the lenticular form of twins. The appearance seems to indicate the discontinuous nature of formation of mechanical twins in Be. Fig. 46b shows an-

interesting kink band where the sharp boundary is clearly seen. Basal slip lines were made broken and symmetrically oriented across the boundary. A difference in density of slip lines is also apparent on the two sides, the less dense halve being the one adjacent to the compression surface. The specimen of this micrograph, Be-152, had a large thickness. Friction of the compression surface and the tendency for bending were increased. The kink band formed under this favorable circumstance.

F. CLEAVAGE and BRITTLENESS of BERYLLIUM

In all the groups of specimens considered above, cracks occasionally appeared. They were generally short in length and numbered not more than four or five in an entire specimen. Examination of the direction of the cracks disclosed they were either along the basal plane or $\{11\bar{2}0\}$ planes.

Beryllium cleaves very readily, especially along the basal plane. In the course of preparing specimens for compression it was all too often that a corner suddenly chipped during grinding, or cracks occurred across the edges. Figure 47a and Figure 47b show such a case. The chips separated from the main body are shown in Figure 47c. X-ray patterns obtained from these pieces confirmed the fracture as basal and $\{11\bar{2}0\}$. Close examination of the two fractures revealed that the basal cleavage was always flat while the $\{11\bar{2}0\}$ cleavages were curved. Figure 47d is a schematic drawing of Figure 47c intended to illustrate this difference more clearly. This phenomenon might be related with the characteristic of crystal imperfectness of beryllium of which much remains to be investigated.

Fig. 44 - (10$\bar{1}$0) slip lines in crystal Be-156, deformed at 500°C (150X).

Fig. 45 - (10$\bar{1}$0) slip lines in crystal Be-152, deformed at 300°C (100X).

Fig. 46a - Twin clusters in crystal Be-155, deformed at 25°C (150X).

Fig. 46b - Kink band, basal slip lines (fine, straight) and (10$\bar{1}$0) slip lines in crystal Be-152, deformed at 300°C (150X).

The area surrounding a crack in another specimen is shown in Fig. 48. A Laue pattern obtained by directing the x-ray beam upon the crack showed the separation of spots and the line of separation followed the hyperbola of one of the $\langle 11\bar{2}0 \rangle$ zones, Figs. 49 and 50. It may also be pointed out that, as shown in Fig. 48, the cracks seemed to follow closely the twin boundaries as did the edges produced by chipping. This appears to be an indication that the $\{11\bar{2}0\}$ cleavages might be initiated by the presence of the weakness of twin surfaces. It should be noted that the twinning direction in $(10\bar{1}2)$, i.e. $[\bar{1}011]$, is also shared by $(1\bar{2}10)$, and the two planes, $(10\bar{1}2)$ and $(1\bar{2}10)$, are perpendicular to each other. Thus a twin along $(10\bar{1}2)$ would transmit its maximum strain on the plane $(1\bar{2}10)$, creating localities of high stress concentration.

Figs. 51 and 52 show a series of fractographs after lumps of beryllium were broken by hammering. Features observed here are twins, secondary cleavages, fissures, striae, fan-like markings, dendritic structures, and inclusions, similar to those observed by Zapffe (28) with many other crystals. No attempt was made to carry out any crystallographic analysis of these fractographs.

The brittleness of beryllium has long been an interesting subject. Sloman (1) attributed it to the presence of oxide films. Gold (15) observed fine particles in the slip bands of beryllium when examining a cleaved surface of a single crystal. The nature of the particles was not identified but they were conceived to be the BeO phase as -

proposed by Sloman. The present investigation offers no affirmation or disproof of this concept. However, examinations of the compressed specimens and also the specimens such as Be-NT2 (Figure #8a) and Be-NT4 (Figure #7a) appeared to afford some at least additional causes for the brittle behavior of beryllium. The availability of many cleavage planes, the aid to fracture offered by twinning, the inclusions, as well as the crystal imperfection--whatever their origin might be--seem all acting in concerted moves to contribute to the brittleness of beryllium.

SUMMARY of RESULTS of EXPERIMENTAL WORK

1. Beryllium single crystals with a square cross section were studied under compression. The results indicate that slip on the basal plane and $\{10\bar{1}0\}$ planes in the original material, twinning on the $\{10\bar{1}2\}$ planes, slip on the basal plane of twinned regions, and cleavages along (0001) and $\{11\bar{2}0\}$ planes were the only mechanisms operating at room temperature, 300°C, and 500°C. The relative prevalence of these several mechanisms has been classified into five groups of orientation.

2. Secondary deformation features such as deformation bands, kink bands were also observed when the strain was inhomogeneous. A peculiar type of band resulted from the change of length of slip direction from plane to plane was found in some specimens with particular orientations.

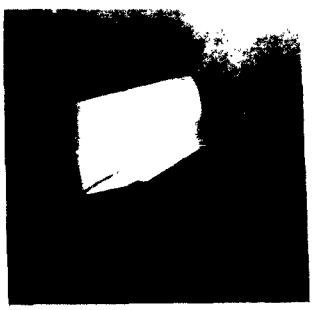

(a)

Be-NT4, actual size

(b)

Be-NT4 fragments, actual size

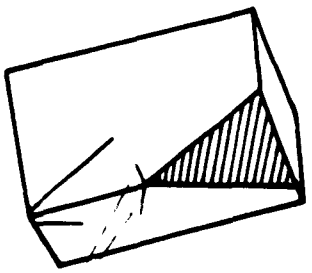

(c)

$(11\bar{2}0)$ cleavage and
(0001) cleavage (shaded)

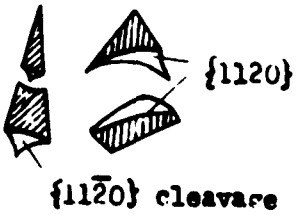

(d)

$(11\bar{2}0)$ cleavage,
(0001) shaded

Fig. 47 - Beryllium crystal Be-NT4

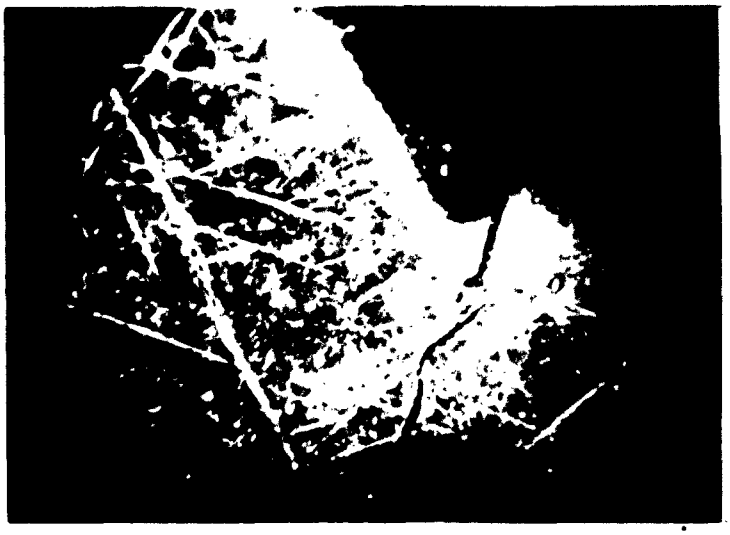

Fig. 48 - Macrograph of crystal Be-NT2, deformed until a crack formed. Note crack changing path to follow a twin boundary (10X).

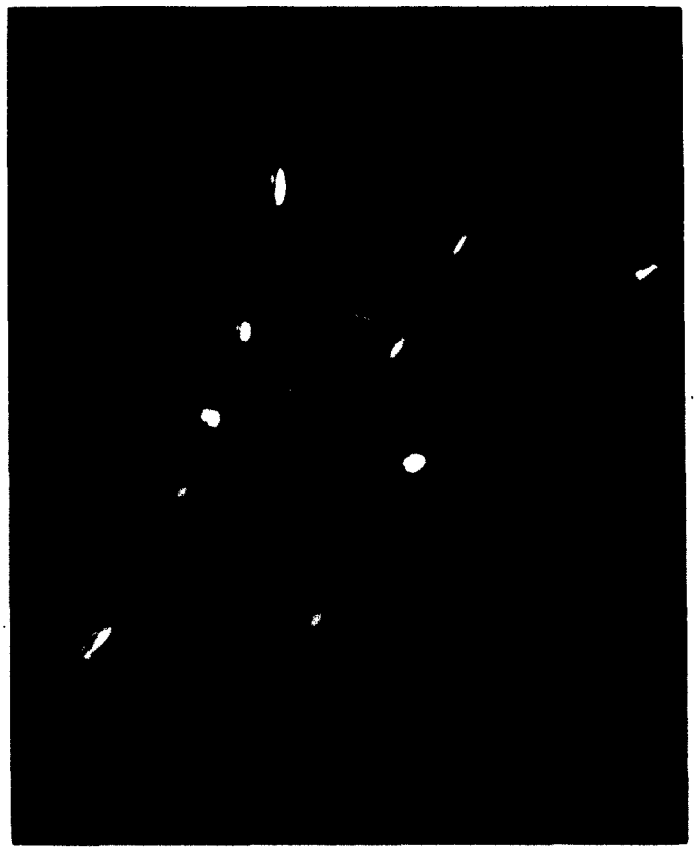

Fig. 49 - Laue taken with beam directed at crack of specimen above. Crack caused separation of spots and the line of separation of spots follows a [1120] zone.

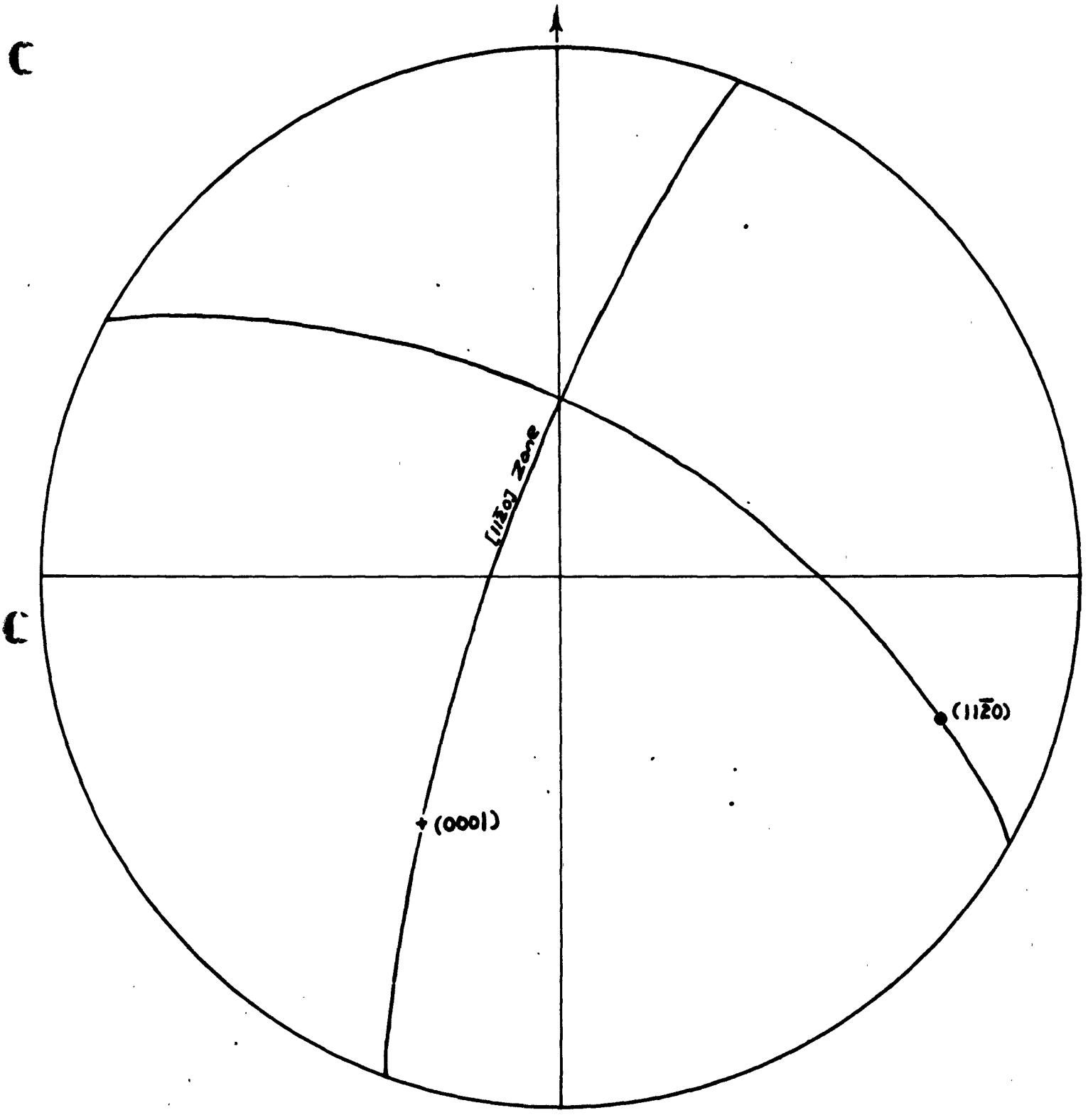

Figure 50 Orientation of Be-NT2

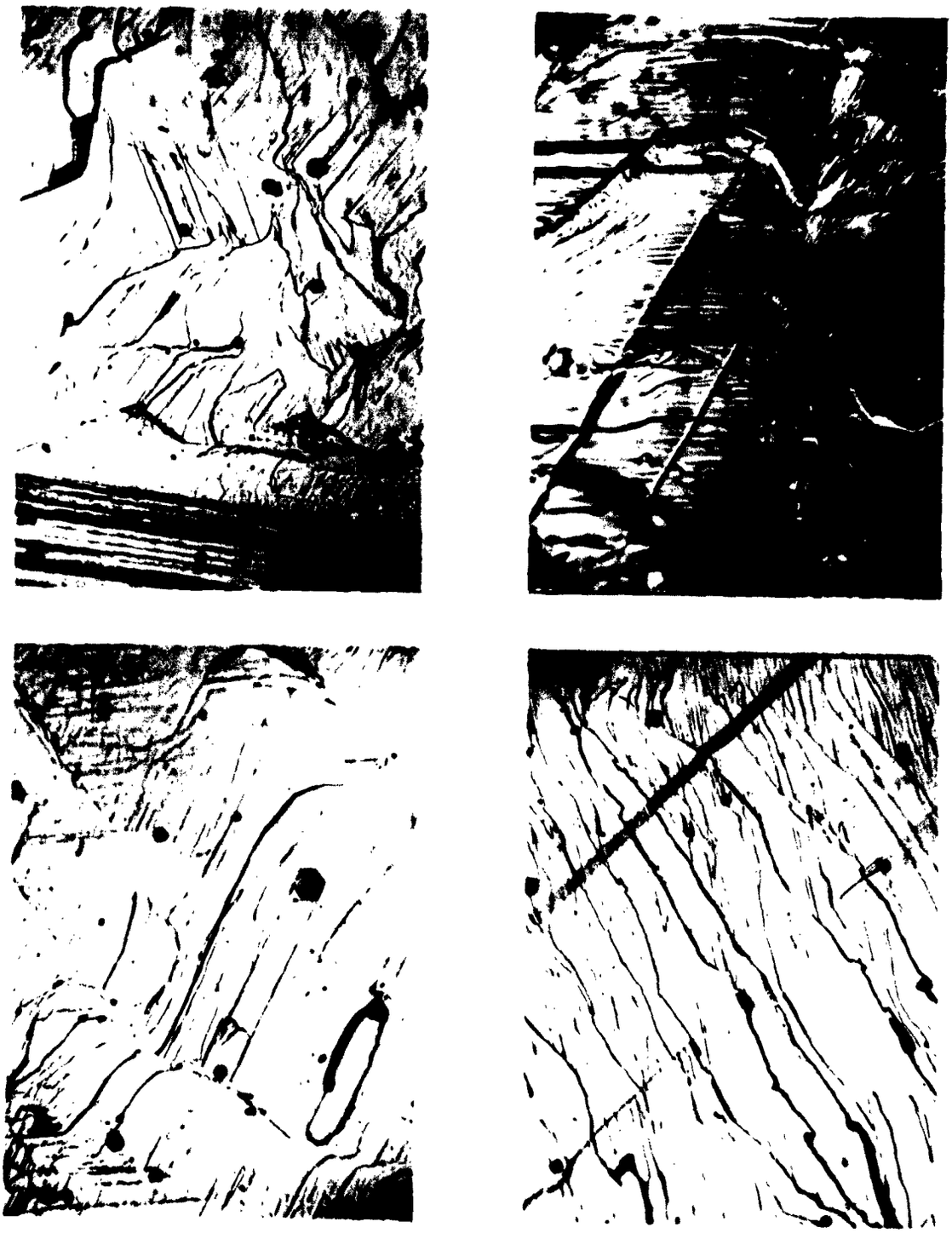

Fig. 51 - Fractographs of beryllium crystals, (100X).

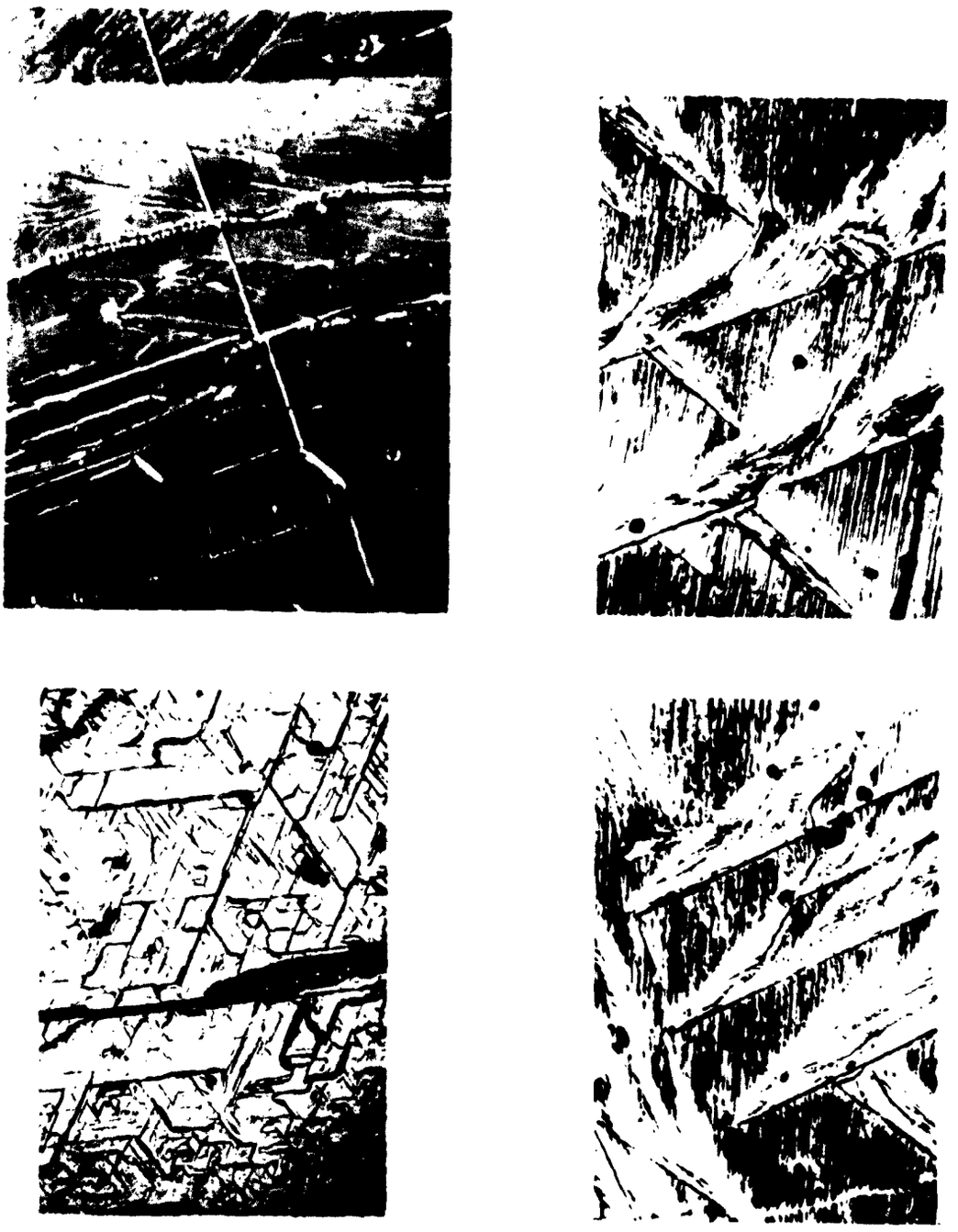

Fig. 52 - Fractographs of beryllium crystals (100X).

3. The critical resolved shear stress for basal slip of Be has been determined at 25° C, 300°C, and 500°C.

4. Basal slip lines generally were found to be straight at room temperature and 300°C. $\{10\bar{1}0\}$ slip lines always appeared wavy and forking at all temperatures.

5. By measuring the displacement of scratches, local shear strains have been calculated and compared to the average.

6. Stored elastic energy prior to fracture for several specimens which suffered little deformatior before breakage has been calculated. The value was found not comparable to the heat of sublimation.

7. As an application of LeChatelier's principle, a selection rule governing the selection of $\{10\bar{1}2\}$ planes for twinning has been given. The rule was found workable at least for beryllium crystals under compression.

PART II ANALYSIS of ATOMIC MOVEMENTS in MECHANICAL TWINNING of METALS and EVOLUTION of FACTORS AFFECTING TWINNING

The past twenty years have seen rapid progresses in the field of plastic flow. The outstanding achievement is undoubtedly the formulation and development of the theory of dislocations. While efforts have been centered around the theoretical aspects of plastic deformation to gain the insight of the fundamental mechanism of this process, the simple approaches of earlier days from crystallography have been somewhat neglected. The experimental study of compression of Be single crystals as described in part I has led to the belief that more understanding of the mechanism of deformation of single crystals solely from a crystallographic standpoint is still in need, especially in the case of twinning. The following pages thus constitute an attempt to make a few analyses of a purely crystallographic nature regarding some of the problems of slip and twinning. Particular attention will be paid to a crystallographic analysis of the mechanism of twinning of HCP metals.

A. TWINNING of HCP METALS

Twinning is generally described as a process of homogeneous shear, where all atoms involved translate in a common plane and a common direction. The displacement of a particular layer of atoms is proportional to its distance from the twinning plane. However, this simple picture is believed only exactly applicable to the cubic structures. As pointed out by Mathewson in 1928 (29), for hcp metals only one fourth of the atoms--

follow the restrictions of a homogeneous shear whereas the rest move irregularly.

1948 Barrett (30) deduced the movements of the atoms during twinning in HCP metals. Four possibilities were suggested. It was pointed out that the postulated atomic movements differed markedly from the ones in cubic structures. Barrett also suggested that the difference "seemed to account for the fact that hexagonal metals form obvious deformation twins while FCC metals do not."

In general, previous works have led to the conclusion that the mechanism of twinning of HCP metals is drastically different from that of cubic structures. However, since twinning is a fundamental mechanism of plastic deformation, it is not too unreasonable for one to think that this fundamental mechanism should not change greatly with the crystal lattices. Furthermore, twinning systems of HCP metals have often been described by the use of two undistorted planes (21). This picture of two undistorted planes is derived from the assumption of homogeneous shear. With this picture it is possible to calculate the amount of shear and the change of thickness of specimen as related to twinning. Work by Bakarian and Mathewson (27) on magnesium showed clearly that the calculations by the aid of Schmid's formulas derived from the assumption of homogeneous shear agreed very well with experimental results. Part I of the present investigation has also offered such agreement in the case of beryllium.

These thoughts lead to the suggestion that the twinning mechanism of HCP metals may very well be similar to a homogeneous shear even if it is not exactly so. If this is true, it may be said that the twinning mechanism of HCP metals is not too different from that of cubic metals.

For most HCP metals, twinning occurs on the $\{10\bar{1}2\}$ planes. Fig. 53 shows a unit cell of HCP structure; the $(10\bar{1}2)$ plane is shown as marked. In order to show correctly the atomic movements with respect to the twinning plane, the arrangement of the atoms in a plane which is perpendicular to the twinning plane and contains the twinning direction (shearing direction) has to be examined. This plane is $(1\bar{2}10)$. Fig. 54 shows such a plane, the open and solid circles represent two different layers of atoms, a/2 apart. The $(10\bar{1}2)$ plane is here shown perpendicular to the paper. The intersection of $(10\bar{1}2)$ and $(1\bar{2}10)$ is $[\bar{1}011]$ which is the twinning direction.

Fig. 55 is a repetition of the unit cells as projected on the $(1\bar{2}10)$ plane. Open and solid circles represent two layers of atoms in the matrix. Open and solid ellipses represent atoms of the corresponding layers in the twin.

During the process of twinning, atoms represented by open circles move to the sites of open ellipses, and solid circles move to solid ellipses. It will be noted, in doing so, the atoms in two original $\{10\bar{1}0\}$ planes of $\sqrt{3}a/6$ apart merge into a single plane of (0001) of the twin. The angle between the basal plane of the matrix and that of the twin is 2θ, where θ is the angle between (0001) and the twinning plane $(10\bar{1}2)$.

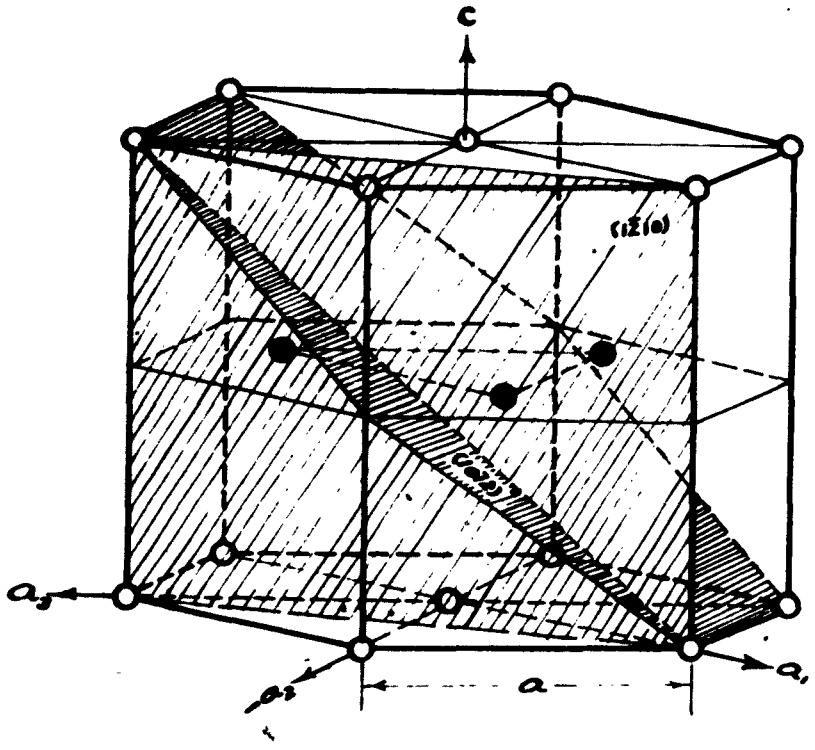

Figure 53 A HCP Unit Cell

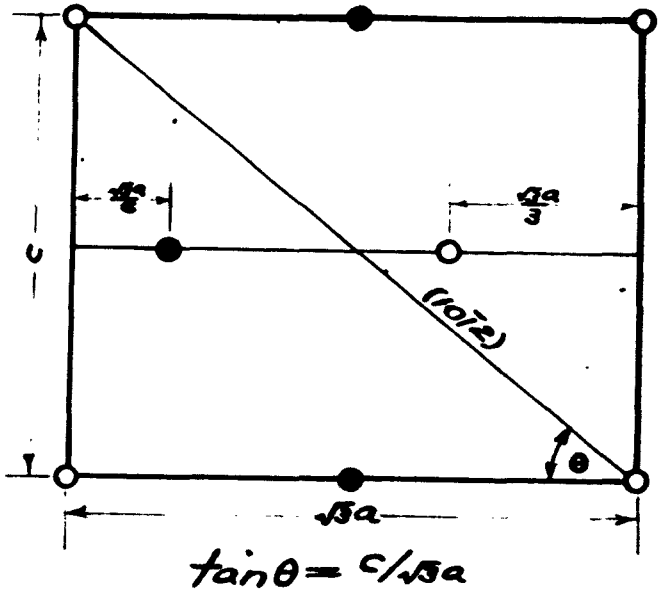

Figure 54

Projection of the Unit Cell on $(1\bar{2}10)$

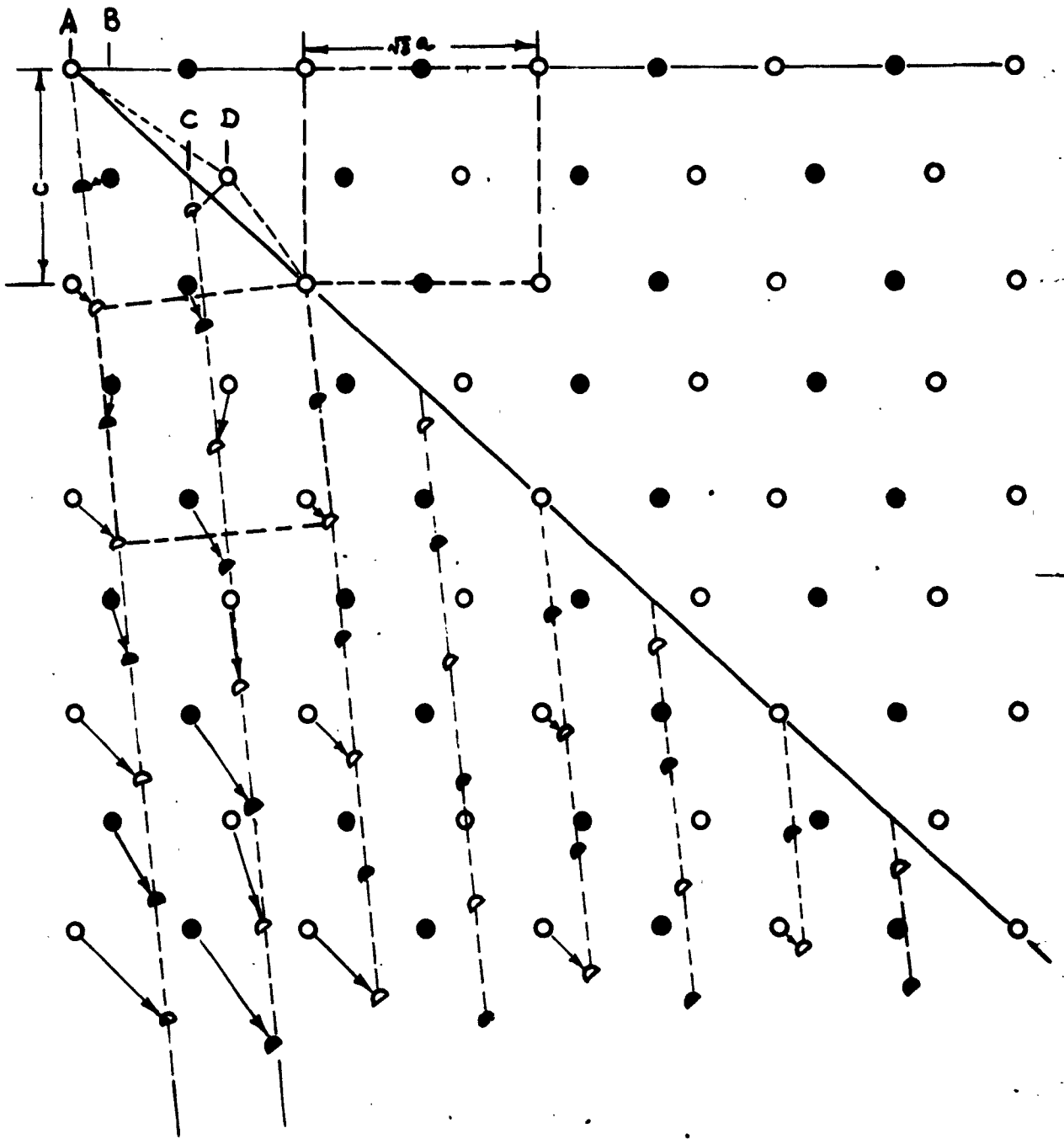

Figure 55 Atomic Movements in Twinning of HCP Metals

Examination of the atoms close to the twinning plane shows that their movements are truly complex. However, when planes farther away from the twin boundary are examined, it will be found the vectors of the atomic movements gradually rotate counter clockwise, towards parallelism of the $(10\bar{1}2)$ plane. The farther the atoms are from the twin boundary, the closer their movements approach to parallel to the twinning plane and direction.

It is possible to select a pair of axes and assign coordinates to positions of all atoms, before and after twinning, in terms of functions of the lattice parameters a and c. From the initial coordinates of an atom and the final coordinates of the same atom after twinning, the direction of the movement of this atom in the process of twinning, can easily be calculated.

Take row A for example, in Fig. 56 with X_1 and Y_1 as the coordinates. The initial ordinates of the atoms in this row can be expressed by a simple function $n_A c$, where n_A is an integer representing the distance of a given atom from the origin in terms of interatomic distances along this row. The abcissa is zero. After twinning, these atoms assume new coordinates which may be represented as $(\frac{n}{2}\sqrt{3}a\cos 2\theta, \frac{n}{2}\sqrt{3}a\sin 2\theta)$ with respect to the same axes, where n is the number of atomic distances from the origin along the newly formed (0001) plane of the twin, i.e., AA' in Fig. 56.

The direction of movements of the atoms in row A can, therefore, be formulated as:

$$\tan\theta_A = \frac{\frac{n}{2}\sqrt{3}\, a \sin 2\theta - n_A c}{n_A \sqrt{3}\, a \cos\theta} \quad \ldots\ldots\ldots\ldots\ldots\ldots (1)$$

Notice that for row A, $n = 2n_A$. Equation (1) can thus be simplified to the form:

$$\tan\theta_A = \tan 2\theta - \frac{c}{\sqrt{3}a \cos 2\theta}$$

Since..... $\tan\theta = \frac{c}{\sqrt{3}a}$,

$$\tan\theta_A = \tan\theta \left(\frac{2}{1-\tan^2\theta} - \frac{1}{\cos 2\theta}\right)$$

Simplifying further, $\tan\theta_A = \tan\theta$

This relation shows $\theta_A = \theta$, i.e., all the atoms in row A move parallel to the twinning plane and twinning direction when they are transferred from matrix to twin positions.

When the same procedure is followed for rows B,C, and D, it is found that the direction of movements of atoms in these three rows is not constant. Their movements can be shown as follows:

$$\mathrm{Cot}\theta_B = \mathrm{Cot}\theta \left\{1 - \frac{3 + (c/a)^2}{3(n_B+1)\left[3-(c/a)^2\right]}\right\} \quad (2)$$

$$\mathrm{Cot}\theta_C = \mathrm{Cot}\theta \left\{\frac{n_C + 2/3}{n_c + \frac{5a^2 - c^2}{2(3a^2 - c^2)}}\right\} \quad (3)$$

$$\mathrm{Cot}\theta_D = \mathrm{Cot}\theta \left\{\frac{n_D + a^2/(3a^2-c^2)}{n_D - c^2/3(3a^2-c^2)}\right\} \quad (4)$$

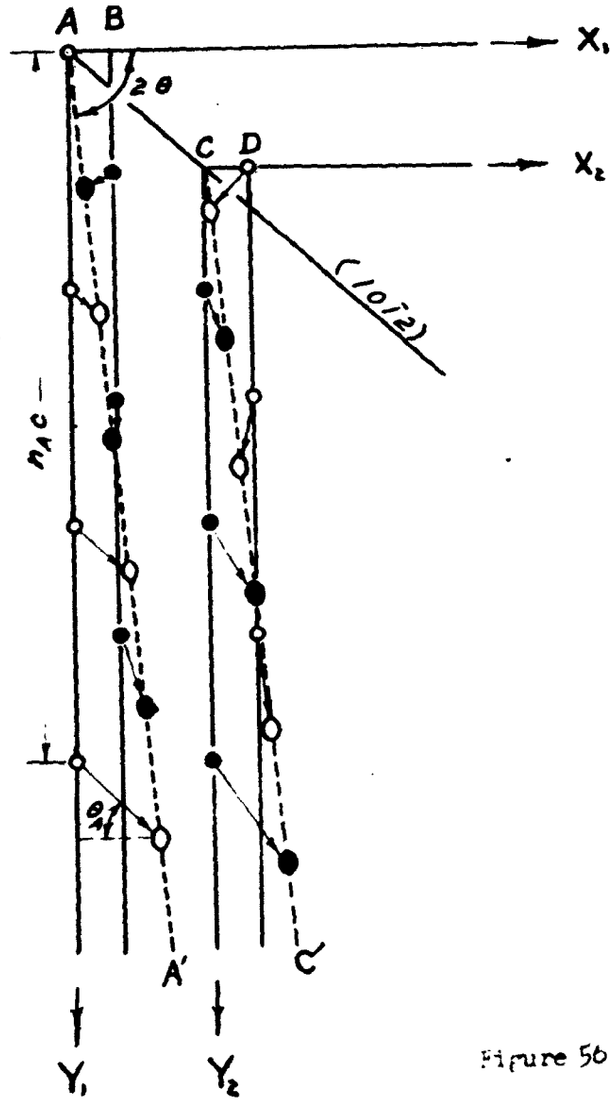

$$\tan\theta_A = \frac{n_A\cdot\sqrt{3}\,a\cdot\sin 2\theta - n_{AC}}{n_A\cdot\sqrt{3}\,a\cdot\cos 2\theta} = \tan\theta$$

$$\cot\theta_B = \cot\theta\left\{1 - \frac{3+(c/a)^2}{3(n_B+1)[3-(c/a)^2]}\right\}$$

$$\cot\theta_C = \cot\theta\cdot\frac{n_C + 2/3}{n_C + \frac{5a^2-c^2}{2(3a^2-c^2)}}$$

$$\cot\theta_D = \cot\theta\cdot\frac{n_D + \frac{a^2}{3a^2-c^2}}{n_D - \frac{c^2}{3(3a^2-c^2)}}$$

Figure 56 Angular Direction of The Atomic Movements

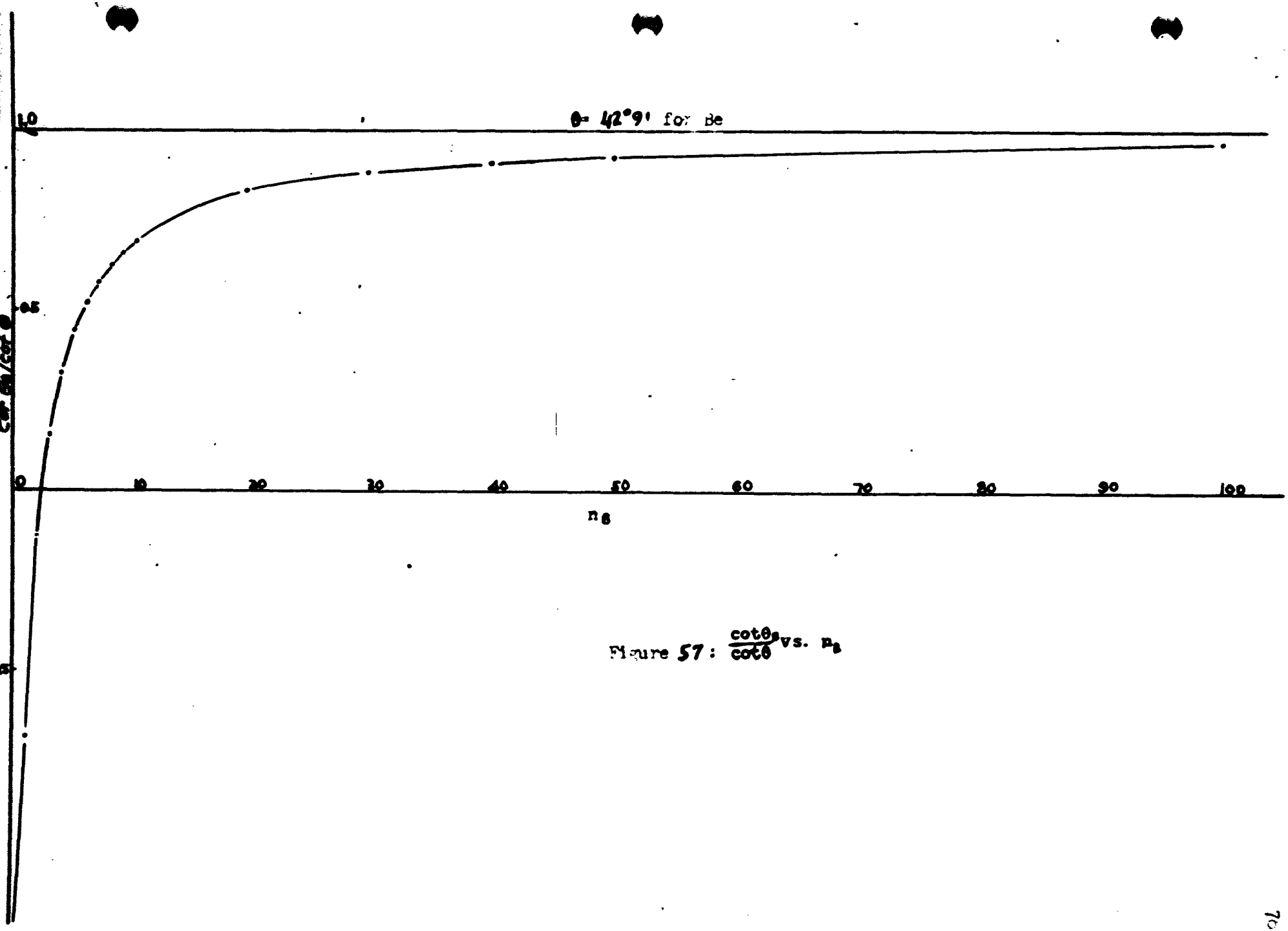

Figure 57: $\frac{\cot\theta_s}{\cot\theta}$ vs. n_s

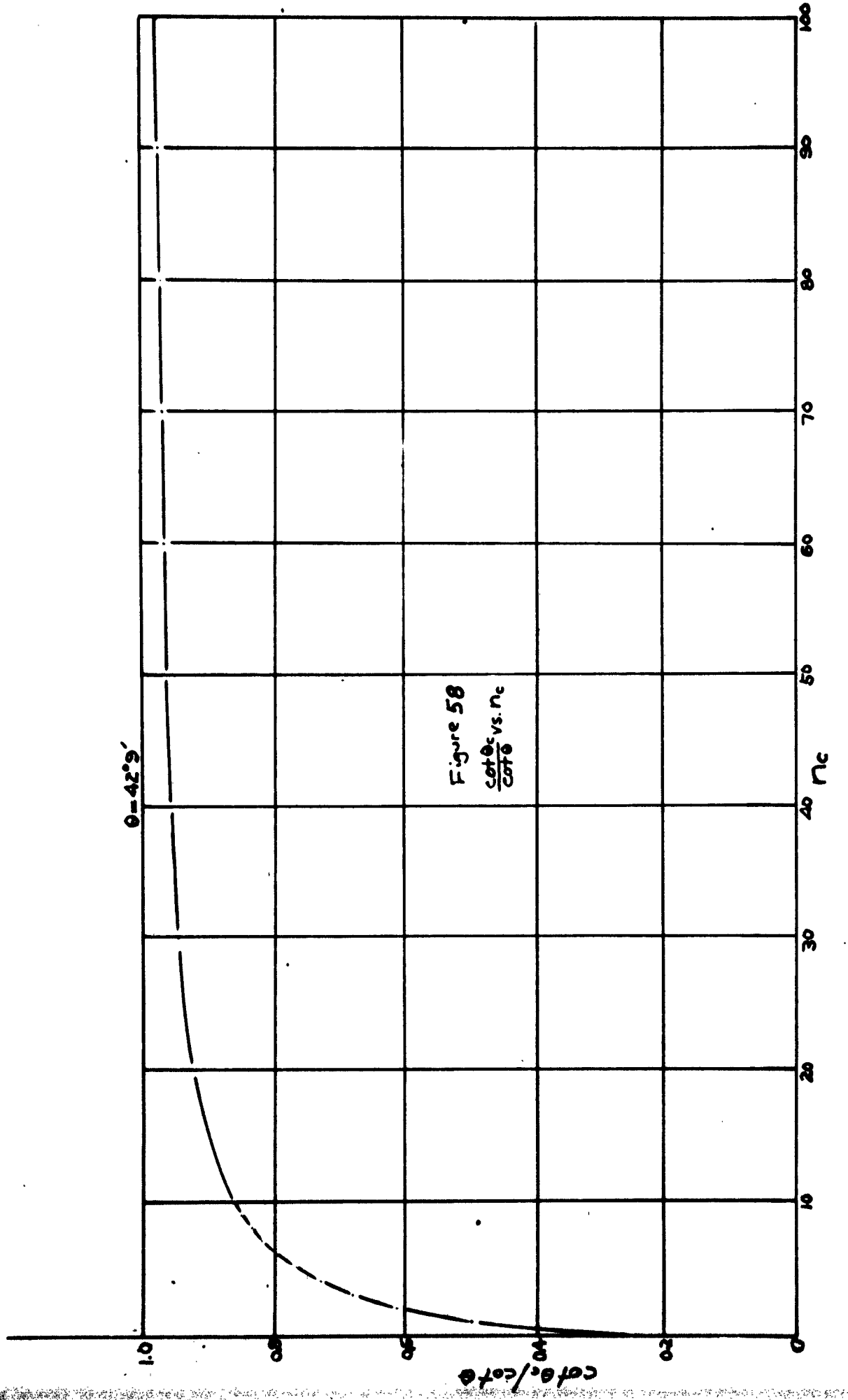
θ=42°9'
Figure 58
$\frac{\cot\theta_c}{\cot\theta}$ vs. n_c
n_c
$\cot\theta_c/\cot\theta$
100
90
80
70
60
50
40
30
20
10
0
1.0
.8
.6
.4
.2

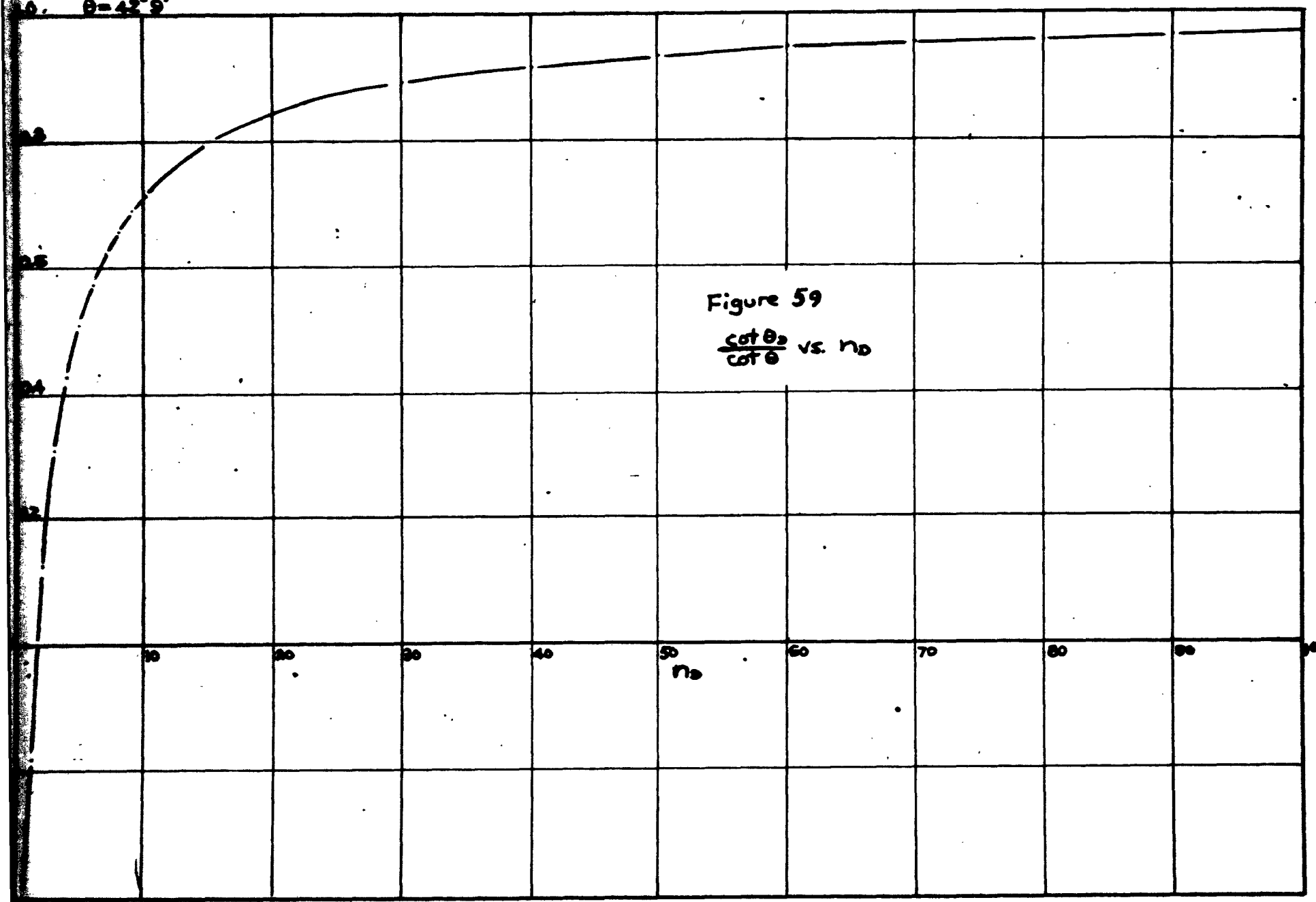

Figure 59

$\frac{\cot \theta_2}{\cot \theta}$ vs. n_D

In all cases, as n_B, n_C, or $n_D \to \infty$; θ_B, θ_C, $\theta_D \to \theta$. This shows that the further away from the interface the atoms are, the more nearly their movements approach parallelism to the twinning plane and direction. By plotting the cotangent of θ_B, θ_C, and θ_D against n_B, n_C, n_D correspondingly for beryllium which has parameters a = 2.2871Å, c = 3.5860Å, it is found that as either of the three n-values reaches 100 the corresponding θ_B, θ_C, or θ_D will be all within 1° of θ. Figs. 57, 58 and 59 show these plots.

In a HCP metal, a twin is generally much more than 100 atomic layers thick. For this reason, the twinning mechanism of a HCP metal, though not exactly a process of homogeneous shear, can rather safely be regarded as such in essence. Calculations based on this assumption, therefore, agree with experimental results. And, this analysis seems to bring the picture of twinning of HCP metals somewhat closer to that of the cubic structures.

The above analysis did not single out the peculiar situation of the first layer of atoms from the twinning plane. Whether this layer of atoms stays in the matrix or moves over to the twin the result is a twin boundary of unsymmetrical counterparts. The most probable way is for this layer of atoms to take up symmetrical positions on the interface with consequently both matrix and twin being in a state of strain.

The comparatively high strain of twin boundaries of HCP metals and the large number of atoms required to move approximately parallel to the twinning plane to offset the irregular movements of the atoms near the interface, all require the twins to be large in size in order to be stable enough to exist. This corresponds with the general observations of twinning in hexagonal metals.

It is not suggested here that the above derived process should be considered as the actual mechanism of twinning in HCP metals. Rather it merely serves as an explanation of the fact that for ordinary purposes, twinning of HCP metals can be treated as a homogeneous shearing process. The above analysis offers a unified mathematical description of how this is accomplished.

This analysis of atomic movement in twinning of HCP metals treats the displacement of atoms over a considerable depth instead of merely in layers adjacent of the interface. Whether mechanical twins are formed through a process where only a few layers of atoms are involved or through a process which involves a minimum of few hundred layers of atoms has not been answered by any conclusive experimental evidence.

However, it was frequently observed in beryllium that on surfaces which had not been repolished after compression, twins sometimes appeared as clusters of fine lines, e.g., Fig. 46a on p. 59. These clusters bore the general outline of a twin. After repolishing the ordinary homogeneous structure of twins took place of the clusters.

The fine structure within the twins - a series of evenly spaced parallel lines - seems to suggest that these twins were not formed by a gradual migration of their boundaries where only few layers of atoms participated at one time. Rather it was an indication of the discontinuous nature of the formation of twins.

B. FACTOR of PERIODICITY

The foregoing analysis deals with only a particular crystal structure, where the twinning elements are experimentally determined. To further extend the analysis of the problem of twinning to other structures, a more general picture may be considered.

Fig. 60a shows a string of atoms. Figs. 60b, 60c, and 60d represent several ways when four strings of atoms are put together in a two dimensional way. These arrangements of atoms can also be regarded as being the cross-sections of a certain crystal lattices.

It is immediately seen that there is no possibility of twinning in the first two cases, whereas the third arrangement does offer the possibility of twinning, as well as the possibility of slip. This situation can be described from several approaches. It could be said that the geometry in the first two cases just does not allow twinning while in the third it does. In this way, one may call it a geometrical factor which governs whether slip or twinning should occur in a particular system.

Figure 60a

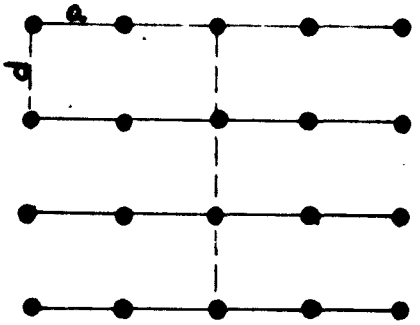

Figure 60b
periodicity - 1
cryst. shear - a/d; slip

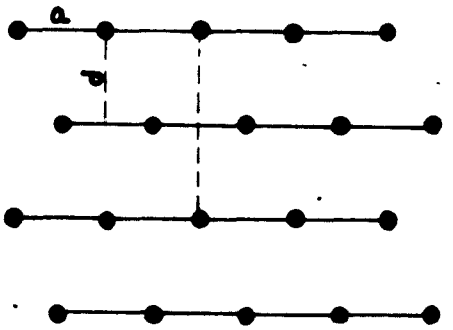

Figure 60c
periodicity - 2
crystall. shear - a/d; slip

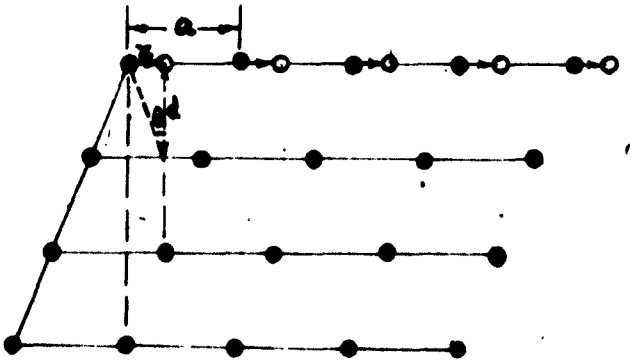

Figure 60d
periodicity - 3
cryst. shear - x/d, twinning

It could also be said that in the first two cases, part of the crystal is already a twin of the rest. The plane in question has already been functioning as a twinning plane. Therefore, no further twinning is allowed. Of course, the plane can serve as a slip plane. In so doing, the arrangement of the atoms will be maintained the same, half of the crystal is still a twin of the other half, and the plane does not lose its original property of being a mirror after slip. In the third case, however, while the plane in consideration is not a twinning plane yet, parts of the crystal on two sides of this plane are not mirror images of each other. Therefore, it may acquire this property, i.e., it offers the possibility of being used as a twinning plane. From this point of view a similarity between slip and twinning is noticed. Both processes will offer in the end the symmetry of twins. The difference is, a slip plane has this property of symmetry all the time, before as well as after twinning; and a twinning plane has this property of symmetry only after being used as such.

A third way to describe it, is by examining the periodicity of the plane in consideration. By periodicity it is meant the period through which the plane directly repeats itself. To assign a periodicity, one simply draws a line through an atom perpendicular to the plane in question to find out how often this line passes through another atom in a similar plane. In the first case, Fig. 60b, obviously the periodicity is 1; in the second case, 2; and the third case, 3. Only when the periodicity is 3 or larger can twinning occur. Otherwise, only slip is possible. In the light of the factor of periodicity, slip may be regarded as a special case of twinning where the periodicity is smaller than 3. Across a slip-

plane every layer of atoms constitutes a twin. Therefore, the two twins will be indistinguishable, or perfectly identical; since the atoms at the interface do not change their neighbors and no boundary could be detected. It is only when the periodicity reaches 3 or larger that a crystallographically distinguishable boundary can exist. Thus, twin of a periodicity of 1 is a slip; twin of a periodicity of 2 is also a slip; and twin of a periodicity of 3 or larger will be a true twin in its conventional sense. Very likely, the larger the periodicity of the twin, e.g., Fig. 61, p.90, the thicker the twin and the more stable the twin boundary will be.

Figs. 62 and 63, p.91, show the twinning of BCC metals. The twinning system $(112)\ [11\bar{1}]$, Fig. 62, possesses a periodicity of 3. For such a periodicity, three layers of atoms will be enough to create a twin of distinguishable boundaries, although such a twin may properly be called a fault. On every third layer within the twin, the atoms move a whole interatomic distance or an integral multiple. A simple equation may describe such a condition as dictated by twinning in this case, as also is seen in Fig. 60d:

$$\tan\theta = \frac{ka}{pd} \qquad (5)$$

Where p is periodicity, k is a constant representing the number of interatomic distances through which atoms of the pth layer translate; and $\tan\theta$ is the twinning shear. In this particular case, p equals 3 and k equals 1.

For this type of twinning, which is exactly represented as a process of homogeneous shear, p and k in this equation must be integers, and k is not always 1. It could be shown, when a particular shear direction is chosen, k and p may be related in such a manner as to give the following ratios:

$$k/p = 1/3,\ 2/4,\ 3/5,\ 4/6,\ 5/7,\ 6/8,\ 7/9,\ \text{etc}.....(6)$$

For all cases where $p \geqslant 5$, the shear direction may be reversed so as to give the smaller strain. Thus modified, the above series will then take the form:

$$k/p = 1/3,\ 2/4,\ 2/5,\ 2/6,\ 2/7,\ 2/8,\ 2/9,\ \text{etc}.....(7)$$

Fig. 61, p.90, is a hypothetical case illustrating twinning of a periodicity of 7. When the shear direction is chosen as shown in the left side of the drawing, the k/p must be 5/7, and the shear, 5a/7d. This will be the case of equation (6). Whereas the reversed direction, shown in the right side of the drawing, will give a k/p of 2/7, and a twinning shear of only 2a/7d. This will be the case of equation (7). Obviously the latter direction should be chosen in calculating the strains.

It will be noted that the ratios in equation (7) are not all in their simplest forms. The denominators are maintained as the same integers as p's are. While the ratio of 2/4 may as well be written as 1/2, a periodicity of 2, nevertheless, will not produce a twin. Thus by maintaining the form 2/4 it will be clear the periodicity must be 4 in order to produce such a twin, which in its thinnest form has only two layers of atoms.

Generally speaking, the larger the periodicity the thicker will be the smallest possible twins. However, a closer examination will show equation (7) may be broken into two parts. For all ratios where the denominators are odd, the denominators or periodicities will represent the number of atomic layers required to form a "unit Twin" For all cases where the denominators are even, the denominators or periodicities represent twice of such layers.

Also, as seen from equation (7), the larger the periodicity the smaller will be the twinning shear, provided a/d being constant. Thus, the thicker a "unit twin", the more easily it will be formed. For cubic metals the symmetry does not allow high periodicity systems. $\{112\}$ or $\{111\}$ twins are all of a periodicity of 3. Twins of such systems could occur in very few atomic layers and unless they are piled up in the right sequence for a very long range, the twins are likely to be so thin as to be hardly noticeable. It seems, as long as the twinning satisfies equation (5), the same thing would prevail.

The $\{10\bar{1}2\}$ twinning of HCP metals can not satisfy equation (5). In the first place, the $(10\bar{1}2)$ planes are not evenly spaced. In the second place, no definite value can be assigned for p in this case. It may be noticed from Fig. 55 that when a line is drawn perpendicular to the $(10\bar{1}2)$ plane through an atom no other atoms are met. The periodicity may be said to be infinity. A $(10\bar{1}2)$ twin, therefore, can not exist only in a few layers of atoms, according to equation (5). Instead, the-

movements of the atoms can only be expressed as equations (1), (2), (3), and (4), as previously described. The large periodicity, associated with a large number of layers of atoms necessary to form a twin and a small twinning shear, may be an explanation for the readiness of formation of large mechanical twins in HCP metals.

$\{10\bar{1}2\}$ twinning of beryllium has a shear of 0.186 based on the assumption of homogeneous shear. Substituting this shear in equation (5), it is found the periodicity of $\{10\bar{1}2\}$ twinning of beryllium is equivalent to about 129. While this value by no means describes the exact nature of twinning of beryllium, the argument remains that twins thinner than this number of atomic layers are not likely to exist and twinning over several hundred layers of atoms can be treated as a homogeneous shear for purposes of making related calculations. Examination of Figs. 57, 58 and 59 has shown this approximation.

It should be noted that the above analysis is solely based on a crystallographic respect. No energy consideration enters into it. Creation of new twin surfaces is associated with an increase of surface energy which must be overcome by the drop of free energy accomodated by twinning if twinning is to be obtained. However, with our present limited knowledge concerning the energy of solid-solid interfaces, it seems that not much more than this very broad statement can now be said.

C. FACTOR of CRYSTALLOGRAPHIC SHEAR

In a crystal lattice, there are obviously more than one type of planes which may possess a periodicity of 3 or larger. As far as periodicity is concerned, these planes will all have the possibility of serving as twinning elements. Yet, in reality, only a few of them are found to be the twinning planes. The same thing is true about slip. A second factor affecting the selection of one particular system as favorable from among a number of possibilities, has to be introduced.

Theories of plastic flow may propose various explanations of how the atoms move while a metal is being deformed. Nevertheless, the net or gross displacements of the atoms to account for the deformation are generally quite simple. In either twinning or slip, when an atom is transferred from the initial to the end position, a crystallographic shear---the ratio of the displacement of an atom to its distance from either the twinning plane or the plane of slip---is accomplished. In Fig. 66b and 66c, the atoms all move one whole interatomic distance during slip and the crystallographic shear is hence a/d. In Fig. 60d, the displacement is only a fraction of the interatomic distance and the crystallographic shear is x/d.

When the atomic displacement is large while the interplanar spacing is small, the crystallographic shear will be high and vice versa. The smaller the crystallographic shear, the more easily will an atom move owing to the fact that the travel of the atom is short and its bond to the neighboring layers weak. This bears the general statement that slip-

prefers to occur in a close packed plane and along a close packed direction.

Examination of Fig. 63 will show the $\{112\}\langle 11\bar{1}\rangle$ system of BCC metals has a periodicity of 3, and the atomic movement for twinning along such a system demands a crystallographic shear of 0.707. However, the $\{112\}\langle 11\bar{1}\rangle$ is not the only system which could offer twinning in BCC metals. Fig. 62 shows another possibility where the twinning plane is $\{11\bar{1}\}$ and the direction $\langle 112\rangle$. The periodicity of this system, $\{111\}\langle 11\bar{2}\rangle$, is also 3, but the crystallographic shear required for twinning along it is now 2.828. This value of shear is four times as large as that of the previous one. For this reason it should be expected that twinning of BCC metals would occur in the $\{112\}\langle 11\bar{1}\rangle$ system rather than in $\{111\}\langle 11\bar{2}\rangle$. The observed Neumann bands in α - Fe verify this point.

Similar examinations can be made for a large number of systems. To illustrate the principle involved, only five of them have been carried out for BCC and FCC structures. The result is summarized in Table 1. Figs. 62 to 69 show the atomic arrangement for each case, they are presented to illustrate the periodicity of each of the systems under consideration.

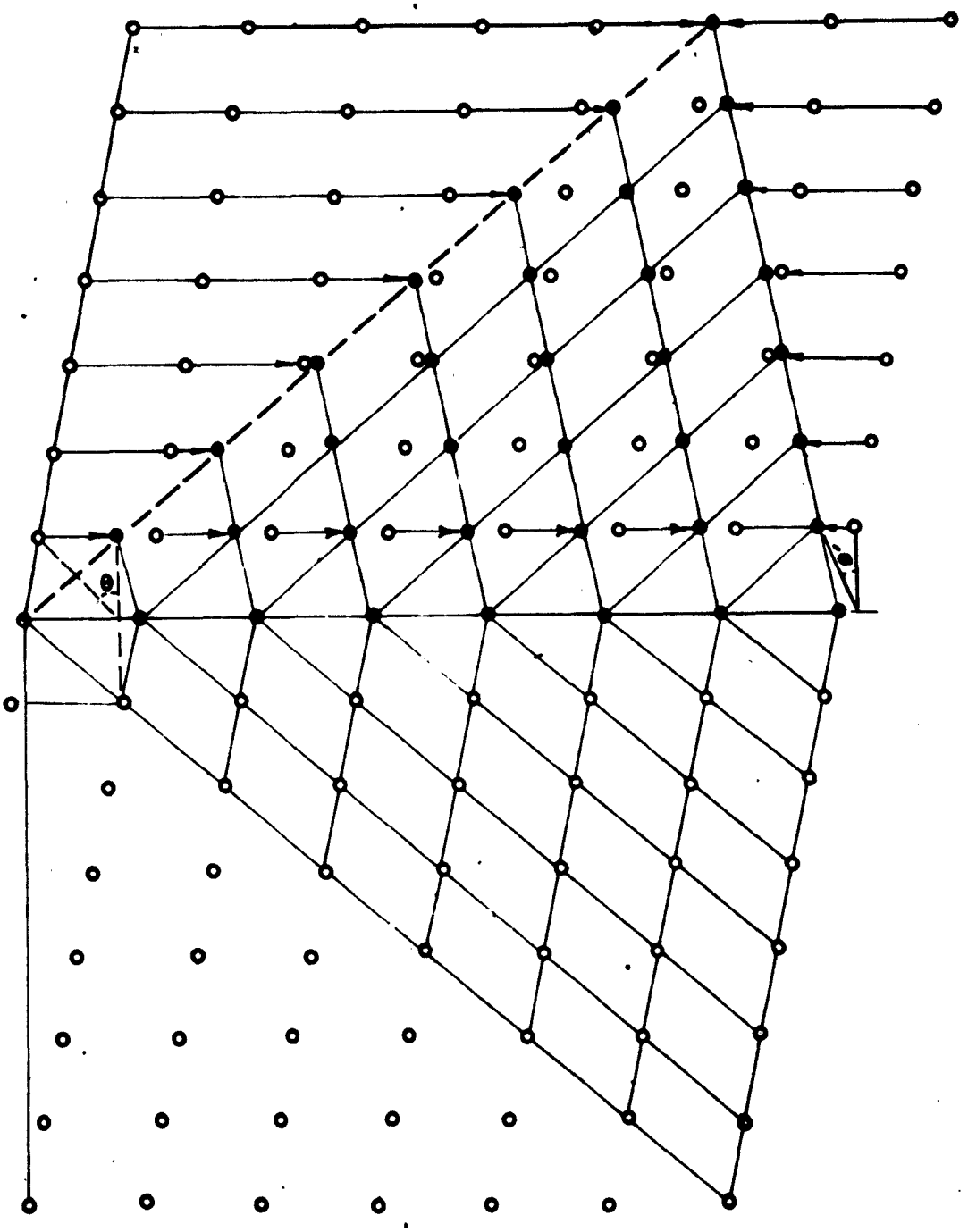

Figure 61 A hypothetical Case of Twinning of Periodicity 7

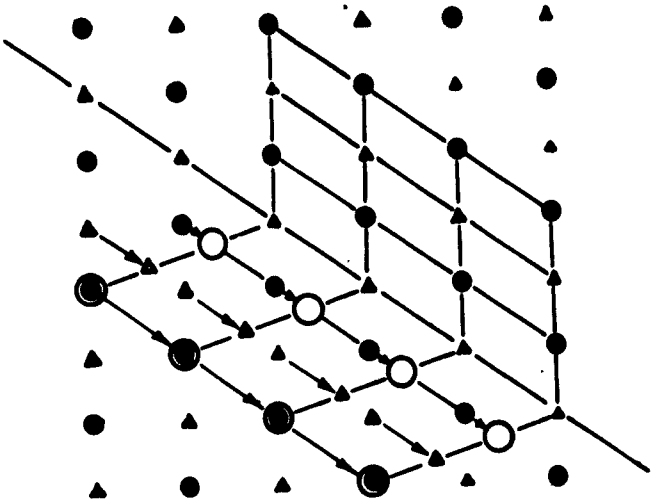

Fig. 62 BCC - $\{11\bar{2}\}\langle 111\rangle$ Twinning System
Plane of Projection - {110}
Periodicity - 3; Crystal shear $\sqrt{2}/2$

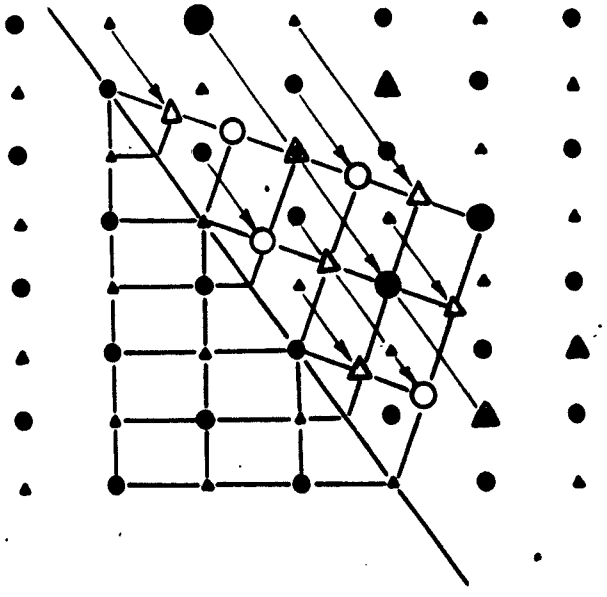

Fig. 63 BCC - $\{\bar{1}11\}\langle 11\bar{2}\rangle$ Twinning System
Plane of Projection - {110}
Periodicity - 3, Crystal shear $2\sqrt{2}$

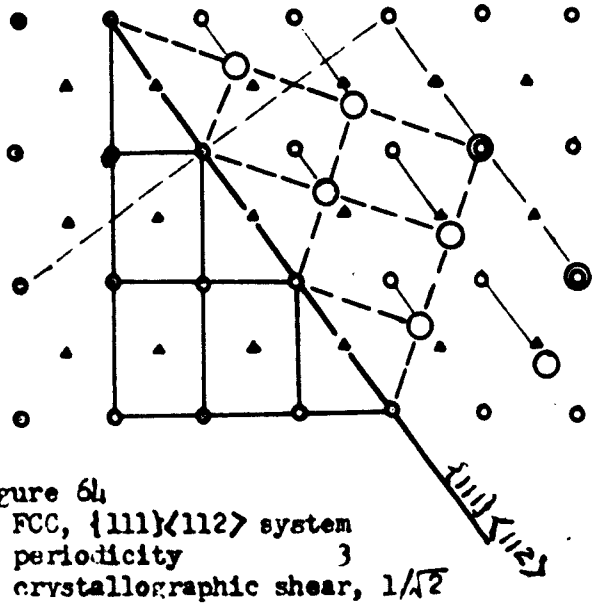

Figure 64
FCC, {111}⟨112⟩ system
periodicity 3
crystallographic shear, $1/\sqrt{2}$

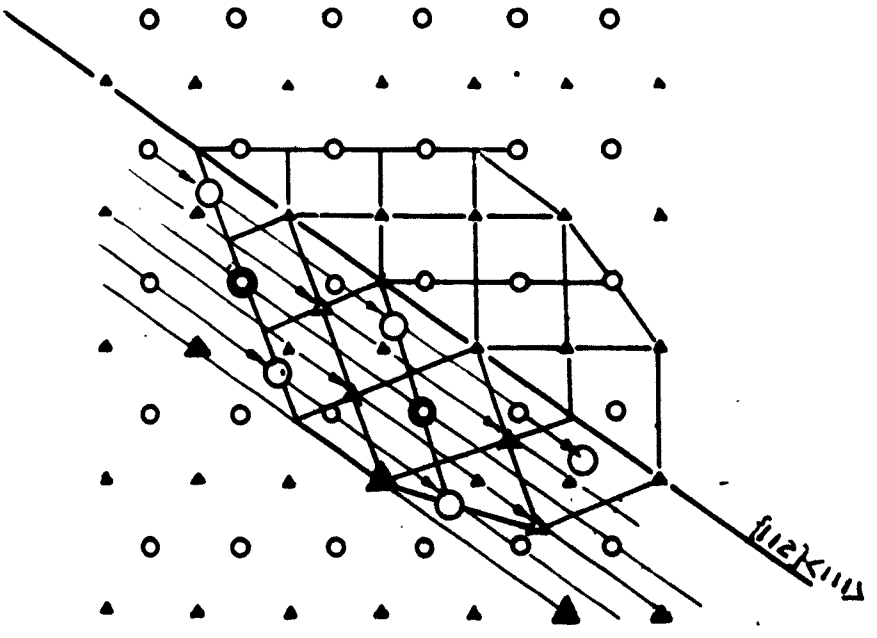

Figure 65 FCC, {112}⟨111⟩ system
periodicity 3
crystallographic shear $2\sqrt{2}$

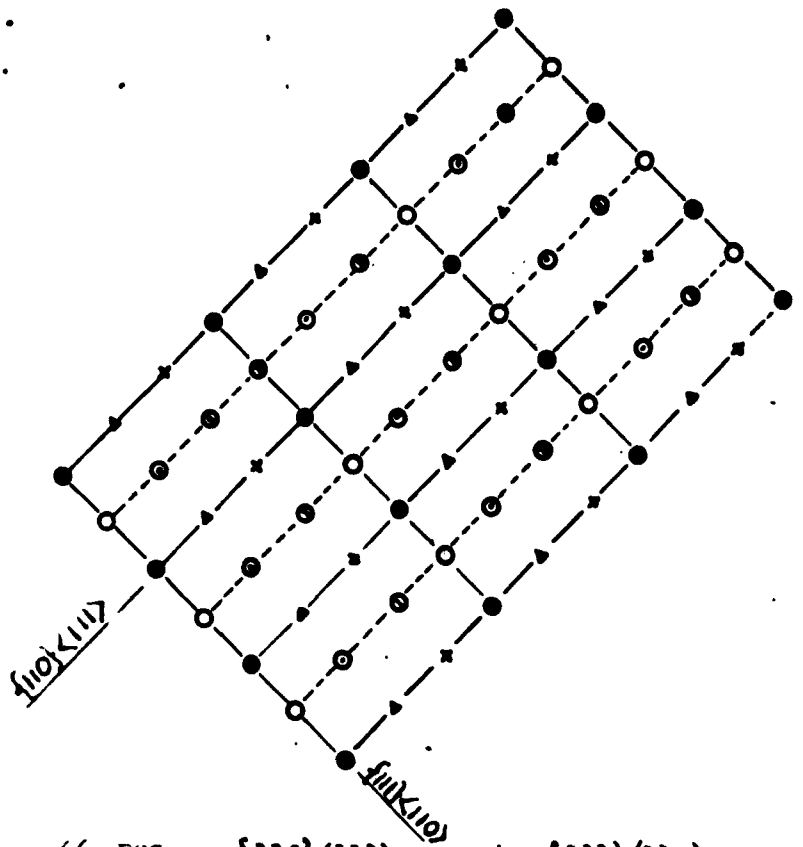

Figure 66 FCC, {110}⟨111⟩, and {111}⟨110⟩ systems
p. $\frac{1}{2\sqrt{5}}$, $\frac{1}{\sqrt{6}/2}$
c.r.
Plane of Proj. {112} (six layers, O's represent three.)

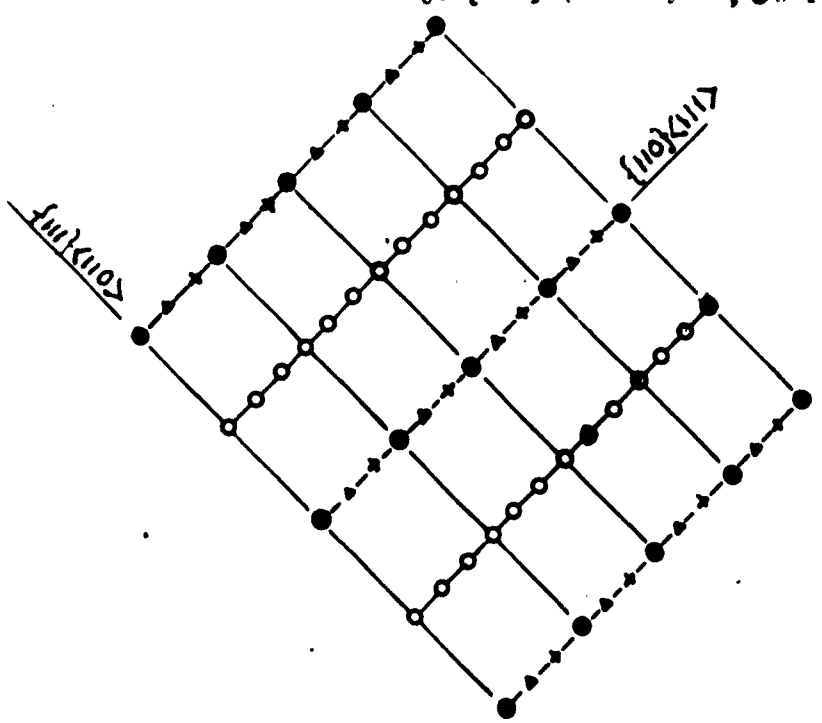

Figure 67 BCC, {110}⟨111⟩, and {111}⟨110⟩systems
p. 1 , 1
c.r. $\sqrt{3}/\sqrt{2}$ $2\sqrt{6}$
Plane of proj. {112} (six layers, O-represent three)

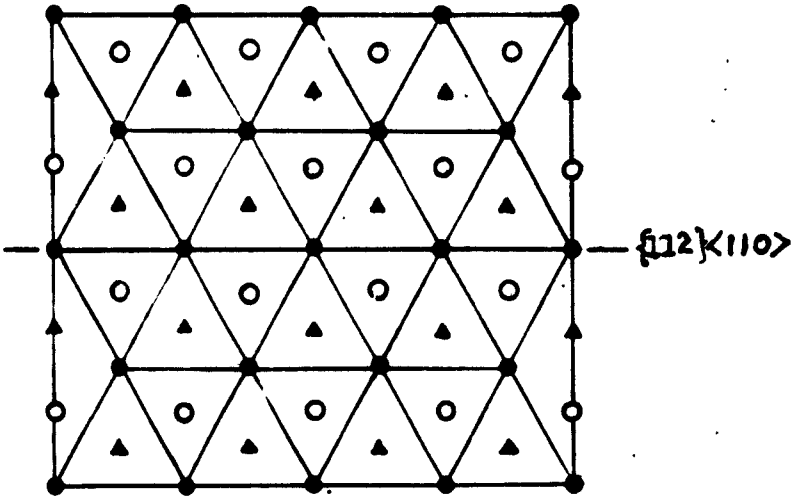

Figure 68 FCC, {112}<110> system
Plane of Projection {111} (3 layers)
Periodicity 2
Cryst. Shear $2\sqrt{3}$ (slip)

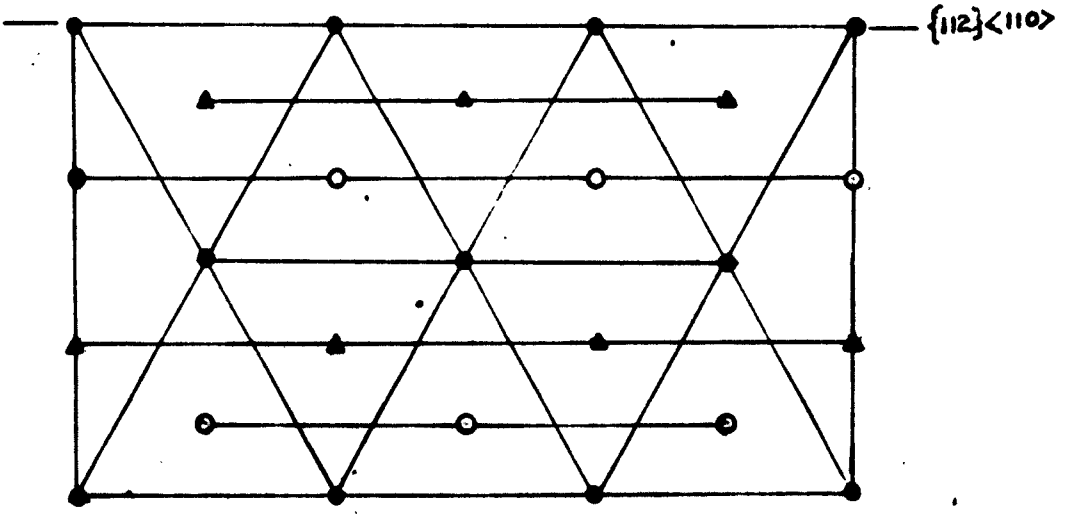

Figure 69 BCC, {112}<110>system
Plane of Proj. {111} (3 layers)
Periodicity 2
Cryst. Shear (slip)

Table I

Periodicity and Crystallographic Shear

of Various Slip and Twinning Systems

of Both BCC and FCC Structures

SYSTEM	F.C.C. P	F.C.C. CRYSTAL.SHEAR	FIGURE	B.C.C. P	B.C.C. CRYSTAL.SHEAR	FIGURE
$\{110\}\langle 111\rangle$	1	$2\sqrt{6}$, 4.900	66	1	1.225	67
$\{111\}\langle 110\rangle$	1	$\sqrt{3}/\sqrt{2}$, 1.225	66	1	4.900	67
$\{112\}\langle 110\rangle$	2	$2\sqrt{3}$, 3.464	68	2	3.464	69
$\{111\}\langle 112\rangle$	3	$\sqrt{2}/2$, 0.707	68	3	2.828	63
$\{112\}\langle 111\rangle$	3	$2\sqrt{2}$, 2.828	65	3	0.707	62

It will be noted, from Table I, in the case of FCC metals both $\{111\}\langle 110\rangle$ and $\{112\}\langle 110\rangle$ systems have a periodicity of either only 1 or 2. Therefore, they can not serve as a twinning system. Only slip is possible for these two cases. To accomplish the slip, the $\{112\}\langle 110\rangle$ system requires a crystallographic shear about three times as large as the $\{111\}\langle 110\rangle$ system does. Hence slip will prefer the $\{111\}\langle 110\rangle$ rather than $\{112\}\langle 110\rangle$. As for twinning, both $\{111\}\langle 112\rangle$ and $\{112\}\langle 111\rangle$ furnish the possibility. The crystallographic shear of $\{112\}\langle 111\rangle$ twinning is four times as large as that of $\{111\}\langle 112\rangle$. As a result, twinning of FCC metals would be expected to prefer the latter system. Although experimentally mechanical twins in FCC metals are not observed, yet the annealing twins do comply with $\{111\}\langle 112\rangle$.

In the case of BCC metals among the three systems of a periodicity of either 1 or 2----- $\{111\}\langle 110\rangle$, $\{110\}\langle 111\rangle$, and $\{112\}\langle 110\rangle$, the $\{110\}\langle 111\rangle$ system offers the smallest crystallographic shear. Slip would therefore choose this system in preference of the other two. By the same reason, twinning in BCC metals will take the system $\{112\}\langle 111\rangle$ instead of $\{111\}\langle 112\rangle$ as previously mentioned.

The analysis based on the factor of crystallographic shear is by no means conclusive. Yet, for the few cases considered, it seems to serve as a possibly improved explanation for some of the generally observed experimental data.

D. FACTORS of STRESS and STRAIN

Both factors of periodicity and crystallographic shear deal with planes and directions of different indices, i.e., different systems for either slip or twinning. To narrow the problem further, it should be noted that even a plane of fixed index has its own multiplicity; so does a crystallographic direction. A specific case is the $\{10\bar{1}2\}$ twinning of HCP metals where there are six $\{10\bar{1}2\}$ planes. As far as periodicity and crystallographic shear are concerned, all six of them are identical. Yet in the twinning of hexagonal metals, it is rarely observed that all of them are active.

In part I, the selection of operative $\{10\bar{1}2\}$ twinning planes of beryllium under uniaxial compressive stress was determined by the relative effectiveness of these planes to accomodate the necessary deformation, i.e., the LeChatelier effect. This, in a broad sense, may be considered as a factor of strain which governs the activity of deformation elements.

A well known example illustrating the factor of stress is the critical resolved shear stress law which has been advanced by Schmid and Boas (21), where particular slip elements are activated from among a number of ones of the same system, according to the magnitude of the shear stress resolved.

Vogel (31) and Steijn (32), in their works on α-iron have incorporated the factor of strain to that of stress. It was observed that the selection of glide plane in α-iron was determined by the interrelation between the resolved shear stress and the relative resistance to shear of all the planes containing the active slip direction. Furthermore, the selection of glide planes was found to be different between compression and tensile tests.

Wu and Smoluchowski (33) have modified the original Schmid and Boas equation by taking into consideration the length of the slip direction. They have found that in aluminum crystals having the dimensions 0.2 by 20mm, there was a tendency for those slip directions which provided the shortest path of slip across the crystal to become active. This was so because such directions would offer the least resistance. Here was an example of the importance of the factor of strain to the selection of even glide directions.

Factors affecting stress and strain are many. The mode of stressing, the geometrical shape of specimens, the material, etc., may all deserve consideration. No generalization is feasible at the present. It might suffice to say that under the constraining conditions of various mechanical tests, the crystal is compelled to accomodate itself to the imposed--

circumstances. Being an anisotropic medium,the crystal would have various paths to do so with different degrees of effectiveness and efficiency. The selection of deformation elements is thus a result of balancing the magnitude of stress and resistance as resolved along these available pathes, with the most efficient one to be the active.

SUMMARY

1. From purely a crystallographic basis, a mathematical formulation of the atomic movements in the twinning of hexagonal close packed metals has been proposed. This serves as a means to describe the transferring of atoms from matrix to the twinned positions. Orderliness to a certain extent could be assigned to the atomic movements.

2. Factor of periodicity has been introduced in an examination of the crystallography of slip and twinning in general, and based on this factor a comparison of the two processes has been discussed.

3. An evaluation has been made of the factors of crystallographic shear, stress and strain, as related to the selection of twinning and slip elements.

REFERENCES

1. H. A. Sloman; Journal Institute of Metals, (1932), 49, p.365.

2. P. W. Bridgman; Proceedings of American Academy Arts & Sciences, 1933, 68, p.27.

3. E. Grueneisen and H. D. Erfling; Ann. d. Phys., (1939), 36, p.357.
   E. Grueneisen and H. D. Erfling; Ann. d. Phys., (1942), 41, p.89.
   E. Grueneisen and H. Andenstedt; Ann. d. Phys., (1938), 31, p.714.
   H. D. Erfling; Ann. d. Phys., (1938-1939), 34(2), p.136.

4. E. A. Owen, T. L. Richards; Phil. Mag., (1936), 22, p.304.

5. A. R. Kaufmann & E. Gordon; Metal Progress, (1947), 52,3, p.387.

6. L. Gold; Rev. Sci. Instr., February 1949.

7. C. H. Mathewson & A. J. Phillips; AIME Tech. Publ. No.53, 1928.

8. E. J. Lewis; Phys. Rev. (1929), 34, p.1575.

9. G. F. Kosolopov, A. K. Trapezenikov; Zhurnal Eksperimentalnay i Theoretischeskay Fisiki, (1936), 6(10), p.1163.

10. F. M. Jeager & J. E. Zanstra; Proc. Acad. Sci., Amsterdam, (1933), 36, p.636.

11. L. Losana; Alluminio, (1939), 8(2), p.67.

12. M. C. Neuberger; Z. Krist., (1935), 92.

13. E. A. Owen, L. Pickup; Phil. Mag., (1935), 20.

14. E. A. Owen, L. Pickup, & I. O. Roberts; A. Krist., (1935), 91(1), p.70.

15. L. Gold; USAECD-2643, AECD-2645, July 1949.

16. Neuberger, M. C.; Z. Krist. 85, p.325-28. 1933.

17. G. I. Taylor & W. S. Farren; Proc., Royal Society London, (1926), 111-A, p.529.

18. F. L. Vogel, Jr.; Master of Science Thesis, University of Pennsylvania

19. F. R. Bichowsky & F. D. Rossini; The Thermochemistry of the Chemical Substances, Reinhold Publishing Corp., New York, 1936.

20. E. Baur and R. Brunner; Helv. Chin. Acta, 17, 1934, 958-69.

21. Schmid and Boas; Plasticity of Crystals, F. A. Hughes & Co., London, 1950.

22. R. F. Miller & W. E. Milligan; Transactions, AIME, Vol. 124, p.229, 1937.

23. E. N. da C. Andrade & C. Henderson; Phil. Trans. Royal Society (London), vol. 244, p.177, 1951.

24. E. Orowan; Nature, (1942), 149, p.643.

25. H. J. Gough; Proc. ASTM, (1933), 33, pt.II.

26. E. N. da C. Andrade & P. J. Hutchings; Proc. Royal Society, London, 148A, 120.

27. P. W. Bakarian & C. H. Mathewson; Trans. AIME, (1943).

28. C. A. Zapffe & C. O. Worden; Acta Crystallographical, 2, 1949, 383-385.

29. C. H. Mathewson and A. J. Phillips; Proc. Inst. Metals Div. AIME, (1928), 445.

30. C. S. Barrett; Cold Working of Metals, ASM (1949), 65.

31. F. L. Vogel, Jr. & R. M. Brick; J. of Metals (1953), May, 700.

32. R. P. Steijn & R. M. Brick; Preprint #36, ASM, 1953.

33. T. L. Wu & R. Smoluchowski, Phy. Rev., (1950), 78, p.468.

34. L. W. McKeehan; Proc. Acad. Sci., (1922), 8, p.270.

35. J. C. McLennan & C. W. Niven; Phil. Mag, (1927), 4, p.387.